C1

BEHAVIOUR OF GOLD IN STREAM SEDIMENTS, HUAI HIN LAEP, LOEI REGION, NORTHEASTERN THAILAND

by

PASAKORN PAOPONGSAWAN

B.Sc., Khon Kaen University, Thailand, 1981

A THESIS SUBMITTED IN PARTIAL FULFILLMENT OF

THE REQUIREMENTS FOR THE DEGREE OF

MASTER OF SCIENCE

in

THE FACULTY OF GRADUATE STUDIES

Department of Geological Sciences

We accept this thesis as conforming

to the required standard

THE UNIVERSITY OF BRITISH COLUMBIA

September 1991

72

In presenting this thesis in partial fulfilment of the requirements for an advanced degree at the University of British Columbia, I agree that the Library shall make it freely available for reference and study. I further agree that permission for extensive copying of this thesis for scholarly purposes may be granted by the head of my department or by his or her representatives. It is understood that copying or publication of this thesis for financial gain shall not be allowed without my written permission.

Department of Geological Sciences

The University of British Columbia
Vancouver, Canada

Date September 25, 1991

ABSTRACT

Stream sediment sampling for gold exploration has encountered various problems: these include location and type of sample to be taken, determination of the appropriate sample size in view of gold particle sparsity, and the apparently erratic distribution of gold in stream sediments. Study of the behavior of gold in stream sediments could help to solve these problems and is needed to guide systematic exploration for gold in Thailand.

The Huai Hin Laep, an intermittent third order stream in Loei region, northeastern Thailand, drains a hilly area underlain by highly weathered sandstones, shales, andesites, and tuffs, blanketed by residual lateritic and podzolic soils. The stream reach is approximately 8 km long with an average gradient of 0.008. The original mixed evergreen forest has been logged and cleared for agricultural purposes.

Active stream sediment samples collected from point bars and pavements along the stream reach were processed to obtain 8 size fractions. Of these, five size fractions between 0.425 and 0.053 mm were separated into heavy and light mineral fractions, and analyzed for gold by fire assay-atomic absorption spectrophotometry. The -0.053 mm sediment fraction was split, pulverized and further split prior to analysis. The corresponding dry-sieved -0.150 mm sediment fraction was also processed and analyzed for gold.

Results show that in both point-bar and pavement samples gold is concentrated in the heavy mineral fractions, whereas in all but six samples, the corresponding light fractions and the -0.053 mm fraction contain < 5 ppb gold. Similarly, thirteen out of the sixteen -0.150 mm sediment samples contain less than 5 ppb gold. Gold content is typically higher at pavement than at point-bar sites where gold concentrations are closely correlated with narrow stream channel, shallow channel depth, high flow velocity, coarse-grained sediment texture and high bed roughness, indicating that higher energy conditions favour accumulations of gold.

Estimates of numbers of free gold particles suggest that analysis of heavy mineral concentrates (between 0.425 and 0.053 mm fraction) from a 40 kg -12 mm field sample from either point-bar or pavement site has a high chance of detecting anomalous gold. In contrast, the probability of reliably detecting gold in a 30 g analytical subsample is very low.

With respect to mineral exploration, conventional stream sediment samples will usually fail to detect the gold anomaly in the Huai Hin Laep. This probably results from the dilution of the Au-rich heavy mineral fractions by the barren light minerals and large amounts of silt-clay. The presence of anomalous concentrations of gold would, however, be recognized through the use of field pan concentrates or heavy mineral separates. During regional surveys, samples

for this purpose should be collected from either pavement sites or high energy point-bar sites characterized by a narrow channel, shallow depth, high flow velocity and large amount of coarse grained sediment along the lower reaches of the third order streams. Subsequently, detailed follow-up surveys should consist of more detailed sampling of either 40 kg -12 mm sediments or field pan concentrates from at least 20 kg of sediments along the stream. Anomalous concentrations of gold at the lower reaches of the stream may result from accumulation of gold by hydraulic processes rather than the location of gold mineralization. High gold concentrations at low energy sites characterized by slow flow velocity, low bed roughness and fine grained sediment texture may indicate proximity to the source of gold.

TABLE OF CONTENTS

LIST OF TABLES

LIST OF FIGURES

ACKNOWLEDGEMENTS

Special thanks are due to Mr. S. Sekthera and Mr. M. Jamnongthai, Economic Geology Division, Department of Mineral Resources, Thailand, for providing access to information and field facilities. Mr. S. Yensabai and his colleagues are thanked for their field assistance.

At the University of British Columbia, sincere appreciation is expressed to D. Feduik, J. Borges, S. Paopongsawan and T. Priest for laboratory work. W.K. Fletcher provided guidance, critical comments and helpful criticism. A.J. Sinclair and M. Church carefully reviewed the manuscript.

Finally, I am grateful to Mr. J. Mossop, the SNC Group, for funding through the Canadian International Development Agency (CIDA).

CHAPTER ONE

INTRODUCTION

1.1 Statement of research problem and approach

Although gold[1] occurrences have been recognized for centuries in many parts of Thailand (Fig. 1-1) and placer gold has been panned from small deposits along river banks and from stream sediments, there was little systematic exploration until 1984 when an extensive mineral exploration program was initiated by the Department of Mineral Resources (DMR) with Canadian International Development Agency (CIDA) support under the Mineral Resources Development Project (MRDP) (Kumanchan, 1987). One aspect of this program was to investigate, and if appropriate, apply geochemical methods to gold exploration. However, with the exception of the recently completed, complementary study by Nuchanong (1991), no detailed orientation studies are available to provide guidelines for design and interpretation of exploration geochemical surveys for gold in Thailand. The objective of this thesis was to remedy this situation.

Studies elsewhere (reviewed later in this chapter) of the exploration geochemistry of gold in stream sediments have shown that:

1) the scarcity of free gold particles can result in difficulty to obtain representative stream sediment samples,

2) the dispersion and distribution of gold as a heavy mineral is extremely erratic because of the variations of

---

[1]Gold refers to the mineral which is an alloy of Au with minor Ag, Cu, Hg etc. Au refers to the element only.

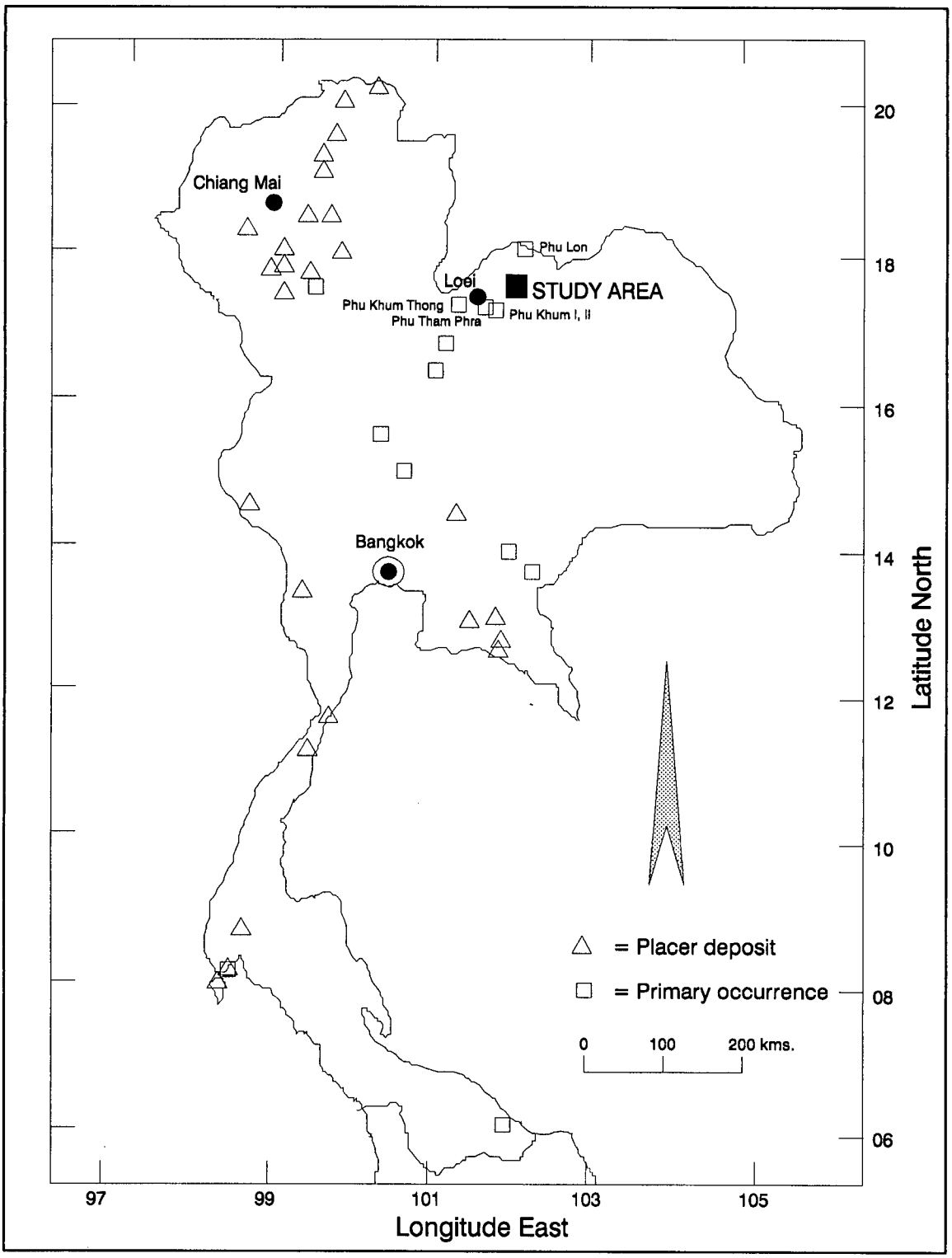

Fig. 1-1. Gold occurrences in Thailand (modified from Vudhichatvanich, 1980; Tate, 1988). Shaded arrow indicates north direction.

local hydraulic conditions that cause gold to accumulate at high energy sites along the stream bed, and

3) contrary to the conventional exploration geochemical dilution model (Polikarpochkin, 1971; Hawkes, 1976), gold concentrations tend to increase downstream away from their source.

Specific objectives of this study were, therefore, to:

1) investigate behaviour of gold in different size and density fractions in order to determine representative stream sediment samples,

2) examine the relations between gold concentrations and stream characteristics (i.e. stream width, channel depth and flow velocity) and stream sediment properties (i.e. mean grain size, sediment sorting, bed roughness and abundances of sediment fractions) in order to understand the hydraulic effects influencing the erratic dispersion of gold, and

3) explore the downstream dispersion of gold in order to provide an optimum guideline for design of exploration geochemical surveys for gold in Thailand.

Several areas of interest were suggested for study by the Geochemical Survey Division, Department of Mineral Resources (DMR). Based on the presence of gold in pan concentrates and site visits in July 1989, the Huai[2] Hin Laep in Loei region, northeastern Thailand was selected. The catchment, described in greater detail in Chapter 2, is a

[2] Huai, in Thai, means stream.

typical third order stream in this region of Thailand with a high soil erosion rate as a result of agricultural land use. Chapter 3 describes collection and analysis of bulk stream sediment samples from the Huai Hin Laep. Stream characteristics and sediment properties and their relations are described in Chapter 4 with respect to stream width, channel depth, flow velocity and sediment textures. In Chapter 5, variations in gold content are then presented in terms of the parameters described in Chapter 4. Variations in gold content are then discussed in Chapter 6 and used as a basis for making recommendations for exploration.

1.2 Gold in stream sediment surveys

1.2.1 Introduction

The behaviour of gold in active stream sediments is poorly understood because of the general scarcity of gold particles relative to clasts of rocks and rock forming minerals, and its apparently extremely erratic distribution in stream sediments. Recently, however, studies in British Columbia, Canada (e.g. Day and Fletcher, 1986, 1987, 1989 and in press; Fletcher, 1990; Fletcher and Day, 1988a, b; Fletcher and Wolcott, 1989, in press; Fletcher and Zhang, 1989) have shown that variations in gold concentrations on stream beds can be understand in terms of sorting of heavy minerals during bedload transport of sediment. The factors

involved are briefly reviewed in the remainder of this chapter.

1.2.2 Distribution of metal anomalies in stream sediments

Polikarpochkin (1971) and Hawkes (1976) have presented the dilution model of metal anomalies of stream sediment downstream of the mineralization. The equation is as follows:

$$Me_m A_m = (Me_a - Me_b) A_t + Me_b A_m \qquad (1\text{-}1)$$

where Me_m is the metal content of mineralization,

Me_a is the anomalous metal content in sediment,

Me_b is the background metal content in sediment,

A_m is the area of exposed mineralization, and

A_t is the area of drainage basin.

This model has several limitations arising from the following assumptions:

1) equal rate of erosion throughout the drainage basin;
2) no chemical interactions of the metal in the stream;
3) constant geochemical background values for the metal;
4) no sampling and analytical errors;
5) single source of mineralization in the basin;
6) no contamination from any sources.

A further implicit, but generally unstated assumption, is that within any one size fraction, the various components of the sediments are transported at the same rate and without

segregation (Fletcher, 1990).

This model works reasonably well for either homogeneously distributed or reprecipitated minerals, for example, the dispersion of Cu in stream sediment anomalies downstream from porphyry-copper deposits (Rose et al, 1979). However, anomaly decay for elements such as Ba, Au, Sn and W hosted in high-density resistate minerals is extremely erratic downstream from the source and does not seem to follow the Hawkes' model (e.g. Ba, Sleath and Fletcher, 1982; W, Saxby and Fletcher, 1986; Sn, Fletcher et al, 1987; Au, Day, 1988, Day and Fletcher, 1987, in press, Fletcher, 1990, Fletcher and Day 1988a, b). Major sources of variability for these elements are placer-forming hydraulic processes that create local enrichments of heavy minerals on the stream bed.

1.2.3 Hydraulic effects

The conditions controlling heavy mineral enrichment are (Slingerland, 1984): i) the settling velocity distributions of the local populations of heavy and light minerals, ii) the long-term hydraulic flow at the site, iii) the average roughness of the bed and iv) the volume of material processed through time. Concentrations of heavy minerals occur at preferred sites and at different scales e.g. bed (10^0m), bar (10^2m), and system (10^4m) scales. Locations of

extremely elevated heavy mineral concentrations (placer deposits) in present-day stream beds are summarized in Slingerland (1984, Table 1), Slingerland and Smith (1986, Table 1) and Day (1988, Table 1-1). Thus, in exploration geochemistry, sampling a stream at different locations will produce a wide range of heavy mineral abundances, particularly at the bed and bar scales (Fletcher, 1990).

1.2.3.1 Hydraulic equivalence

The tendency of grains of different minerals to be deposited together is described by the concept of hydraulic equivalence, that is grains having equal fall velocity tend to be hydraulically equivalent. The concept of hydraulic equivalence is generally attributed to Rubey (1933) and Rittenhouse (1943). Use of this concept refers to settling velocity equivalence as determined by Stokes' law or modifications of it (Tourtelot, 1968). This sorting process results in small particles of high density being deposited together with larger, less dense mineral particles. Although the concept of settling equivalence is useful, it is not sufficient by itself to explain the concentration of detrital heavy minerals. It is therefore necessary to consider other mechanisms influencing the formation of placers.

1.2.3.2 Entrainment sorting

Entrainment sorting is the separation of grains into distinct populations of different size, density, and shape by differential pick-up off a bed to produce lag deposits (Slingerland, 1984). The characteristic of this mechanism is that like-size and like-shape particles of heavy minerals accumulate together on the bed because the larger light mineral particles protruding higher into the flow are more susceptible to entrainment.

Grigg and Rathbun (1969) defined the critical shear stress for the initial motion for different size and density of spherical particles of quartz, monazite, lead and gold in water at 20^{o}C using Shields' criterion as a function of grain diameter. The results (Fig. 1-2) showed that for grain diameters finer than 0.10 mm the shear stress required to initiate motion is directly related to grain density, whereas for larger grains the critical shear stress is a function of both grain size and grain density. Additionally, Reid and Frostick (1985) showed that when beach bars are under low flow stresses, entrainment equivalence acts as a sorting mechanism tending to homogenize the size distribution of light and heavy mineral particles. This implies that size alone is an important factor controlling entrainment (Steidtmann, 1982).

Slingerland (1977, 1984) and Komar and Wang (1984) showed that entrainment sorting was controlled by the size

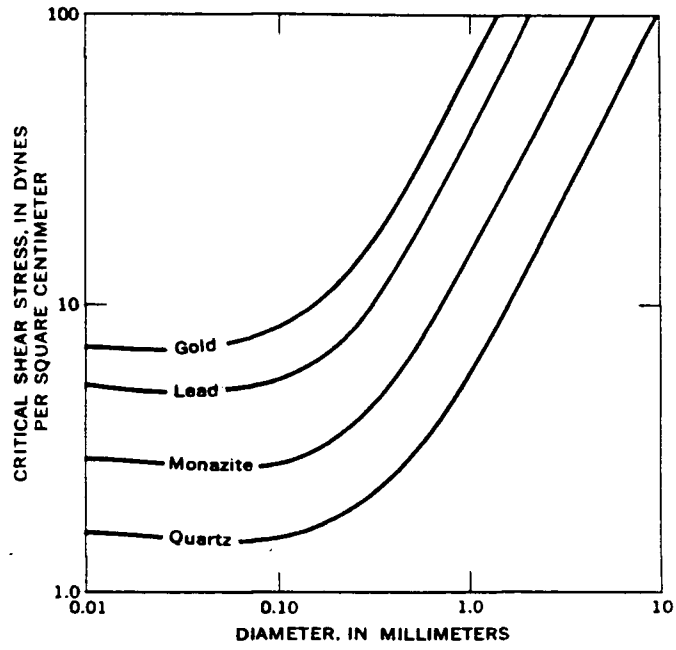

Fig. 1-2. Relation of critical shear stress in water at 20°C to grain diameter for spherical grains of quartz, monazite, lead, and gold (from Grigg and Rathbun, 1969).

and density of minerals under different Reynolds' criteria and bed roughness. However, Slingerland and Smith (1986) pointed out that these results applied only to similarly sized sediments on a plane bed. It was not possible to predict from Figure 1-2 which sizes of different-density minerals would be entrained together from a natural bed. They concluded that winnowing, armoring and hiding are important in entrainment sorting in mixed bed roughness.

Recently, Kuhnle and Southard (1990) empirically studied in flume experiments the response of a mixture of lights and much finer heavies to a range of imposed flows in a gravel-bed channel. Over a wide range of flows and sediment feed rates, a layer of highly concentrated heavy minerals formed at the base of the active layer before equilibrium transport of the heavy minerals was attained. Once deposited, entrainment of finer (< 1 mm) heavy minerals would be unlikely at any flow strength. This also suggests that for fine grained sizes, density is an important control on the entrainment mechanism.

1.2.3.3 Dispersive or shear sorting

Dispersive or shear sorting is a vertical fractionation of particles into different layers within a concentrated granular dispersion caused by dispersive pressures in a moving bed layer or a grain flow (Slingerland, 1984 and Slingerland and Smith, 1986). This sorting mechanism occurs

due to the dispersive pressures arising from grain collisions (Sallenger, 1979). A similar effect is produced by kinetic sieving, wherein smaller grains fall between larger ones (Middleton, 1970). Both cases produce inversely graded deposits (larger or denser grains deposit on top).

In the case of grain collisions, Sallenger (1979) showed that i) along any one horizon of a grain flow composed of light and heavy grains of different sizes, a heavy grain would be smaller than an associated light grain and ii) heavy minerals generally increased in concentration with depth in the lamination. In the case of kinetic sieving, smaller or denser grains fall downward between larger grains resulting in coarse and less heavy minerals staying above the smaller grains (Slingerland, 1984). Nevertheless, Komar and Wang (1984) suggested that dispersive sorting was less important than entrainment sorting. Dispersive sorting may, however, act to feed larger light mineral grains to the top of the mobile layer where their protrusion ensures that they are subject to entrainment. This leaves a lag of smaller heavy minerals (Reid and Frostick, 1985).

1.2.3.4 Interstice entrapment or trapping

Interstice entrapment may be the best mechanism to explain heavy mineral concentrations associated with much coarser sediments where the difference between grain sizes

of light and heavy minerals cannot effectively be explained by settling or entrainment equivalence. If grains are already in motion, denser particles may be trapped or selected out of the waning bed load in preference to less dense particles because they test the bed more often, and once in place are not reentrained (Slingerland and Smith, 1986). A possible process for trapping is that the larger framework particles are deposited first, immediately after extreme flood events, while the heavy minerals accumulate later as part of a matrix which selectively filters into the pores of the streambed (Reid and Frostick, 1985). This agrees well with results of a recent study by Day and Fletcher (in press) at Harris Creek, south central British Columbia, Canada.

Beschta and Jackson (1979) and Frostick et al (1984) empirically studied the infiltration of fine sediments into a coarse-grained streambed. They concluded that fine particles blocked pores of the near-surface coarse-grained streambed and prevented further intrusion. Reid and Frostick (1985) further suggested that clogging in coarsening upwards gravels prevents heavy mineral concentration by entrapment, and that these are unlikely to be sites of placer formation. In contrast, where gravels are progressively fine upwards the pores tended to be packed uniformly, providing greater potential for placer development. This trapping mechanism agrees well with the trapping of alluvial gold in Precambrian conglomeratic gold deposits (Smith and Minter,

1980) in the Witwatersrand basin.

1.2.3.5 Transport equivalence

Slingerland (1984), Fletcher and Day (1988b) and Day and Fletcher (in press) used the modified stochastic bedload transport equation of Einstein (1950) to estimate transport equivalence of low- and high-density minerals in real streams by using the transport ratios of low-density to high-density minerals (e.g. quartz:magnetite and quartz:gold) for different bed roughness conditions. They found that for both low- and high-density minerals, fine particles (< 0.053 mm) behaved very similar, but that coarse high-density minerals tended to preferentially accumulate at high bed roughness sites. Day and Fletcher (in press) further showed that decreasing gradient along a stream's longitudinal profile might result in increasing gold concentrations downstream away from the source.

1.2.4 Sampling considerations

The sampling distribution of very rare mineral grains (e.g. gold, cassiterite, diamond, etc.) in rocks, soils and stream sediments can be described by the Poisson distribution (Koch and Link, 1970; Ingamells, 1981) which is defined as

$$P_{(n)} = \mu^n * e^{-\mu}/n! \qquad (1\text{-}2)$$

where μ is the expected number of particles and $P_{(n)}$ is the probability of n particles occurring in the sample. The confidence limit at significance level Á for the mean (μ) can be estimated from the chi-squared (X^2) distribution (Zar, 1984) as

$$(X^2_{(1-Á/2),2N})/2 \leq \mu \leq (X^2_{(Á/2),2(N+1)})/2 \qquad (1\text{-}3)$$

where N is an estimate of μ.

The implications of the above equations to stream sediment sampling for gold are illustrated in the following example. Gold is assumed to be distributed evenly, as free spherical particles (diameter 0.175 mm), throughout the sediment at a concentration of 200 ppb Au. The gold content of other minerals is considered negligible. Representative samples weighing 250 g are taken from the sediment. Assuming that the gold density is 15 g/cm^3, the expected weight of gold is therefore 50 μg (based on bulk concentration). The mass of each spherical gold particle (density = 15 g/cm^3, diameter = 0.175 mm) is 42.11 μg. Therefore, the expected number of gold particles (μ), on average, is 1.19.

Using the Poisson distribution equation (1-2), the probability that the sample will contain no free gold ($P_{(0)}$, n = 0) is 0.3042. Thus, there is a 30.42% chance that the anomaly will go undetected (Fig. 1-3a). If the sample weighs 30 g (approximately 1 assay ton), then μ = 0.14 and $P_{(0)}$ =

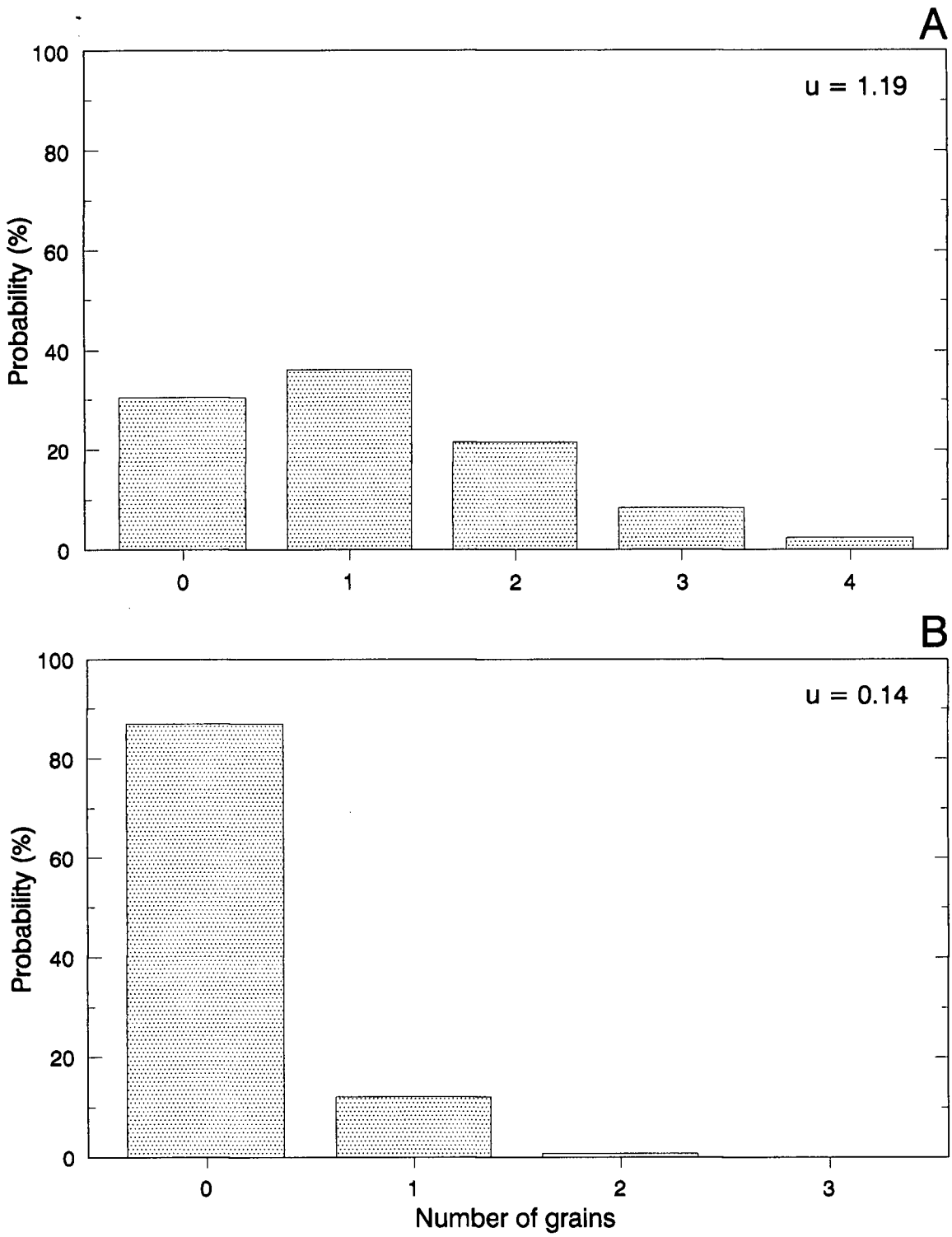

Fig. 1-3. Poisson probabilities of detecting gold particles a) expected number of gold particles (μ) = 1.19, b) expected number of gold particles in 30 g analytical sample (μ) = 0.14.

86.94% (Fig. 1-3b). However, if a single particle of gold happens to be present in the sample ($P_{(1)}$ = 12.17%) then the analysis would be 1400 ppb, 7 times the true concentration of 200 ppb. This result has led to the term "nugget effect" to describe erratically high Au values resulting from the presence of a single or very few gold particles in a small sample (Ingamells, 1981).

Variation in the particle size and sample size used for analysis will have a dramatic effect on the result obtained. Assume that the stream sediment comprises five equally proportioned size fractions (200, 150, 100, 75 and 50 microns), and each contains 100 ppb Au as free spherical particles. A 1000 gram field sample provides 200 grams of each fraction for analysis. Representative 10 and 30 gram subsamples split from each size fraction are analyzed for Au by FA-AAS. Using equation 1-2, the probabilities of these samples (200, 30, and 10 gram) containing no gold particles ($P_{(0)}$, n = 0) are shown in Figure 1-4. Results are strongly dependent on grain size and sample size. The scarcity of gold particles in coarse sediment fractions leads to a high probability of Au not being detected, whereas in the fine size fractions there is a greater chance of detecting Au.

Clifton et al (1969) pointed out that, based on the binomial distribution, an adequate sample size providing an acceptable precision (relative errors of +54 and -34% (±44% on average), at the 95% confidence level) should contain at least 20 particles of gold. The relations between particle

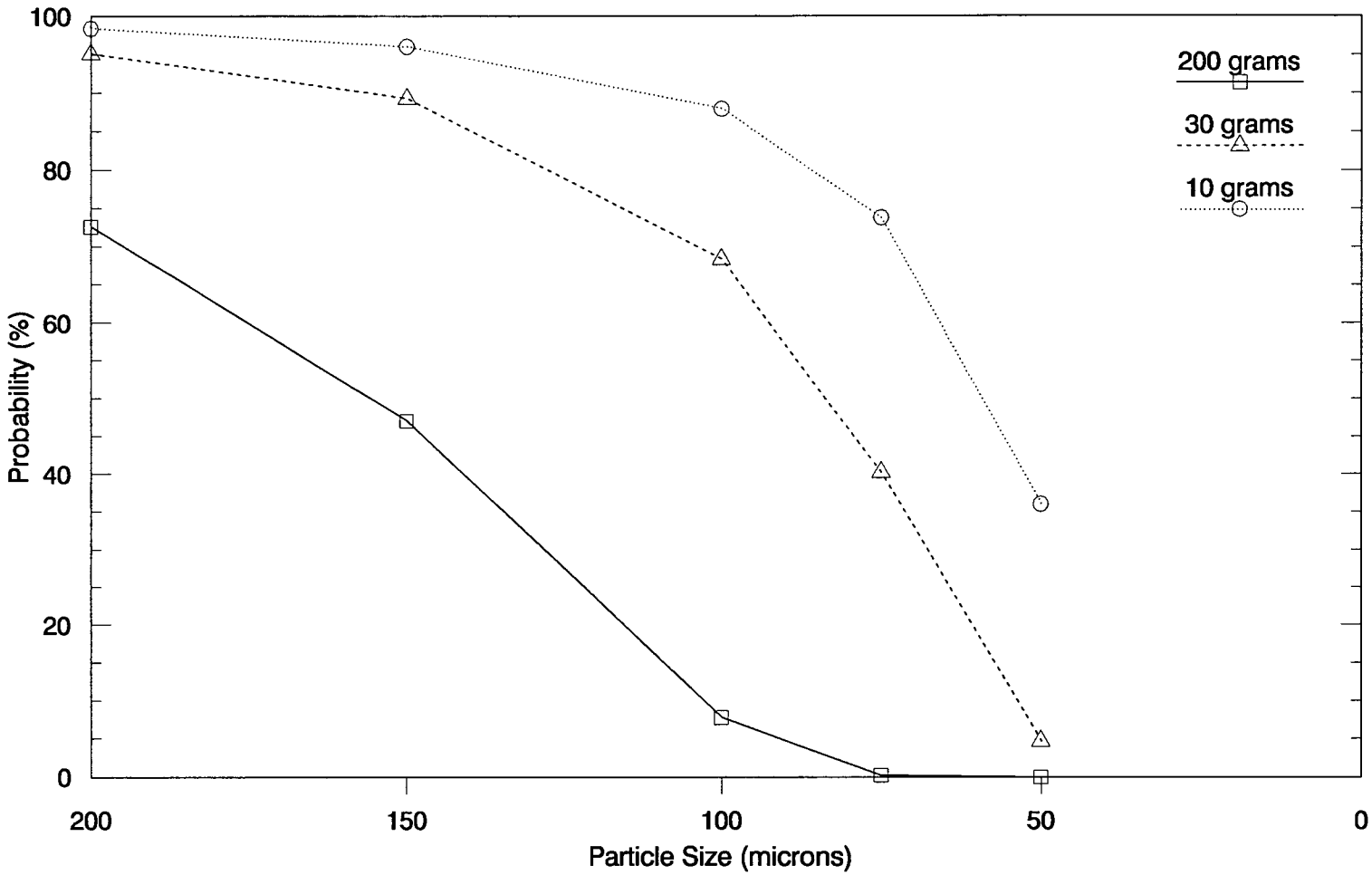

Fig. 1-4. Poisson probability of detecting no gold particle as a function of grain size and sample weight.

size, particle shape and the minimum sample size required to contain 20 gold particles are presented in Figure. 1-5.

1.2.5 Field studies of heavy minerals in streams

Recently, several studies of the behaviour of heavy minerals and free gold particles in gravel-bed streams have been carried out, for example, gold in British Columbia, tungsten in Yukon Territory, Canada, and cassiterite in a mountain stream in Malaysia. The purpose of these studies was to solve the problems of extremely erratic and irreproducible results of stream sediment surveys for rare heavy mineral grains.

Fletcher et al (1987) used analysis of variance (ANOVA) to evaluate reduction of among-site/within-site variance of Sn concentrations in the same size fraction at low and high energy sites and between size fractions, in a Malaysian mountain stream. They found that local hydraulic conditions control the accumulation of cassiterite, and that there is no relation between the magnitude of an anomaly and proximity to its source.

Saxby and Fletcher (1986b) used the geometric mean concentration ratios (GMCR) to estimate local hydraulic effects on heavy minerals (W, in this case) in a Yukon Territory stream. The GMCR is based on analysis of the same size fraction of paired sediment samples from high- and low-energy environments:

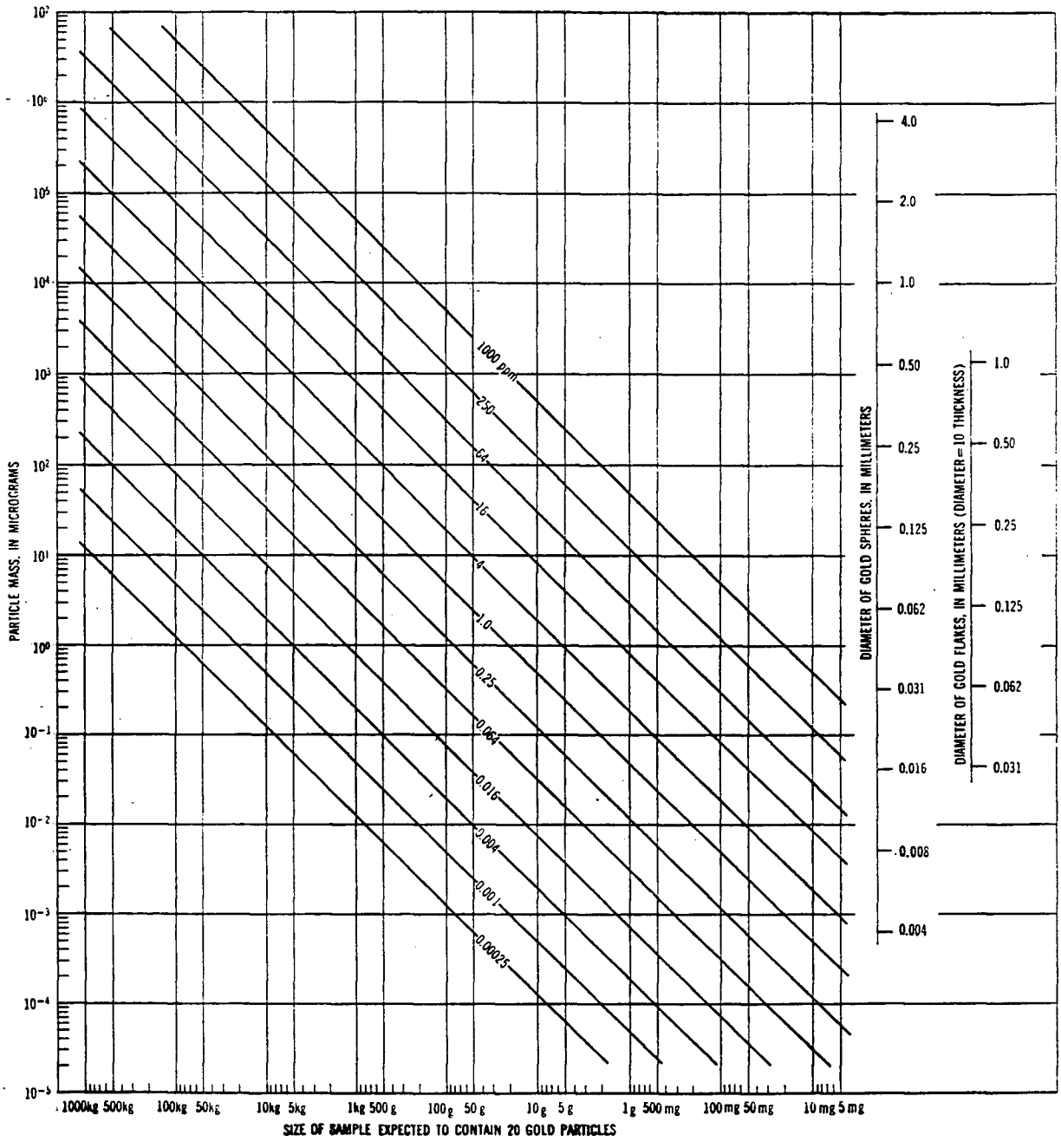

Fig. 1-5. Relations between particle size and the size of sample required to contain twenty gold particles (after Clifton et al, 1969).

$$GMCR = \text{antilog}\ \{(\text{Sum}_{1}^{n}\ \log_{10}CR)/n\} \qquad (1\text{-}4)$$

$$CR = C_{he}/C_{le}$$

where CR = concentration ratio,

C_{he} = concentration of a mineral for high energy site,

C_{le} = concentration of a mineral for low energy site,

n = the number of pairs.

They also found that, like cassiterite (Fletcher et al, 1987), hydraulic effects are dependent on grain size and density, and are reduced in fine sediment fractions. Although local hydraulic variability can be minimized by use of the fine size fractions, it at the same time can remain an important source of noise in drainage geochemical surveys if very large sediment samples are processed to obtain representative heavy mineral concentrates.

In the Harris Creek, south central British Columbia, Day (1988) and Day and Fletcher (1986) estimated numbers of gold particles and then used the Poisson distribution (equation 1-2) to determine an adequately representative field sample size. They found that, because of the scarcity of gold particles it was necessary to field screen 60 kg of -2 mm sediment from up to 250 kg of bulk sediment. Day (1988), Day and Fletcher (1989) and Fletcher and Day (1988b) also used GMCR to evaluate downstream dispersion trends for gold in stream sediment and the influence of hydraulic effects on heavy-mineral concentrations. They found that local hydraulic processes resulted in downstream erratic

geochemical dispersion patterns of gold between associated high- and low-energy environments, but variations were reduced for fine grained (e.g. < 0.053 mm) fractions. Further investigations, Day and Fletcher (in press) and Fletcher (1990) have shown that gold in the Harris Creek is preferentially accumulated at high bed roughness sites and as the stream gradient decreases downstream. These results are consistent with field observations (Day and Fletcher, 1989; Fletcher and Day, 1988b) and with bedload transport models (Slingerland, 1984; Slingerland and Smith, 1986).

Based on the above it is apparent that 1) large sediment is required for a representative sample for gold and 2) the dispersion of gold in stream sediment depends mainly on local hydraulic processes and channel physical characteristics. This study will investigate the behaviour of gold in a fluvial environment different from that of the Harris Creek, British Columbia.

CHAPTER TWO

DESCRIPTION OF STUDY AREA

2.1 Location and access

The Huai Hin Laep catchment is in the Na Duang district (map scale 1:50,000, series L 7017, sheets 5444 III and 5443 IV), about 50 kilometres east of Loei (Fig. 2-1). The study area is accessible by an all-season hard-surface road from Loei.

2.2 Basin morphology and topography

The catchment of the Huai Hin Laep (Fig. 2-2) is asymmetrically shaped with an area of approximately 8 square kilometres. Topographically, the catchment is undulating low relief lying on a plateau that becomes increasingly dissected from northwest to southeast at elevations of approximately 400 to 320 metres above mean sea level.

The Huai Hin Laep is a third order (as represented on the map scale of 1:50,000) intermittent tributary of the Huai Kho Lo. The stream is approximately 6.5 kilometres long (measured from the topographic map) with an average gradient of approximately 0.01. However, from field measurements, the stream is about 8.8 kilometres long. Because the valley is not well-developed, it is assumed that valley length equals stream length from the topographic map and that channel length equals the field measurement (8.8 km). Sinuosity can therefore be estimated. By definition, sinuosity is the ratio of channel length to valley length (Chorley et al,

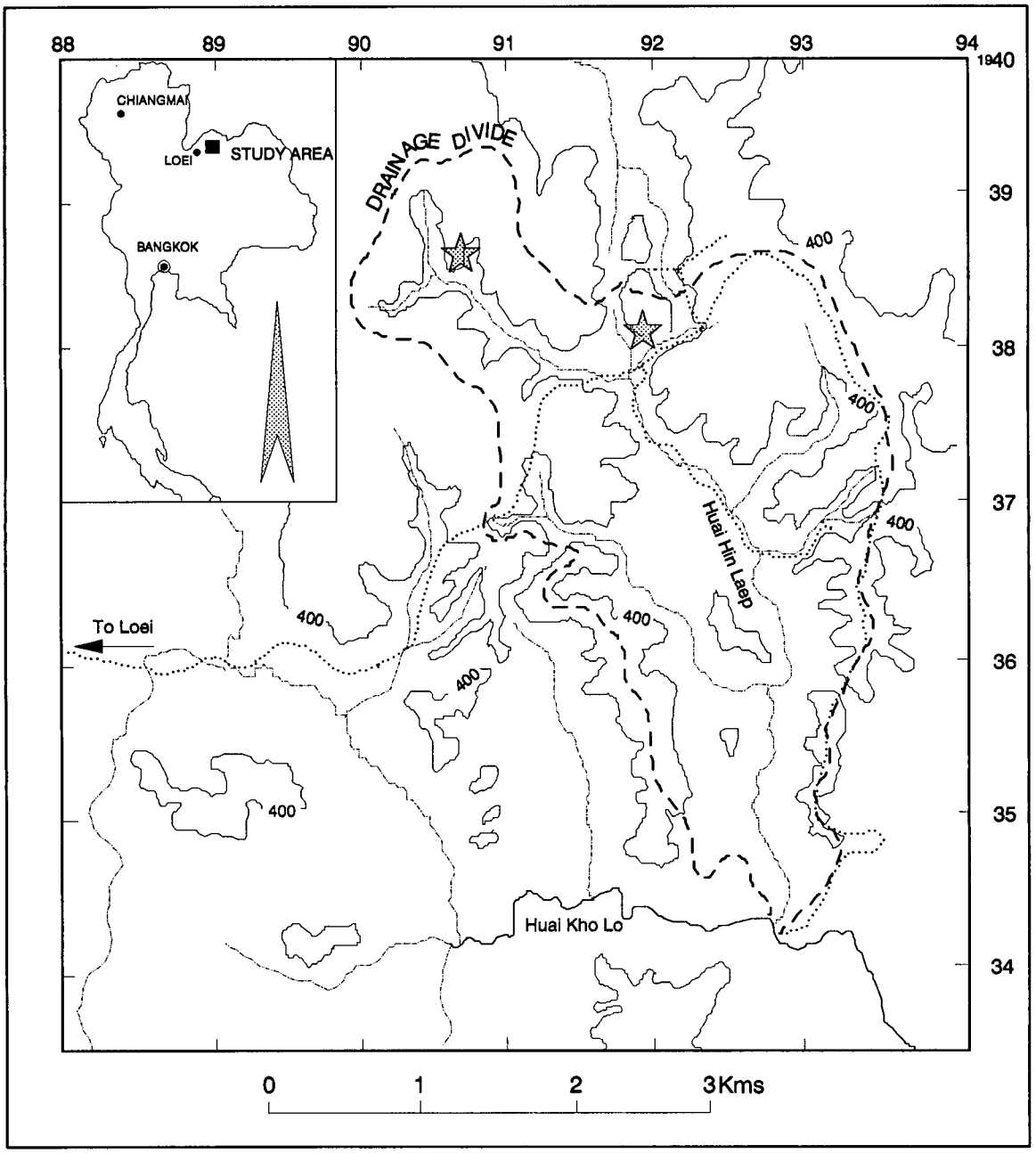

Fig. 2-1. Location and topography of the drainage basin of the Huai Hin Laep study reach (contour lines are at 400 m ASL, dotted lines are hard surface roads; dashed line is catchment boundary; shaded stars are supposed bedrock sources of gold mineralization; shaded arrow indicates north direction).

Fig. 2-2. Topography of the Huai Hin Laep drainage basin.

1984 and Schumm, 1985). Stream meanders are constrained by adjacent hill slopes, so the channel is considered to be straight with sinuosity = 1.35, where the dividing point between straight and meandering channels is 1.5 (Selby, 1985).

Pavement riffles (Fig. 2-3a), pools and point bars (Fig. 2-3b) are typical channel forms. On average, pavements consist primarily of gravel and coarse sand with about 10% silt and clay. They are formed at the topographic high area of the stream channel located between a pair of point bars. Pools and point bars are paired, with the pools on the outer part of stream bends. Point bars, on the inside of channel bends, also consist mainly of gravel but contain more silt and clay (~ 17%) than pavement.

2.3 Stream longitudinal profile

The Huai Hin Laep study reach, between an elevation of about 380 m and 315 m above mean sea level, is 7,763 metres long with the average gradient of 0.008 (Fig. 2-4). Gradient decreases from 0.013 at the stream headwater to 0.003 at the confluence with the main stream, the Huai Kho Lo. There were no major rainfalls during the sampling period and stream discharge remained nearly constant. Stream width at water level ranged from about 0.5 m at riffles to 6.5 m at pools, with depths ranging from about 0.5 to 0.9 m, respectively. Flow velocity varied from stagnant to about 1 m/second.

A

B

Fig. 2-3. Principal bedforms of the Huai Hin Laep, a) sandy gravel pavement and b) sandy gravel point bar.

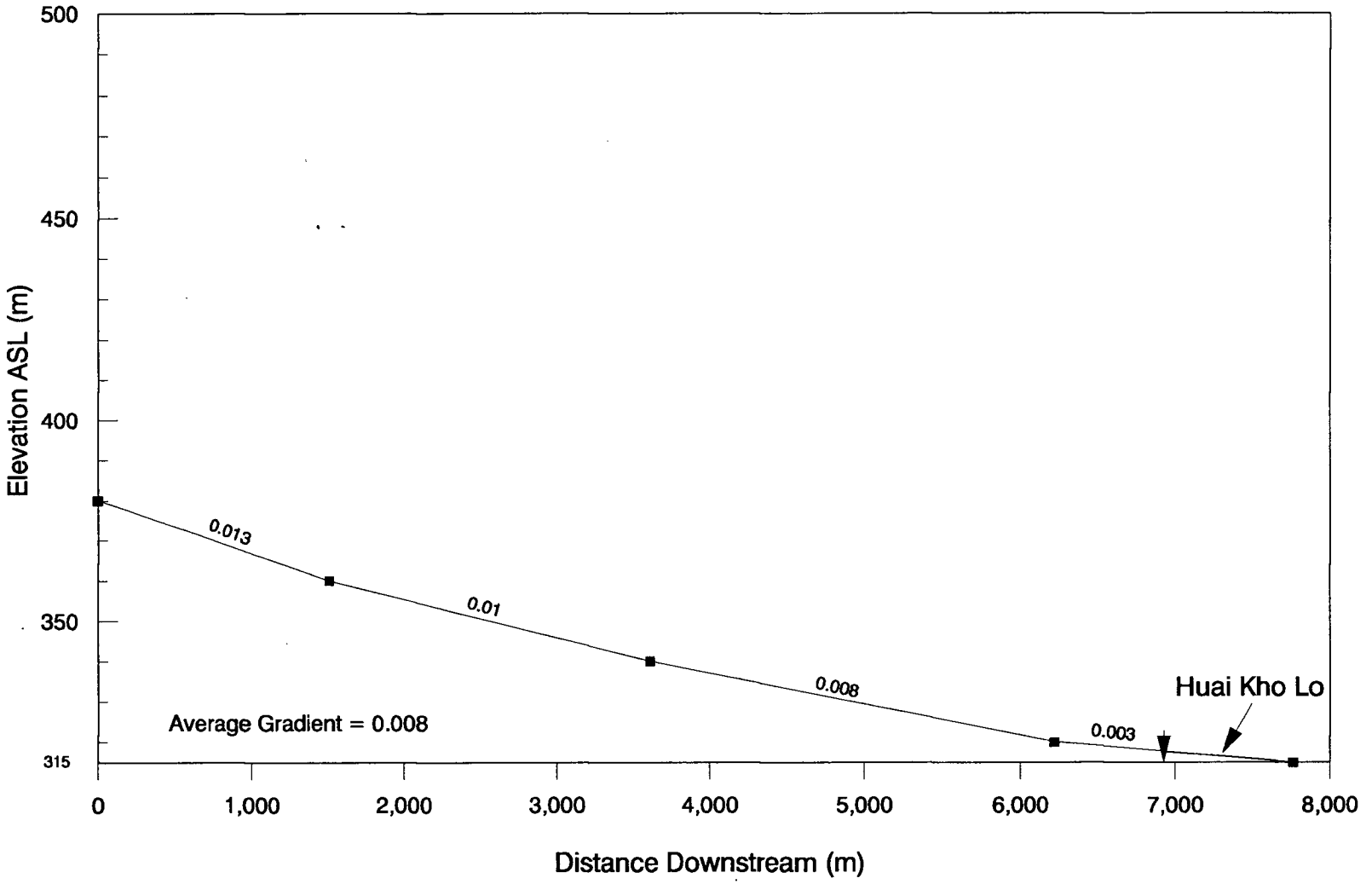

Fig. 2-4. Stream long profile, showing average gradient between 380 and 315 m above mean sea level. The whole section is 7,763 m long. Arrow indicates confluence with the Huai Kho Lo.

2.4 Geology

Geology of Loei region (Appendix) has been studied by Charoenpravat et al (1976). The area is underlain by Silurian-Devonian (SD) to Lower Permian (P_1) sedimentary rocks and Permo-Triassic (PTR) igneous rocks. Detailed geology of the study area is shown in Fig. 2-5.

The Silurian-Devonian (SD) unit consists of shales, phyllitic shales interbedded with sandy shales, actinolite schist, phyllite, hornfelsic rocks, meta-tuff and sandstones. Quartz veins occur in fractures. The Devonian unit (D) consists of shales interbedded with grey thin bedded chert, limestone and volcanic tuffs. The Carboniferous unit (C_1) comprises grey shales, well-bedded sandstones, conglomeratic sandstone, conglomerate and grey limestone. These three rock units are overlain by thickly bedded to massive Permian limestone (P_1). Volcanic rocks (PTR-v) are mainly rhyolite porphyries, rhyolitic tuffs and andesites.

All rock units have undergone low grade metamorphism, are tightly folded, and are intruded by numerous stocks and dykes of hornblende granodiorite, hornblende diorite and pyroxenite which is partly altered to serpentinite.

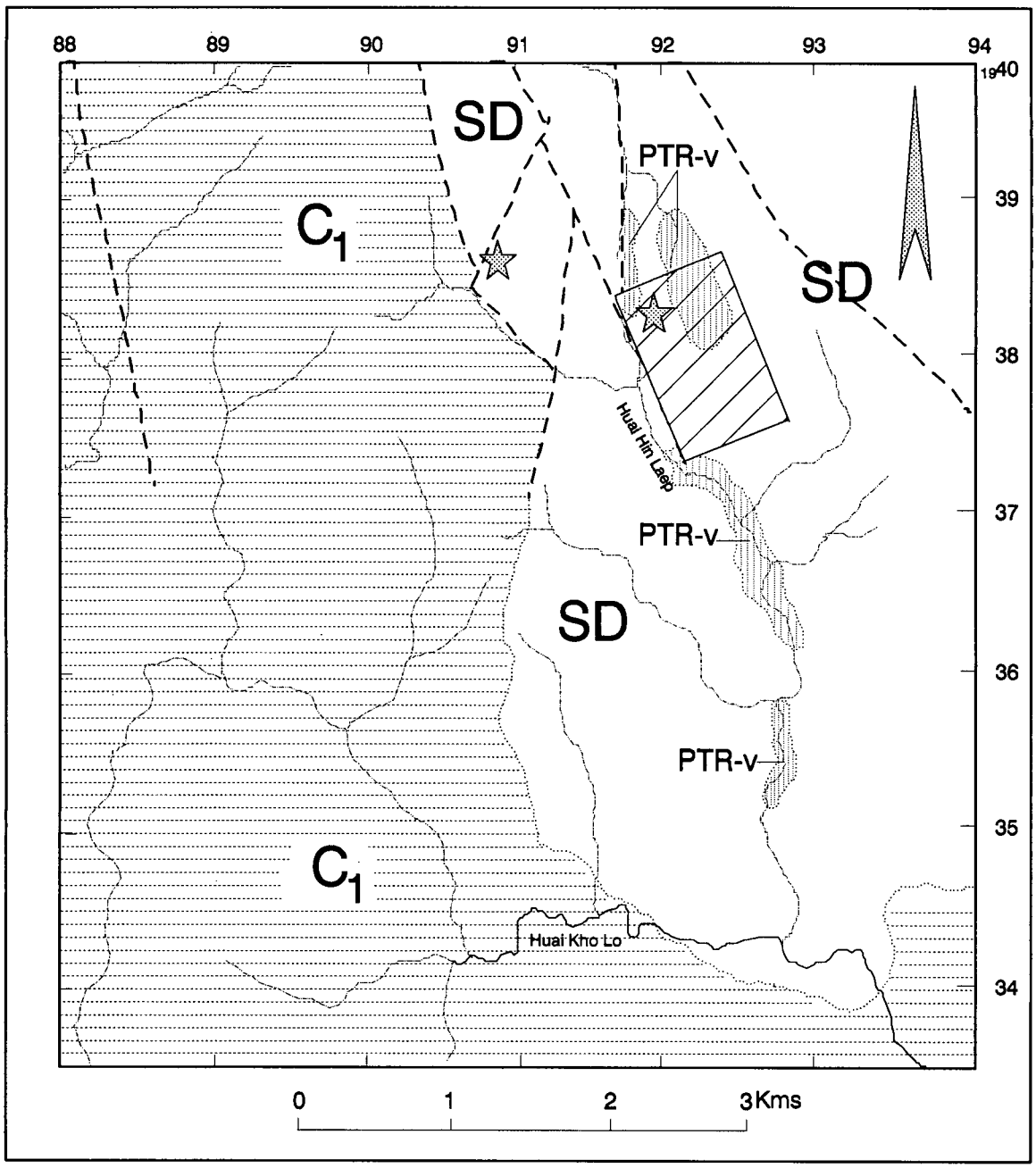

Fig. 2-5. Detailed geology of the Huai Hin Laep drainage basin (SD = Silurian-Devonian; C_1 = Carboniferous; PTR-v = Permo-triassic volcanic rocks; shaded stars are supposed bedrock sources of gold mineralization; labeled rectangular indicates DMR grid soil sampling area).

2.5 Source of gold in the Huai Hin Laep

Although visible gold is common in pan concentrates from the Huai Hin Laep, its exact bedrock source is not known. Analysis of B horizon soils collected from the supposed source of gold mineralization (Fig. 2-5) failed to detect a gold anomaly (Yensabai and Jamnongthai, 1990). However, based on several gold-quartz vein occurrences related to porphyry and skarn deposits in the Loei region (Fig. 1-1) [e.g. Phu Tham Phra (Kumanchan, pers. comm., 1989; Nuchanong, 1988; Tate, 1988), Phu Lon (Vudhichatvanich et al, 1980; Tate, 1988), Phu Khum Thong, Phu Khum I and Phu Khum II (Kumanchan, pers. comm., 1989)], the gold is thought (Yensabai, pers. comm., 1989) to be associated with quartz vein float found in two areas near the headwaters of the Huai Hin Laep.

2.6 Climate, soils, vegetation and land use

The Loei region has a monsoonal climate with a long rainy season from May to October, winter season from November to February, and summer season from March to April. Average annual rainfall is approximately 1100 mm, and average annual temperature about 28^{o}C.

Soils are residual laterites and podzols derived from highly weathered parent materials (Soil Survey Division, 1975). The effect of weathering has been recorded to a depth

of 20 to 90 m at Phu Tham Phra 40 km west of the study area (Pholphan and Siriratanamongkol, 1967).

Four soil pits in the study area show that soil is developed to a depth of 80 cm at hill tops, increasing to 2 meters at the base of the slope. Soils are yellowish to reddish brown and consist mainly of silt and clay with less than 20% sand and coarser particles (Fig. 2-6). At hill top sites, soil profiles (Fig. 2-7) are poorly developed and contain numerous quartz and parent rock fragments. At the base of the slope, however, these fragments are absent (Fig. 2-8). The soil profile has been modified by cultivation to a depth of about 30 cm.

Vegetation in this region was originally a mixed evergreen forest (Smith et al, 1968). However, because of a rapid increase of population in the past two decades, the forest has been logged and cleared (Fig. 2-9) for agriculture. Ridges and hill tops are now occupied by open bamboo forest whereas hill slopes and low lands are converted to corn and cotton fields. Parts of the area include abandoned farmlands now occupied by second generation brush and shrubs.

Logging and then ploughing and tilling for agriculture have increased rates of soil erosion (Lekhakul, 1990). Although the amount of soil erosion in the study area is not known, Pookcharoen and Ruaisoongnoen (1986) have reported that in Chaiyaphum province, about 120 km south of Loei, soil losses were 0.86 and 0.56 tonnes/ha/year in a 5-year

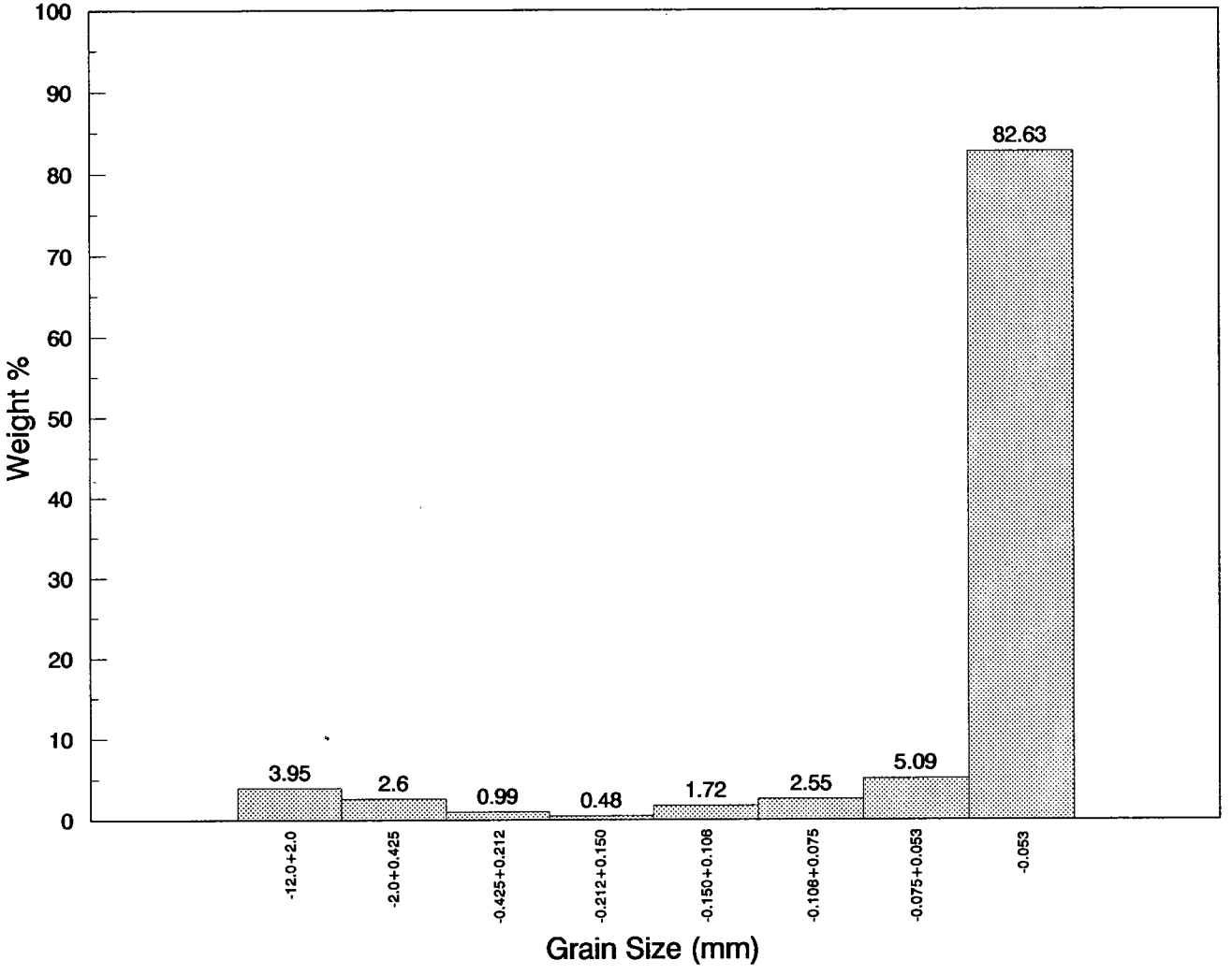

Fig. 2-6. Grain size distribution of the C horizon soil.

A_p

yellow brown
(7.5 YR 5/6)
silty clay loam
cultivated

BC

brown
(5 YR 4/8)
clayey silt loam
rock fragments

C

reddish brown
(2.5 YR 4/6)
silty clay
rock fragments

Fig. 2-7. Soil pit at the hill tops showing A, BC and C horizons.

A_p

grey brown
(10 YR 3/2)
clayey silt loam
cultivated

B

yellow brown
(10 YR 5/8)
sticky
clayey silt loam

BC

yellow brown
(10 YR 6/4)
very sticky
clayey silt loam
few rock
fragments

C

yellow brown
(10 YR 5/6)
sticky
clayey silt loam

Fig. 2-8. Soil pit at the base of slope showing A_p, B, BC and C horizons.

Fig. 2-9. Land use on the Huai Hin Laep drainage basin showing forest logged and cleared for agriculture.

Acacia auriculaeformis and *Leucaena leucocephala* plantation, respectively. In Kalasin province, about 200 km east of Loei, soil loss in corn field was up to 4.6 tonnes/ha/year (Lekhakul, 1990). Similar situations occur in the Huai Hin Laep basin, where erosion of large amounts of silt and clay into the stream appears to result from the practice of ploughing lateritic soils to plant corn just before the onset of the rainy season.

CHAPTER THREE

METHODOLOGY

3.1 Field sampling

Field sampling was undertaken in July-August 1989 during the rainy season. Fortunately, this was a short, relatively dry period that improved accessibility and made sampling easier. Where possible, bulk samples of point bar and pavement sediments were obtained. In most locations, however, only a sample of either point bar or pavement was available. A total of 101 stream sediment samples were collected from 43 locations (Fig. 3-1). Pan-concentrate samples were also collected at each site.

Stream sediment samples were collected by shovelling (with as little water as possible) sediment on to a 12 mm wire screen above a 40 liter plastic tub (60 cm diameter). The plastic tub was placed on a strong plastic tarpaulin to prevent the loss of coarse materials (>12 mm) while sieving. At each sampling site, approximately 65 to 100 kilograms of sediment was processed to yield approximately 40 kg of material finer than 12 mm. This was then transferred to strong plastic bags and weighed. The weight of material larger than 12 mm was also recorded prior to it being discarded. In addition pan-concentrates were obtained at every site by taking four shovel-fulls of sediment into a standard cone-shaped wooden bowl and panning. Heavy minerals retained in the wooden bowl were examined for visible gold grains, which were counted using a hand-lens, and then stored in a small plastic bag.

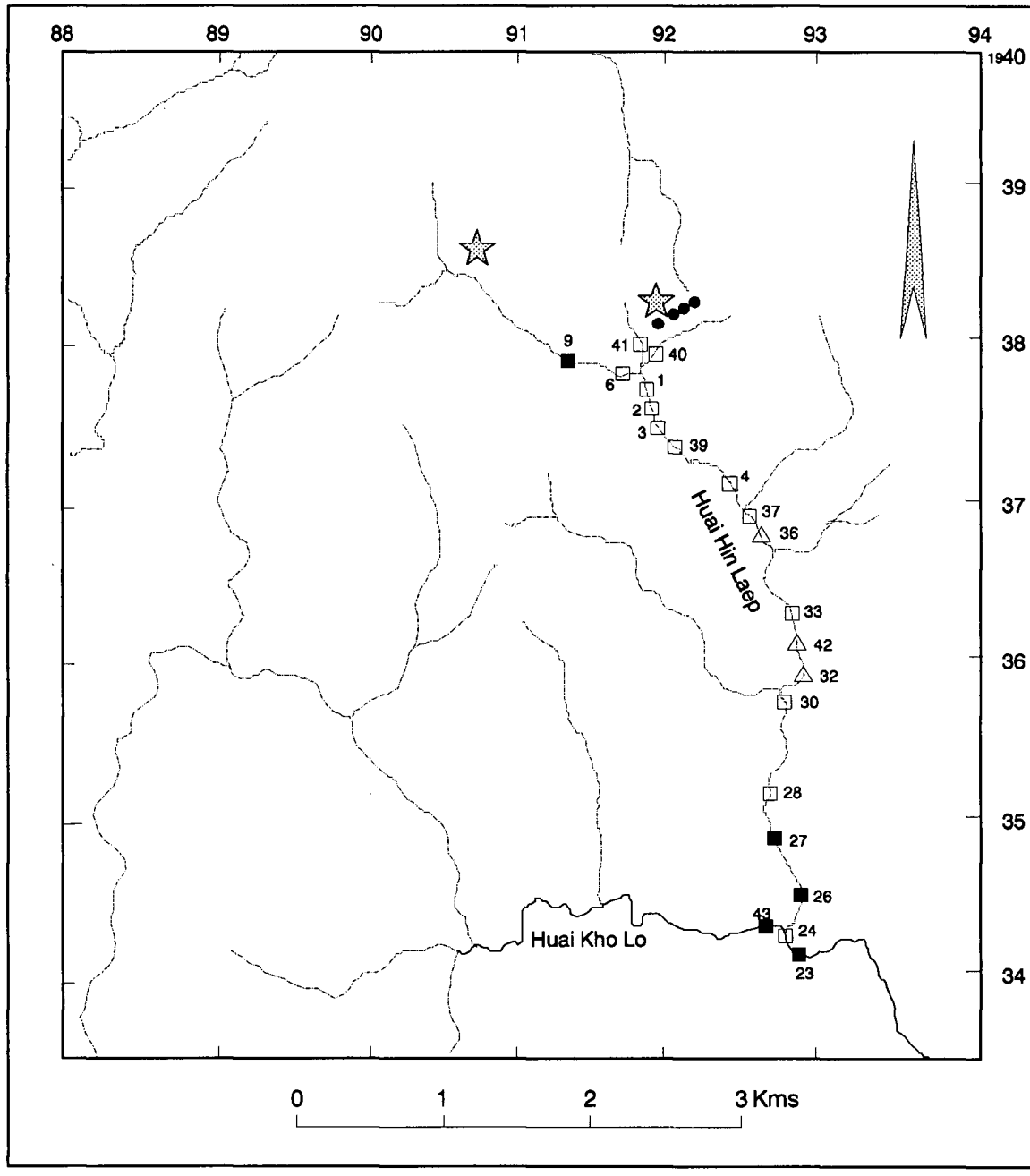

Fig. 3-1. Sample locations on the Huai Hin Laep (open squares = point bars; open triangles = pavements; solid squares = point bar and pavement; solid circles = soil pits; shaded stars = supposed bedrock sources of gold mineralization; shaded arrow indicates north direction).

A plan sketch was drawn at each location to show approximate dimensions and shapes of channel features (point bar and pavement), local bed sediment texture, sample location and flow direction. Stream width was measured across the water surface and stream depth by vertically placing a scale to the streambed and reading the value at water level. Stream flow velocity was determined by timing the movement of a float over a given distance. Other field data such as water colour, bank vegetation and erosion, and log-jams were also recorded and the bed photographed.

A total of 22 soil samples, including 4 pan-concentrates from each C horizon, were also collected from four soil pits along a northeast traverse line of an earlier geochemical survey by the DMR (Fig. 3-1). The soil profile was subdivided into the horizons presented in section 2.6. Each horizon was then sampled systematically from the bottom up in order to avoid possible contamination from overlying horizons.

3.2 Sample preparation

3.2.1 Stream sediments

Laboratory preparation procedures for stream sediment samples are illustrated schematically in Fig. 3-2. They were prepared in two phases with slightly different processes being used in each.

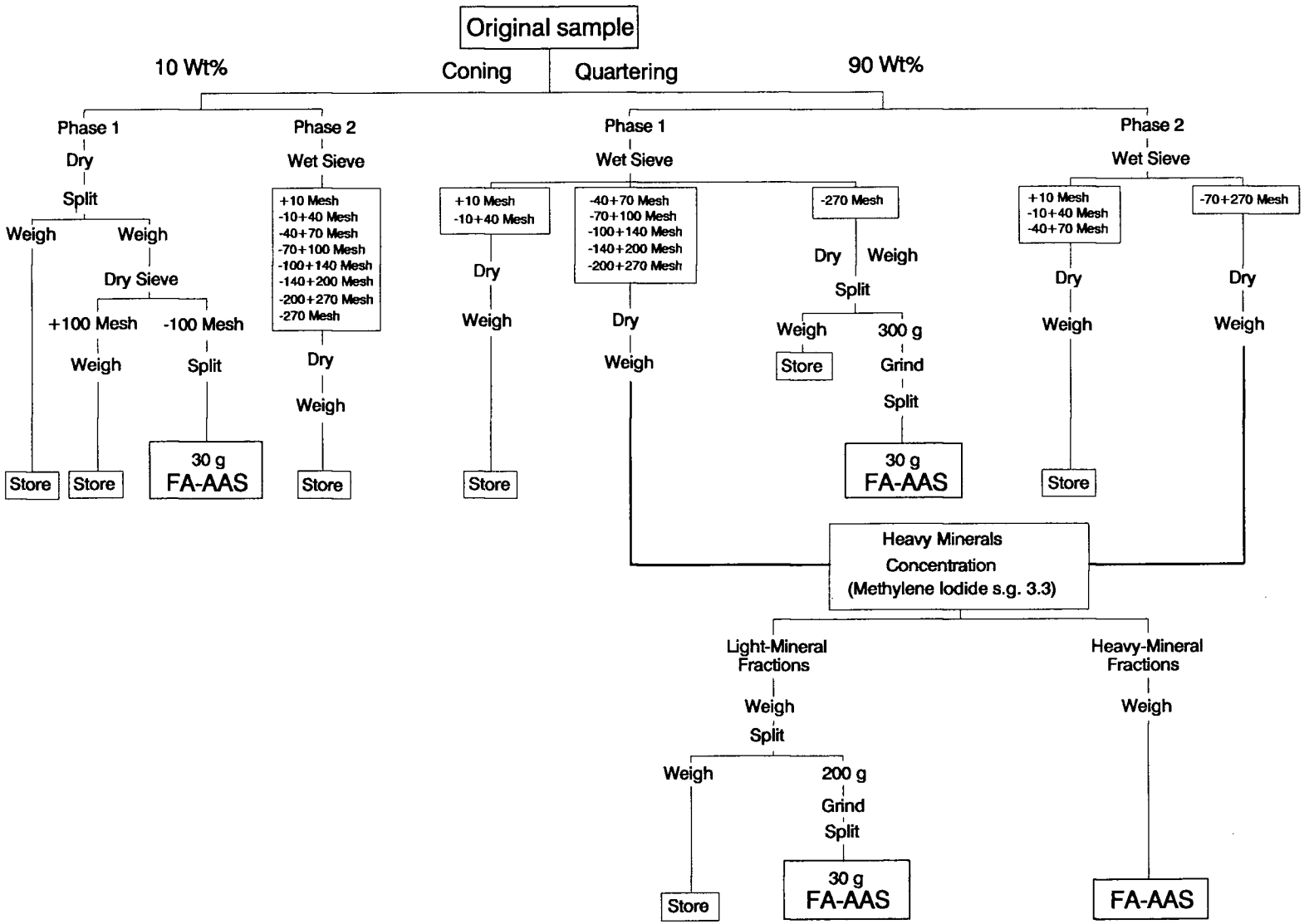

Fig. 3-2. Flow sheet for sample preparation and analysis.

In the first phase, sixteen sediment samples from 14 locations were selected for wet sieving. The entire wet sediment sample was weighed and homogenized, by coning and quartering on a strong plastic tarpaulin, to obtain two portions of different sizes.

The smaller portion, amounting to about ten percent of the entire wet weight (i.e. about 4 kg), was oven-dried at 80°C, disaggregated and weighed. It was then further split, with one half being manually dry-sieved through a 0.150 mm screen and the other half stored. Sediment coarser than 0.150 mm was weighed and stored, and that finer than 0.150 mm split to obtain approximately 30 grams for gold analysis.

The larger portion was processed by wet sieving using a recirculating water system, which Day (1988) showed to be much more effective than dry sieving for removing fines from coarser fractions. Eight size fractions were obtained: +2.0, -2.0+0.425, -0.425+0.212, -0.212+0.150, -0.150+0.106, -0.106+0.075, -0.075+0.053, and -0.053 mm. The seven size fractions coarser than 0.053 mm were dried at 80°C and weighed. Settling of the -0.053 mm fraction was accelerated by addition of a few milliliters of dilute organic flocculating agent (Catfloc, Calgon Laboratories). After a few days, the clear water was pumped off and discarded. Sediment was then washed into several shallow glass trays, dried at 80°C and weighed. The whole process of wet sieving was, however, very time consuming, with 4 days typically being required to process a single sample.

Heavy mineral concentrates were separated from the five size fractions between 0.425 and 0.053 mm using methylene iodide (specific gravity 3.3). All fractions were allowed to dry and were then weighed. No further preparation was required for the -0.425+0.212 mm heavy mineral fraction prior to determination of Au. However, because of their small sizes, the -0.212+0.150 and -0.150+0.106 mm, and the -0.106+0.075 and -0.075+0.053 mm heavy mineral fractions were combined prior to analysis.

Light mineral fractions greater than 200 grams were split to obtain approximately 200 grams which were then pulverized in a hardened steel ring mill. A 30 gram subsample of the pulverized material was taken with a Jones riffle splitter for analysis. Minus 0.053 mm samples were disaggregated using a metal roller and split using a Jones riffle splitter to obtain approximately 250 to 300 grams samples. These were then pulverized in the ring mill and further split to obtain 30 gram subsamples for analysis. Any remaining material was stored for future use.

A medium sand-sized (-0.425+0.212 mm) heavy mineral concentrate from a selected sample was visually examined under a binocular microscope. The sample was then split several times (using a microsplitter) to obtain a very small portion which was mounted on a polished grain-mount using a method developed by J. Knight and Y. Douma at the University of British Columbia. The mount was polished and carbon-coated for scanning electron microscope examination.

In the second phase, after obtaining Au results of the first phase, eleven stream sediment samples from 7 locations were selected and processed using a slightly different procedure. The smaller portion was wet-sieved to obtain eight size fractions for textural analysis. The larger portion was also wet-sieved to obtain four size fractions: +2.0, -2.0+0.425, -0.425+0.212 and -0.212+0.053 mm. A heavy mineral concentrate (S.G. > 3.3) was then prepared for the -0.212+0.053 mm fraction. The -0.053 mm fraction was discarded.

3.2.2 Pan concentrates

Visible particles of free gold were separated from five field pan concentrates and counted under a binocular microscope. The particles were then placed on SEM stubs coated with nail polish and immersed in acetone vapour for a few seconds allowing the particles to settle into the polish (J. Knight, pers. comm., 1990). Stubs were then carbon coated prior to SEM examination. Subsequently, gold particles were removed from the stubs, using acetone, and mounted for cross-section polishing. The polished samples were carbon-coated prior to analysis.

3.3 Analysis

3.3.1 Analysis of sediments and heavy minerals for gold

A total of 217 sediment samples were analyzed for Au by fire assay-atomic absorption spectrophotometry at Chemex Laboratories, North Vancouver, British Columbia. The detection limits for gold in heavy mineral concentrates depend on the weight of the heavies, whereas the detection limit for gold in light mineral and sediment fractions is 5 ppb with a 30 g analytical subsample.

Duplicate samples, randomly selected from approximately 10% of all samples (Fletcher, 1981) from light mineral and sediment fractions, were analyzed together with five gold standard samples as a quality control program. Results of duplicate analyses are listed in Tables 3-1 and 3-2. All but six samples are at or below the detection limit ($\leq$5 ppb). Thus, the midpoint value (2.5 ppb) is taken for those below the detection limit for further statistical evaluation.

A scatterplot of primary and recommended Au values versus duplicate and gold standard analyses is shown in Fig. 3-3. The 21 pairs of < 5 ppb gold of duplicate samples were discarded, and Au values from 6 pairs of duplicate and 5 from gold standards samples were normalized by making the log transformation prior to regression analysis. The square of the correlation coefficient (r^2) is 0.896 (n = 11,

Table 3-1. Duplicate analyses for gold concentrations (ppb) in light and -0.053 mm sediment fractions. The reported detection limit is 5 ppb.

Sample		Analysis	
Number	Fraction	First	Second
89-PP-16	-0.150 mm	<5	5
89-PP-96	-0.150 mm	<5	10
89-PP-94	-0.150 mm	<5	5
89-PP-67	-0.150 mm	<5	<5
89-PP-68	-0.150 mm	<5	<5
89-PP-16	-0.425+0.212 mm	<5	<5
89-PP-81	-0.425+0.212 mm	<5	<5
89-PP-87	-0.425+0.212 mm	<5	<5
89-PP-65	-0.425+0.212 mm	<5	<5
89-PP-96	-0.212+0.150 mm	5	15
89-PP-75	-0.212+0.150 mm	<5	<5
89-PP-100	-0.212+0.150 mm	<5	<5
89-PP-68	-0.212+0.150 mm	<5	<5
89-PP-09	-0.150+0.106 mm	<5	<5
89-PP-70	-0.150+0.106 mm	<5	<5
89-PP-65	-0.150+0.106 mm	35	100
89-PP-94	-0.106+0.075 mm	<5	<5
89-PP-67	-0.106+0.075 mm	5	<5
89-PP-68	-0.106+0.075 mm	<5	<5
89-PP-96	-0.075+0.053 mm	<5	<5
89-PP-10	-0.075+0.053 mm	<5	<5
89-PP-89	-0.075+0.053 mm	<5	<5
89-PP-64	-0.075+0.053 mm	<5	<5
89-PP-16	-0.053 mm	<5	<5
89-PP-79	-0.053 mm	<5	<5
89-PP-22	-0.212+0.053 mm	<5	<5
89-PP-55	-0.212+0.053 mm	<5	<5

Table 3-2. Analyses of gold standard samples.

Sample Number	Values	
	Recommended	Analysis
STSD-3 # 54[1]	6.8	<5
MA-2[2]	1860	1810
GTS-1[2]	346	360
STSD-1 # 433[1]	8	15
GTS-1[2]	346	305

[1] recommended values based on Lynch (1990)

[2] recommended values based on Steger (1986)

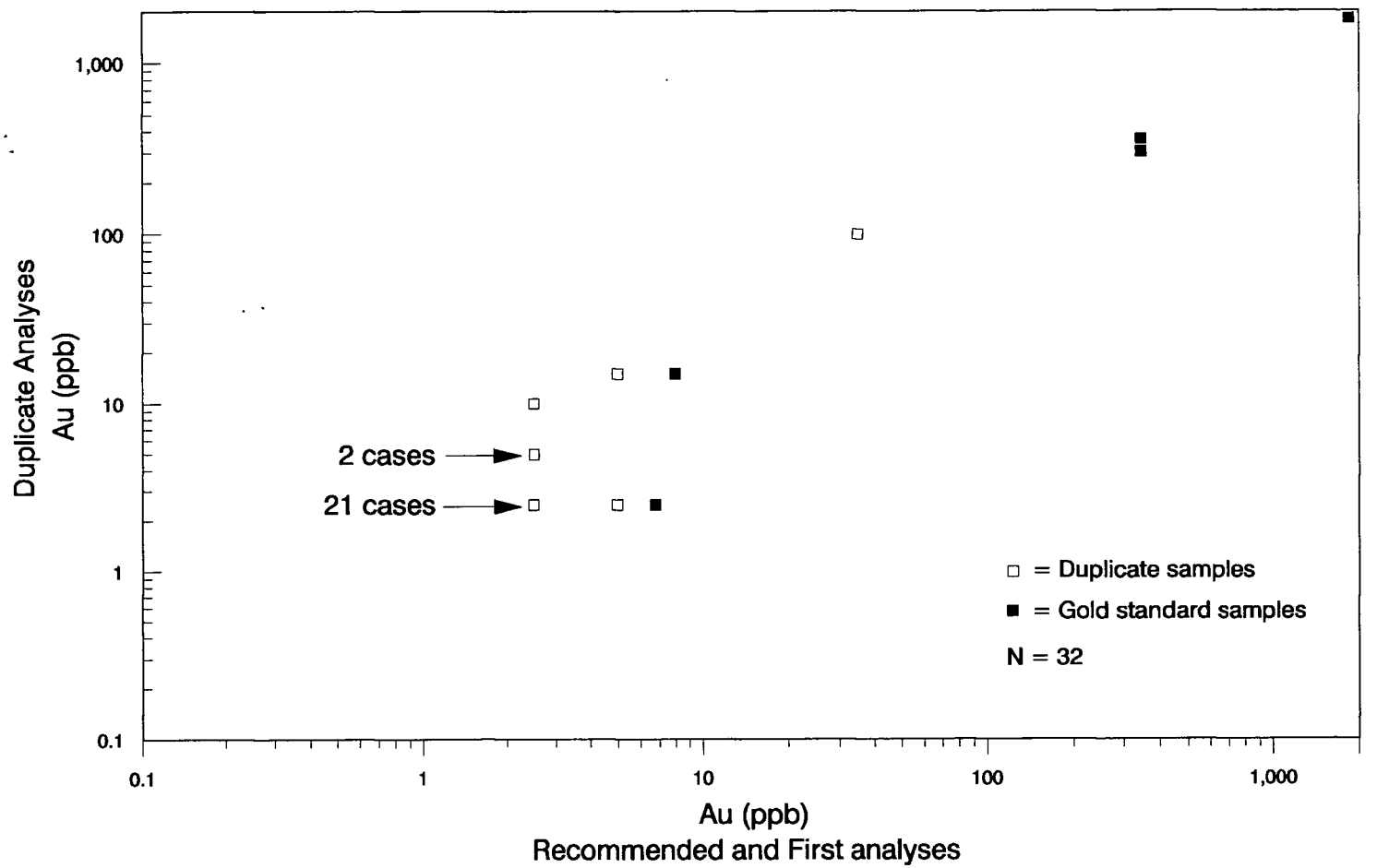

Fig. 3-3. Scatterplot for duplicate Au analysis of the light mineral fraction, -0.053 mm sediment fraction and versus recommended value for gold standard samples.

standard error of estimation = 0.349) indicating that Au values obtained from the duplicate and gold standard analyses are close to the primary and recommended values.

Gold analysis results are therefore considered to be sufficiently precise and accurate for the purpose of this study.

3.3.2 Examination of heavy mineral concentrates and gold particles

Selected heavy mineral concentrates were examined under the binocular microscope to obtain grain morphology. Polished sections of the grains were then examined using a SEMCO NANOLAB 7 scanning electron microscope (SEM) operating at 15 kV, equipped with a Kevec Unispec System 7000 energy dispersive system, to identify heavy mineral compositions.

Mounted gold particles were also examined under the SEM. Each gold grain was photographed with backscatter secondary electron imaging to obtain grain morphology. Two axial dimensions (a and b axes) of each particle were estimated from the SEM photographs. The third (c) axis was estimated under a reflected light microscope.

Polished sections of gold particles were quantitatively analyzed for Au, Ag, Cu and Hg using an SX-50 Cameca electron microprobe and operating conditions modified from Knight and McTaggart (1986). Current was 100 nA on aluminium

with an accelerating potential of 20 kV. Counting time for background was 10 seconds on each side of the peaks and 30 seconds on the peaks. Data were reduced using the phi-rho-xi data reduction method (J. Knight, pers. comm., 1990). Detection limits for Au and Ag were 0.05% (Knight and McTaggart, 1986), Cu 0.025% and Hg 0.65% (Knight, pers. comm., 1990). Where possible, each particle was analyzed 3 times - once in the core and twice at opposite parts of the outer edge.

CHAPTER FOUR

STREAM CHARACTERISTICS AND SEDIMENT PROPERTIES OF THE HUAI HIN LAEP

4.1 Introduction

As reviewed in Chapter 1, studies in the Harris Creek, British Columbia, have shown that accumulations of gold in streams are related to physical characteristics of the stream and stream sediments at both bar and reach scales (Day and Fletcher, 1986, 1989, in press; Fletcher, 1990; Fletcher and Day, 1988b; Fletcher and Wolcott, 1989, in press). The purpose of the present study was to determine if the same, or similar, factors controlled distribution of gold in the Huai Hin Laep, a typical stream in northeastern Thailand. Specifically, it was intended to evaluate

1) gold concentrations in different size and density fractions to determine criteria for a representative field sample for gold,
2) accumulation of gold in different environments, and
3) dispersion and distribution of gold along the Huai Hin Laep.

With respect to 2) and 3), relations between gold concentrations and properties of either the stream channel (i.e. stream width, channel depth and flow velocity) or sediments (i.e. mean grain size, sediment sorting, bed roughness and abundance of sediment) are of both theoretical interest and practical significance for design and interpretation of stream sediment surveys for gold. The first part of this chapter therefore describes and tests stream characteristics and sediment properties for any

systematic relations that might influence distribution of gold. Distribution of heavy minerals is also described with respect to stream and sediment properties.

In order to avoid i) bias from the single gold-rich anomalous sample near the supposed source of gold, and ii) the effects of contamination of sediment draining from tributaries at the stream headwater and dilution by sediment from the Huai Kho Lo, relations between stream characteristics and sediment properties are primarily examined in that part of the reach between the supposed source of gold and the confluence with the Huai Kho Lo (1,055 to 6,223 m). However, relations along the entire reach are also presented for purposes of comparison and to indicate possible outcomes of routine geochemical surveys.

Where statistical tests, such as Wald-wolfowitz total-number-of-runs test (Bradley, 1968), Spearman rank correlation coefficient and two-sample t test[1] (Snedecor and Cochran, 1989), are used the 90% ($P_{0.10}$) confidence level is used to evaluate the outcome. This rather low level of significance is used on an exploratory basis to ensure that meaningful relations between parameters will not be overlooked.

---

[1] two-sample t test is used to test the difference between the means of two independent samples when the two population variances are not equal.

4.2 Stream characteristics

There was no rainfall during the sampling period and stream discharge appeared to remain constant. Stream geometry data (i.e. width at water surface, channel depth, and flow velocity) for point-bar sites are plotted with respect to distance downstream in Fig. 4-1. Although stream width (Fig. 4-1a) and channel depth (Fig. 4-1b) vary quite erratically, stream width seems to systematically decrease between 2,500 and 5,500 m while flow velocity (Fig. 4-1c) increases. Based on the Wald-wolfowitz total-number-of-runs test (Table 4-1), these variations are not significant. However, along the entire reach there are too few segments (runs) for variation in stream width and flow velocity, relative to median cut-off values, to be entirely random.

4.3 Sediment properties

4.3.1 Sediment size distributions in point-bar and pavement

Dry weights of eight size fractions obtained from wet sieving of sediments in the laboratory are used to study sediment size distribution. Sediment sizes larger than 12 mm are excluded in order to avoid bias from rejection of large cobbles (i.e. larger than about 30 cm) during field sampling.

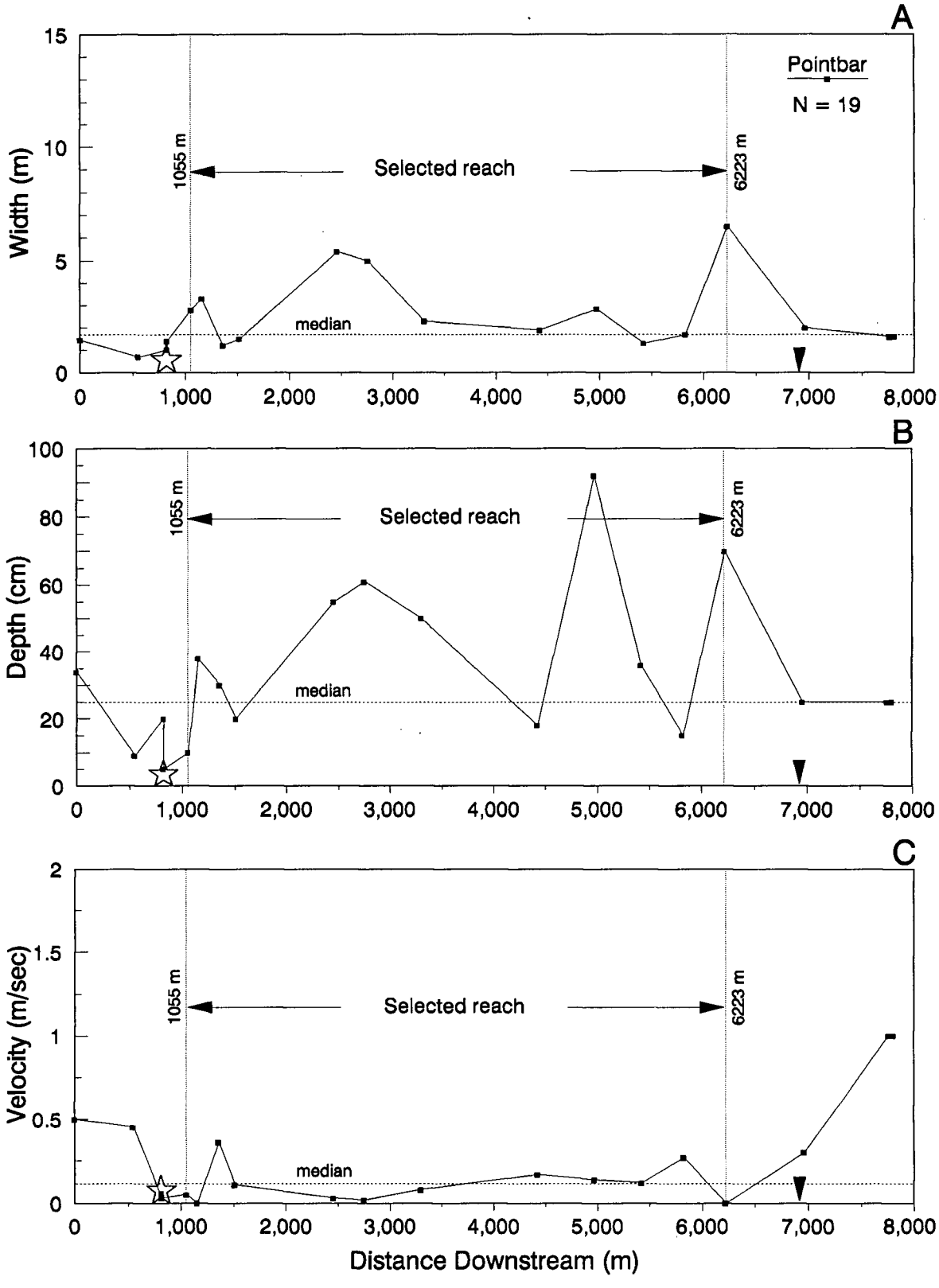

Fig. 4-1. Downstream trends of a) stream width, b) stream depth and c) flow velocity at point-bar sites.

Table 4-1. Results of the Wald-wolfowitz total-number-of-runs test (μ) for trends of stream characteristics at point-bar sites along the entire reach and between supposed source of gold and the confluence with the Huai Kho Lo (1,055 and 6,223 m).

Fraction/ Source of Variation	Cut point (median)	N n_1 (+)	N n_2 (-)	μ	$P(\mu)$
Whole reach					
Point bar (N = 19)					
Width	1.70	10	9	7	0.0500*
Depth	0.25	12	7	9	0.3339
Velocity	0.12	10	9	7	0.0500*
Between supposed source of gold mineralization and the confluence with the Huai Kho Lo (1,055 and 6,223 m)					
Point bar (N = 12)					
Width	2.55	6	6	7	0.5000
Depth	0.37	6	6	8	0.2724
Velocity	0.10	6	6	5	0.1129

N = total number of samples
n_1 = number of samples above median
n_2 = number of samples below median
μ = total number of runs above and below the median

* = statistically significant at 95% confidence level

Grain size distributions, using mean values for point-bar (n = 19) and pavement (n = 7) samples, are plotted on histograms (Fig. 4-2) and semi-logarithmic graph paper (Fig. 4-3). The histogram of point-bar sediments (Fig. 4-2a) shows a strongly bimodal distribution consisting mainly of gravel and coarse-sand (~ 80%), and silt and clay (~ 17%). Medium and fine-sand sizes are scarce (~ 3%). The central tendencies of grain size distribution are arithmetic mean (M) = 3.65 mm, median (D_{50}) = 1.80 mm. Sorting (S_0) is calculated from

$$S_0 = (Q_3/Q_1)^{1/2} \qquad (4\text{-}1)$$

where Q_3 is the third quartile (that diameter which has 75% of the distribution smaller and 25% larger than itself), and Q_1 is the first quartile (that diameter which has 25% of the distribution smaller and 75% larger than itself). It has a value of 2.89 indicating normally sorted sediment (Trask in Krumbein and Pettijohn, 1938). It should be noted that values of the median (D_{50}) and sorting (S_0), obtained from the cumulative curve (Fig. 4-3), are slightly different from those obtained from statistical estimation (listed in Table 4-2).

Pavement sediments also have a strongly bimodal size distribution (Figs. 4-2b, and 4-3) and again consist mainly of gravel and coarse-sand (~ 89%) and silt-clay (~ 9%) with only minor amounts (~ 2%) of medium and fine sand. Distribution parameters of pavement sediments are mean (M) = 4.70 mm, median (D_{50}) = 3.20 mm and sorting (S_0) = 2.52

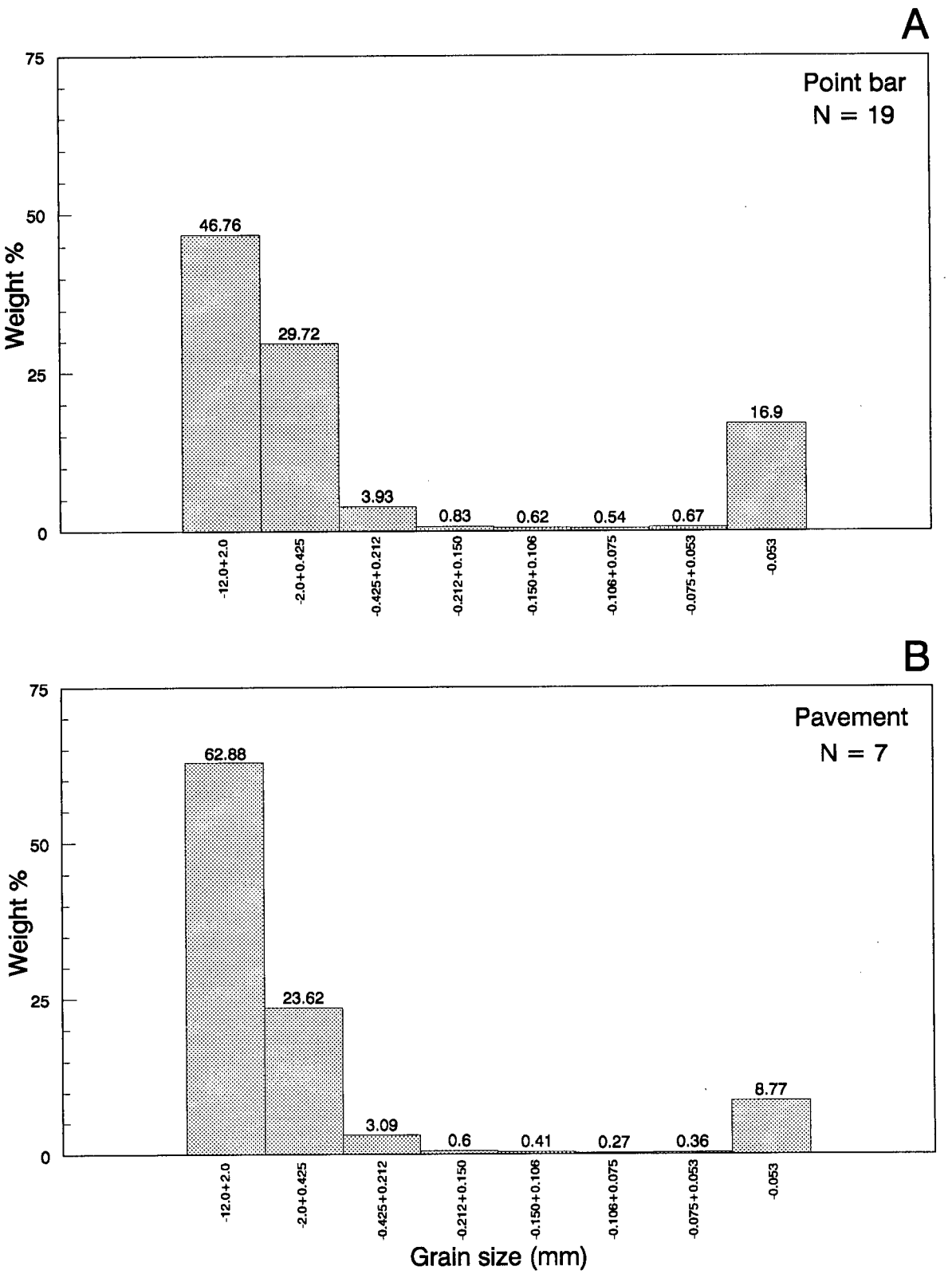

Fig. 4-2. Mean weight percents of sediment size distribution in a) point bar (n = 19) and b) pavement (n = 7).

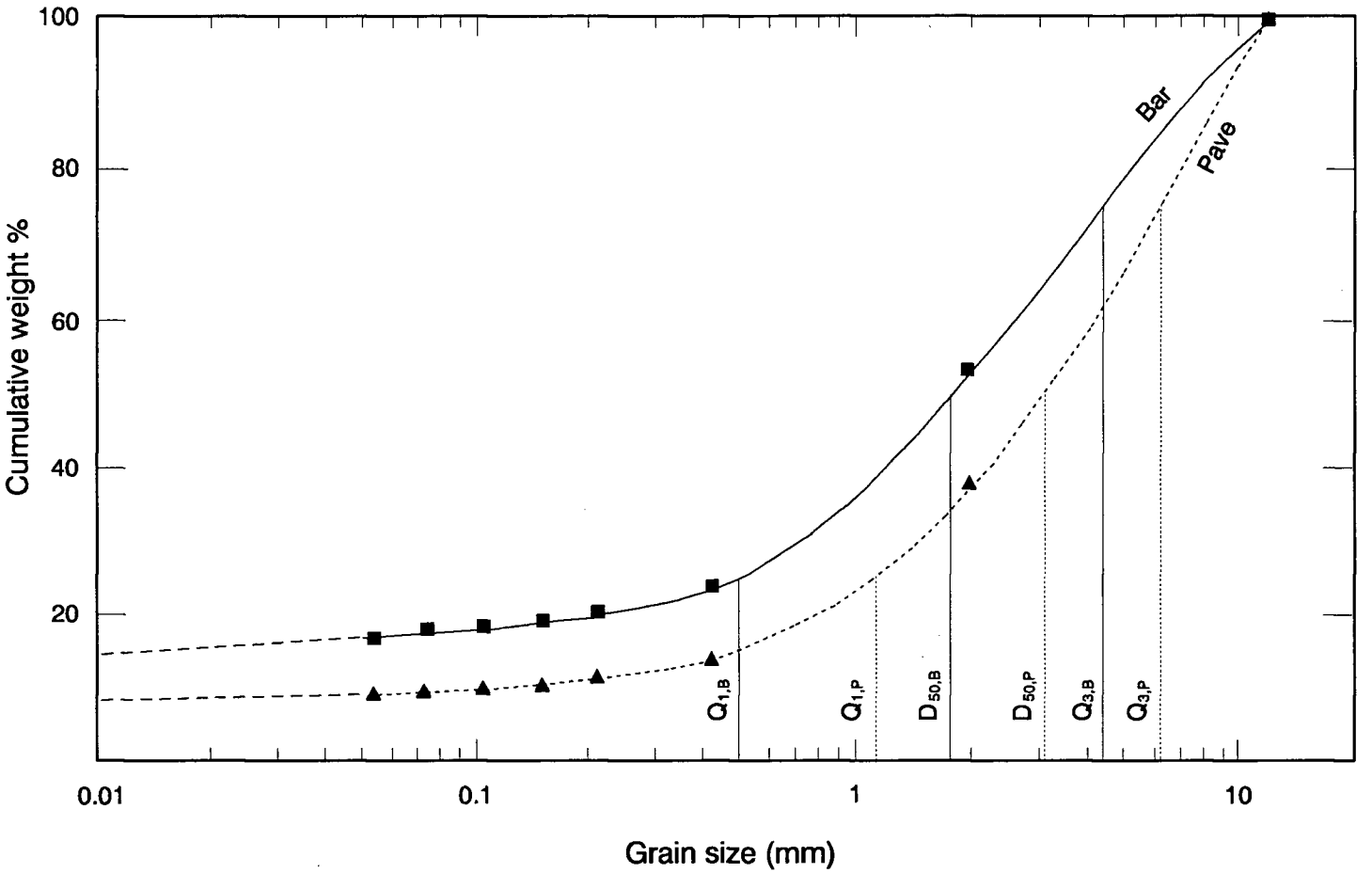

Fig. 4-3. Cumulative curves for sediment size distributions using mean weight percent for point-bar (solid square) and pavement (solid triangle) showing determination points for Q_1 - first quartile, Q_3 - third quartile and D_{50} - median.

Table 4-2. Summary of mean grain size (M_0), median (D_{50}), sediment sorting (S_0) and bed roughness (D_{65}) of the entire sediment at point-bar and pavement sites.

Sample	Mean (mm) (M_0)	Median (mm) (D_{50})	Sorting (S_0)	D_{65} (mm)
Point-bar (n = 19)				
PP-22	4.46	2.60	2.11	4
PP-16	4.67	2.80	1.93	4
PP-96	1.58	0.11	8.37	1
PP-98	1.45	0.14	8.37	5
PP-09	3.88	2.00	2.48	3
PP-08	3.99	2.10	2.47	3
PP-06	3.46	1.70	2.63	2.5
PP-94	2.89	1.30	12.45	15
PP-10	4.72	3.00	2.28	2
PP-89	2.87	1.25	1.81	5
PP-81	4.38	2.50	2.29	20
PP-75	4.40	2.50	2.13	15
PP-73	3.11	1.60	1.82	10
PP-70	4.08	2.40	3.16	70
PP-67	4.68	3.50	2.99	15
PP-64	4.36	2.60	2.40	10
PP-59	3.15	1.30	2.48	5
PP-55	3.15	1.30	2.85	35
PP-56	4.11	2.30	2.73	35
Mean	3.65	1.95	3.57	13.66
Std	0.98	0.90	2.88	17.02
Pavement (n = 7)				
PP-23	4.52	2.70	2.19	10
PP-87	5.58	4.30	1.79	30
PP-100	5.07	3.60	2.00	15
PP-79	4.74	3.00	2.10	15
PP-68	3.92	2.15	3.16	30
PP-65	4.42	2.80	2.37	50
PP-58	4.66	3.00	2.25	50
Mean	4.70	3.08	2.27	28.57
Std	0.52	0.69	0.44	16.51

indicating well sorted sediments.

Summaries of the arithmetic mean (M), median (D_{50}), sorting (S_0) and bed roughness (D_{65}) are given in Table 4-2. (Bed roughness (D_{65}) is estimated from photograph taken at each site before sample collection and therefore includes the sediment fraction larger than 12 mm).

Because the distribution of sediments from both point-bar and pavement sites is bimodal, probability plots (Fig. 4-4), using the method of Sinclair (1976), have been used to identify the two component populations. Results show, for example, that for point-bar sediment 89-PP-94 two populations can be distinguished by an inflection point of the curve at about 0.07 mm (68%). Similarly, for pavement sediment 89-PP-100 the cut point is at about 0.07 mm (93%). The central tendencies of the coarse grained component of point-bar sediments are mean (M_C) = 2.66 mm and sorting (S_C) = 2.16, indicating well sorted sediment. Distribution parameters of coarse grained pavement sediments are mean (M_C) = 3.80 mm and sorting (S_C) = 2.38, also indicating well sorted sediment. Summary statistics for coarse grained sediment characteristics from point-bar and pavement sites are listed in Table 4-3. It is self-evident that sorting (S_C) of the coarse grained sediment, particularly at point-bar sites, is better than sorting (S_0) of the entire sediment.

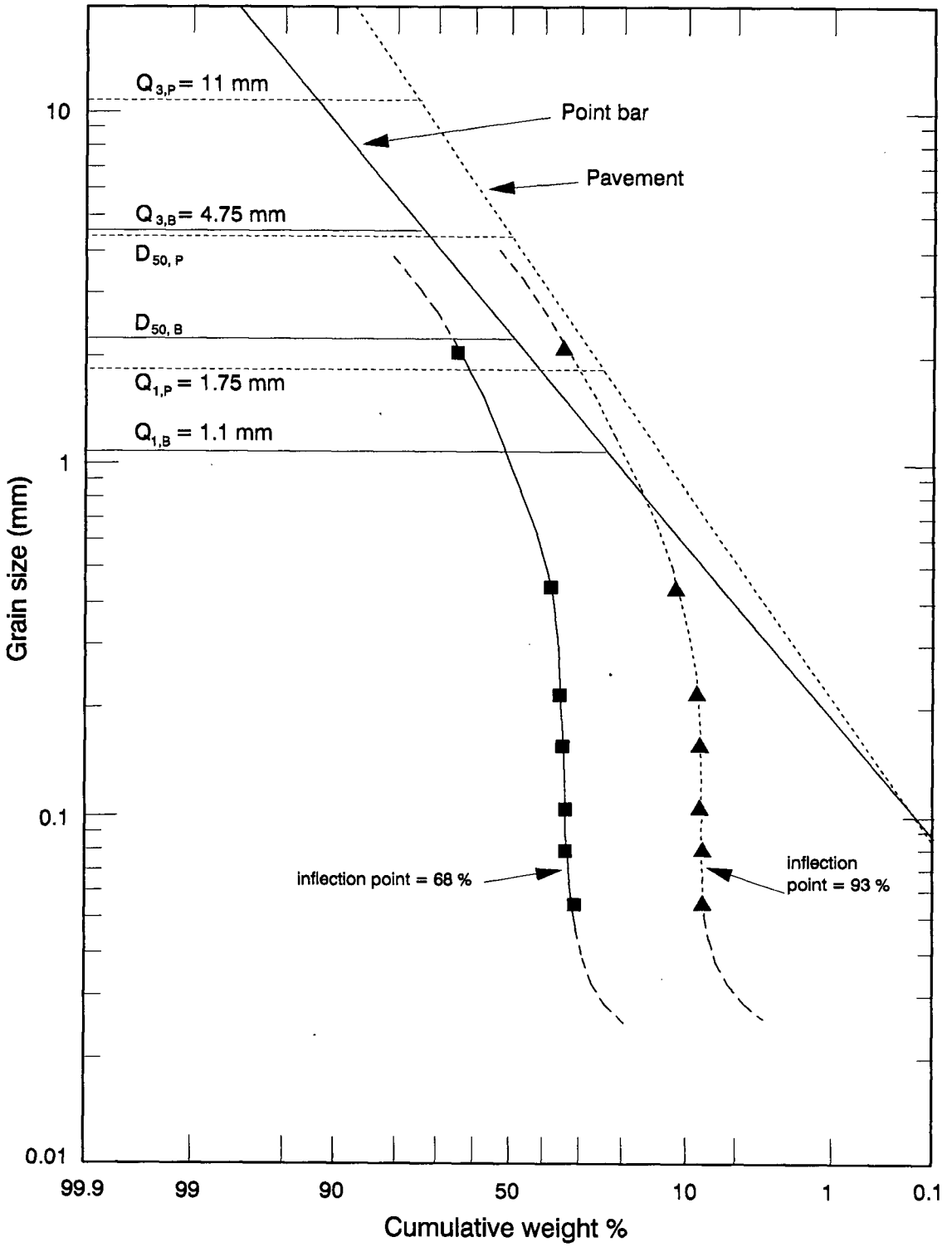

Fig. 4-4. Probability plots for sediment size distributions of 89-PP-94 (point bar, solid square) and of 89-PP-100 (pavement, solid triangle). The straight lines are partitioned log-normally distributed coarse-grained populations (cf. Sinclair, 1976).

Table 4-3. Summary characteristics of coarse grained component of sediment from point-bar and pavement sites.

Sample	Proportion (%)	Mean (mm) (M_C)	Sorting (S_C)
Point-bar (n = 19)			
PP-22	91	3.00	2.03
PP-16	93	2.80	1.65
PP-96	50	1.25	2.38
PP-98	50	1.25	1.98
PP-09	84	2.50	1.91
PP-08	83	2.90	2.22
PP-06	79	2.25	1.85
PP-94	68	2.30	2.08
PP-10	91	3.65	2.24
PP-89	74	1.75	1.99
PP-81	87	3.20	2.16
PP-75	90	2.90	2.03
PP-73	90	1.60	1.70
PP-70	85	3.20	2.65
PP-67	85	6.70	3.32
PP-64	88	3.30	2.10
PP-59	92	1.50	2.14
PP-55	87	1.70	2.15
PP-56	91	2.80	2.49
Mean	82.11	2.66	2.16
Std	12.84	1.23	0.37
Pavement (n = 7)			
PP-23	90	3.50	2.44
PP-87	95	5.20	2.10
PP-100	93	4.50	2.44
PP-79	93	3.40	2.19
PP-68	84	2.90	2.66
PP-65	90	3.40	2.49
PP-58	91	3.70	2.35
Mean	90.86	3.80	2.38
Std	3.53	0.78	0.19

Coarse grained component of sediment is separated at the inflection point (Fig. 4-4) for an individual sample, for example, 89-PP-94 at 0.07 mm and 89-PP-100 at 0.07 mm.

4.3.2 Comparison between textures of sediments at point-bar and pavement

Comparisons of sediment texture between point-bar and pavement are carried out using a two-sample t test (at the 90% ($P_{0.10}$) confidence level) to examine the differences between mean grain size (M_0), sediment sorting (S_0), mean grain size (M_C) and sorting (S_C) of coarse grained component, bed roughness (D_{65}) and abundance of sediment fraction. These parameters are evaluated in the part of the reach between 2,753 and 6,223 m because of: 1) the absence of pavement sites in the upper part of the reach, and 2) possible statistical bias resulting from inclusion of sediment at sites downstream of the confluence with the Huai Kho Lo. Results (Table 4-4) show that only the weight percents of gravel and silt-clay differ significantly, with gravel being more abundant in pavement and silt-clay (-0.053 mm) in point-bar sediments.

4.3.3 Downstream trends of sediment texture at point-bar and pavement sites

Downstream trends in mean grain size (M_0), sediment sorting (S_0) and bed roughness (D_{65}) from point-bar and pavement sites are shown in Fig. 4-5. The corresponding parameters, mean grain size (M_C) and sorting (S_C)) for the coarse grained component are shown in Fig. 4-6. In the

Table 4-4. Statistical two-sample t test for the difference between means of sediment characteristics from point-bar and pavement sites in the reach between 2,753 and 6,223 m.

Null hypothesis:
μ Wt% sediment in point-bar = μ Wt% sediment in pavement

Fraction/ Source of Variation	N	Mean	S	S_e	Degrees of Freedom
Mean grain size (M_0)					
Point-bar	7	3.9829	0.7035		
Pavement	5	4.7460	0.6303		
				0.3954	9
T_{Calc} = -1.79	$T_{(9, 0.10)}$ = 1.833	Null hypothesis accepted			
Sorting (S_0)					
Point-bar	7	2.3714	0.5306		
Pavement	5	2.2840	0.5323		
				0.3111	9
T_{Calc} = 0.28	$T_{(9, 0.10)}$ = 1.833	Null hypothesis accepted			
Mean (M_C)					
Point-bar	7	3.2357	1.6834		
Pavement	5	3.8800	0.9418		
				0.8394	10
T_{Calc} = -0.84	$T_{(10, 0.10)}$ = 1.812	Null hypothesis accepted			
Sorting (S_C)					
Point-bar	7	2.2786	0.5398		
Pavement	5	2.3760	0.2283		
				0.2590	9
T_{Calc} = -0.42	$T_{(9, 0.10)}$ = 1.833	Null hypothesis accepted			
Bed roughness (D_{65})					
Point-bar	7	20.7143	22.2539		
Pavement	5	28.0000	14.4049		
				11.4164	10
T_{Calc} = -0.69	$T_{(10, 0.10)}$ = 1.812	Null hypothesis accepted			

Table 4-4. (continued).

Fraction/ Source of Variation	N	Mean	S	S_e	Degrees of Freedom
Weight % sediment					
-12.0+2.0 mm					
Point-bar	7	51.5886	11.6471		
Pavement	5	63.5700	9.6571		
				6.3793	10
T_{Calc} = -1.94	$T_{(10, 0.10)}$ = 1.812		Null hypothesis rejected		
-2.0+0.425 mm					
Point-bar	7	29.4543	10.9667		
Pavement	5	23.2760	3.5941		
				5.1490	8
T_{Calc} = 1.39	$T_{(8, 0.10)}$ = 1.860		Null hypothesis accepted		
-0.425+0.212 mm					
Point-bar	7	3.2843	1.5434		
Pavement	5	2.9440	1.7384		
				0.9510	8
T_{Calc} = 0.35	$T_{(8, 0.10)}$ = 1.860		Null hypothesis accepted		
-0.212+0.150 mm					
Point-bar	7	0.7429	0.3742		
Pavement	5	0.6160	0.5085		
				0.2535	7
T_{Calc} = 0.47	$T_{(7, 0.10)}$ = 1.895		Null hypothesis accepted		
-0.150+0.106 mm					
Point-bar	7	0.4914	0.2597		
Pavement	5	0.4060	0.3739		
				0.1818	7
T_{Calc} = 0.44	$T_{(7, 0.10)}$ = 1.895		Null hypothesis accepted		
-0.106+0.075 mm					
Point-bar	7	0.3257	0.1306		
Pavement	5	0.2580	0.2321		
				0.1044	6
T_{Calc} = 0.59	$T_{(6, 0.10)}$ = 1.943		Null hypothesis accepted		

Table 4-4. (continued).

Fraction/ Source of Variation	N	Mean	S	S_e	Degrees of Freedom
-0.075+0.053 mm					
Point-bar	7	0.4986	0.1737		
Pavement	5	0.3660	0.3192		
				0.1421	6
T_{Calc} = 0.84	$T_{(6, 0.10)}$ = 1.943		Null hypothesis accepted		
-0.053 mm					
Point-bar	7	13.6114	4.4919		
Pavement	5	8.5620	3.7784		
				2.4716	10
T_{Calc} = 2.11	$T_{(10, 0.10)}$ = 1.812		Null hypothesis rejected		

N = number of samples Mean = population mean
S = standard deviation S_e = standard error of difference

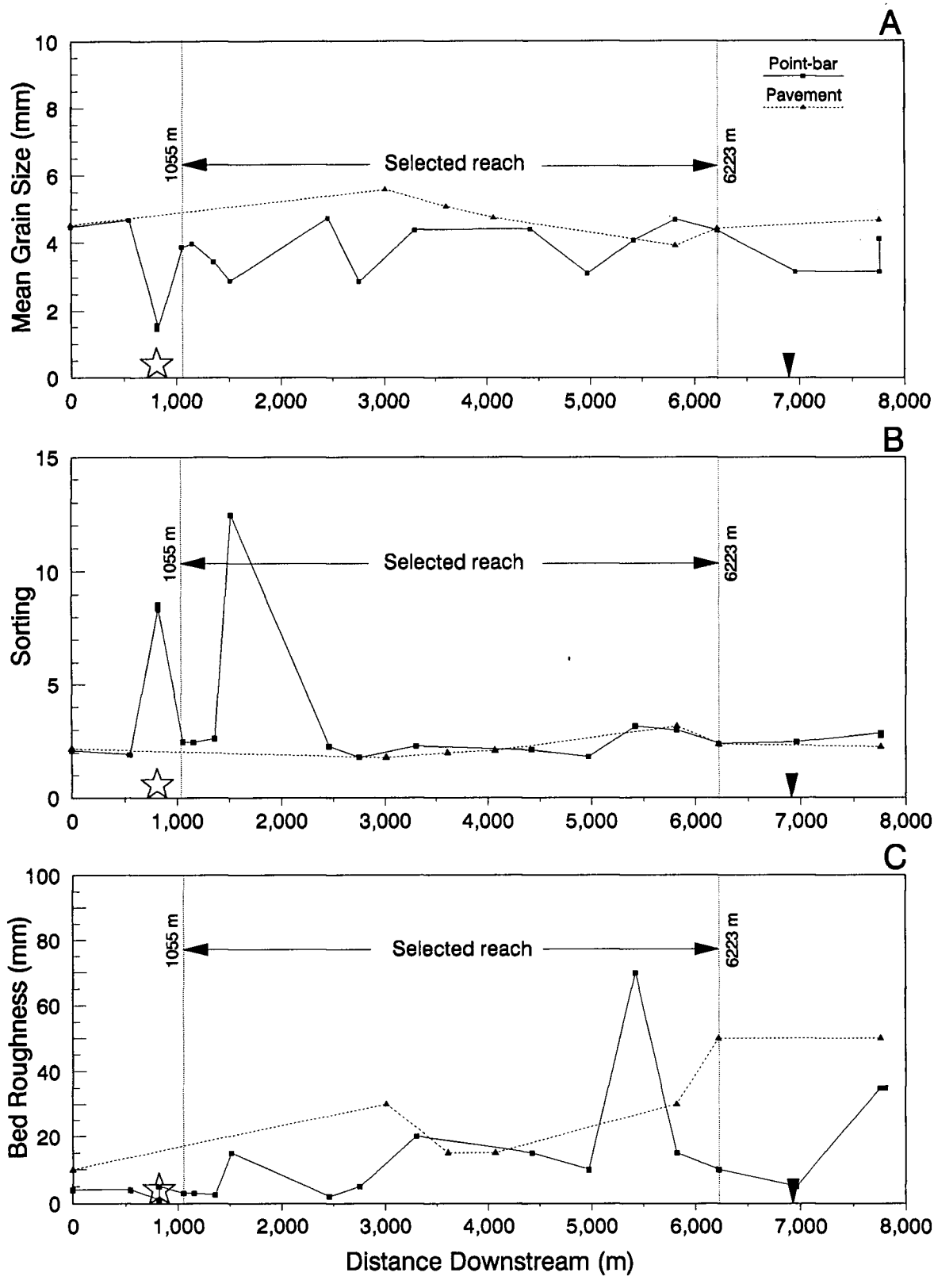

Fig. 4-5. Downstream trends of a) median grain size (M), b) sediment sorting (S_0) and c) bed roughness (D_{65}) of point bar (solid square) and pavement (solid triangle) sediments.

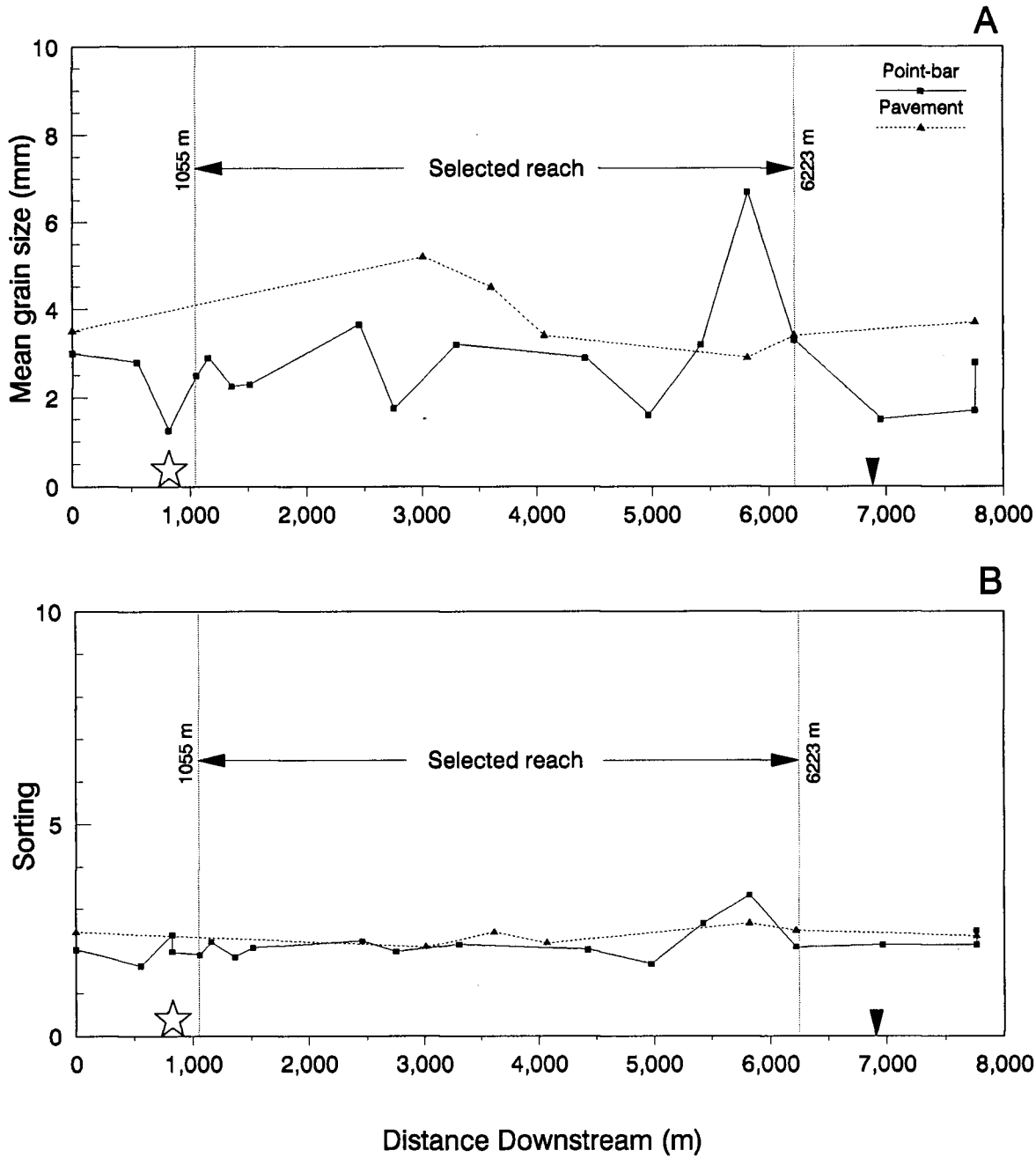

Fig. 4-6. Downstream trends of a) mean grain size (M_C) and b) sediment sorting (S_C) of coarse grained sediment component from point-bar (solid square) and pavement (solid triangle).

selected reach (between 1,055 and 6,223 m), no systematic trend in mean grain size (both M_0 and M_C) of point-bar sediments is apparent. However, mean grain size (both M_0 and M_C) of pavement sediments appears to decrease slightly between 3,000 and 6,000 m and then increases again. Sediment sorting (S_0) of point-bar sediments in the upper part of the stream is very erratic with very poor sorting at 820 and 1,500 m. Sorting (S_0) of pavement sites increases (poorly sorted) slightly from 2,753 to 5,500 m and then decreases (better sorted) again. Sediment sorting (S_C) of coarse grained component of both point-bar and pavement sediments is roughly constant throughout the reach. Bed roughness at point-bar sites shows a very erratic trend, but appears to increase at pavement sites from 3,600 m towards the confluence with the Huai Kho Lo. Results of the Wald-wolfowitz total-number-of-runs test (Table 4-5), suggest that these trends are significant for sediment sorting (S_0) and bed roughness (D_{65}) at point-bar sites, and for mean grain size (M_0) and sediment sorting (S_0) at pavement sites.

The distributions of sediment fractions finer than 12.0 mm are shown in Fig. 4-7. In the reach between 1,055 and 6,223 m, variations in gravel and coarse sand (between 12.0 and 0.212 mm) content of point bars are erratic and no systematic trends are apparent. However, the abundances of sediment fractions finer than 0.212 mm seem to decrease between 1,500 and 4,500 m and then increase again further downstream. Gravel content of pavements decreases between

Table 4-5. Results of the Wald-wolfowitz total-number-of-runs test (μ) for variations of sediment textures at point-bar and pavement sites along the whole reach and between the supposed source of gold and the confluence with the Huai Kho Lo (1,055 and 6,223 m).

Fraction/ Source of Variation	Cut point (median)	N n_1 (+)	N n_2 (-)	μ	P(μ)
Whole reach					
Point bar (N = 19)					
Mean (M_0)	3.99	10	9	11	0.4016
Sorting (S_0)	2.48	10	9	8	0.1207
Mean (M_C)	2.80	10	9	11	0.4016
Sorting (S_C)	2.14	9	10	12	0.2349
Bed roughness	5.00	12	7	6	0.0251*
Pavement (N = 7)					
Mean (M_0)	4.66	4	3	4	0.3580
Sorting (S_0)	2.19	4	3	3	0.1126
Mean (M_C)	3.50	4	3	4	0.1126
Sorting (S_C)	2.44	4	3	6	0.0911*
Bed roughness	30.00	4	3	4	0.3580
Between the supposed source of gold and the confluence with the Huai Kho Lo (1,055 and 6,223 m)					
Point bar (N = 12)					
Mean (M_0)	4.04	6	6	6	0.2724
Sorting (S_0)	2.44	6	6	4	0.0346*
Mean (M_C)	2.90	7	5	8	0.2331
Sorting (S_C)	2.09	6	6	8	0.2724
Bed roughness	10.00	7	5	4	0.0384*
Pavement (N = 5)					
Mean (M_0)	4.74	3	2	2	0.0633*
Sorting (S_0)	2.10	3	2	2	0.0633*
Mean (M_C)	3.40	4	1	3	0.2071
Sorting (S_C)	2.44	3	2	4	0.2563
Bed roughness	30.00	3	2	3	0.3313

N = total number of samples
n_1 = number of samples above median
n_2 = number of samples below median
μ = total number of runs above and below the median

* = statistically significant at higher than 90% confidence level.

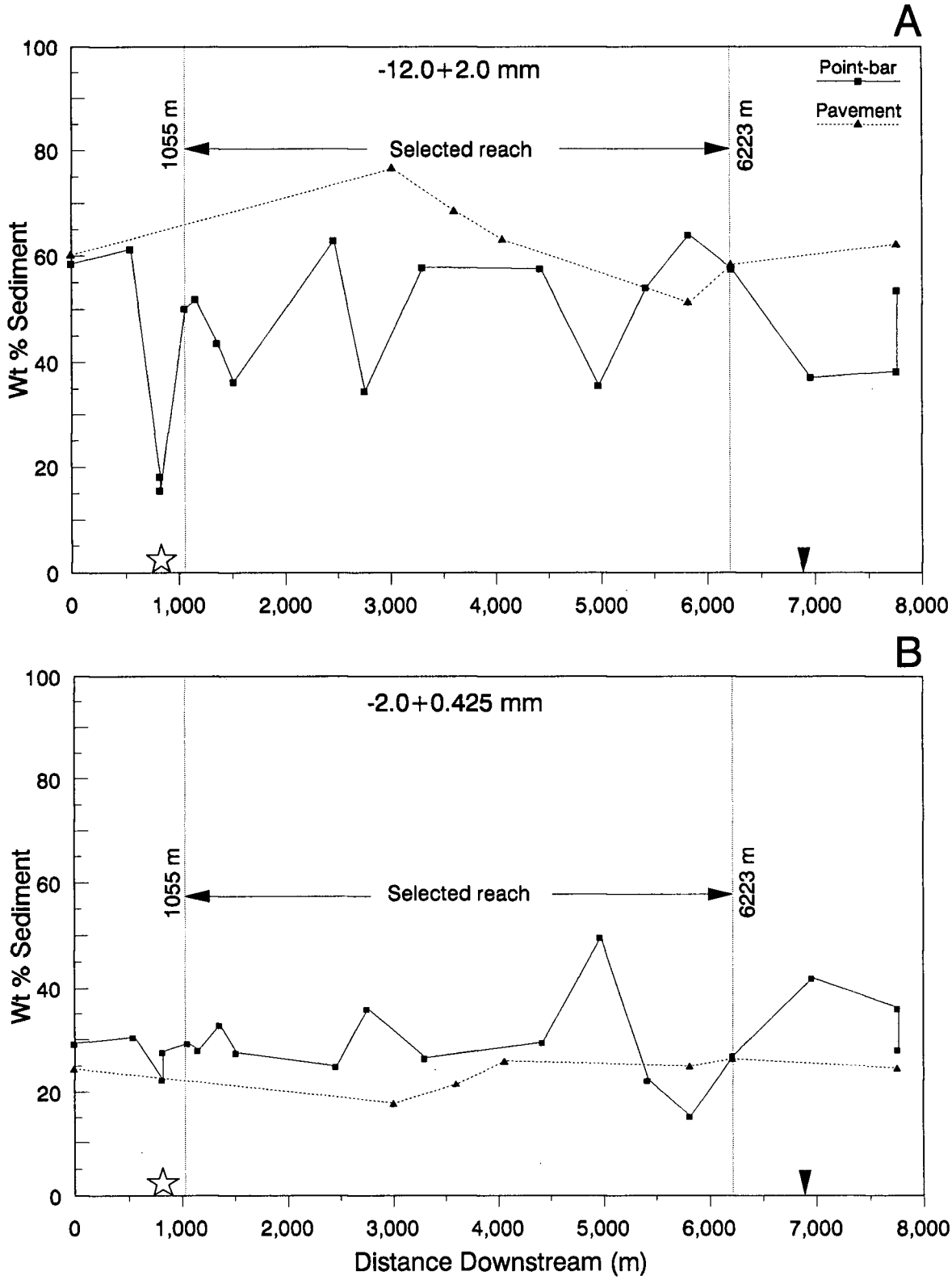

Fig. 4-7. Downstream trends of weight percent sediments at point bars (solid squares) and pavements (solid triangles) in a) -12.0+2.0 mm fraction, b) -2.0+0.425 mm fraction,

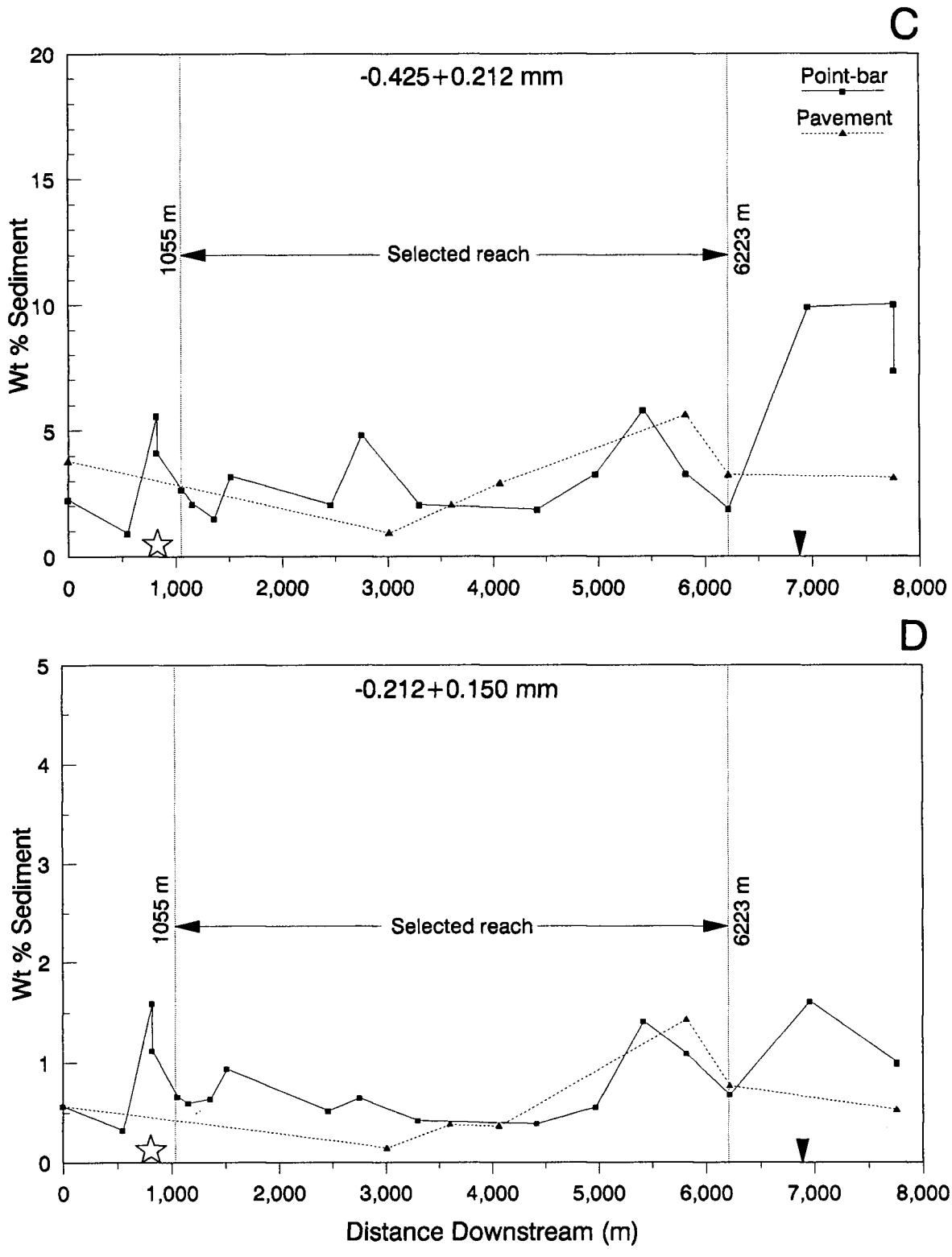

Fig. 4-7. (continued) c) -0.425+0.212 mm fraction, d) -0.212+0.150 mm fraction,

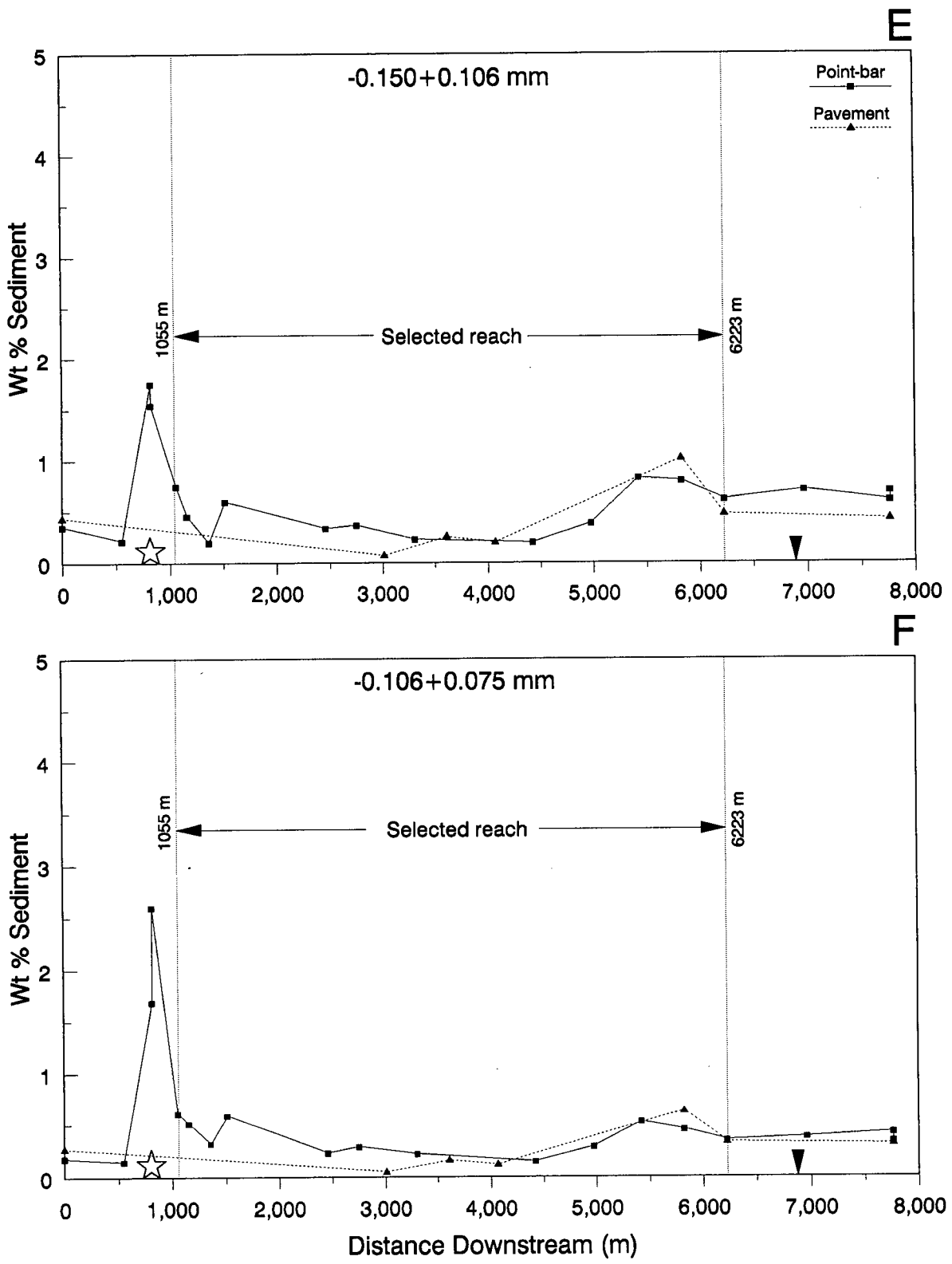

Fig. 4-7. (continued) e) -0.150+0.106 mm fraction, f) -0.106+0.075 mm fraction,

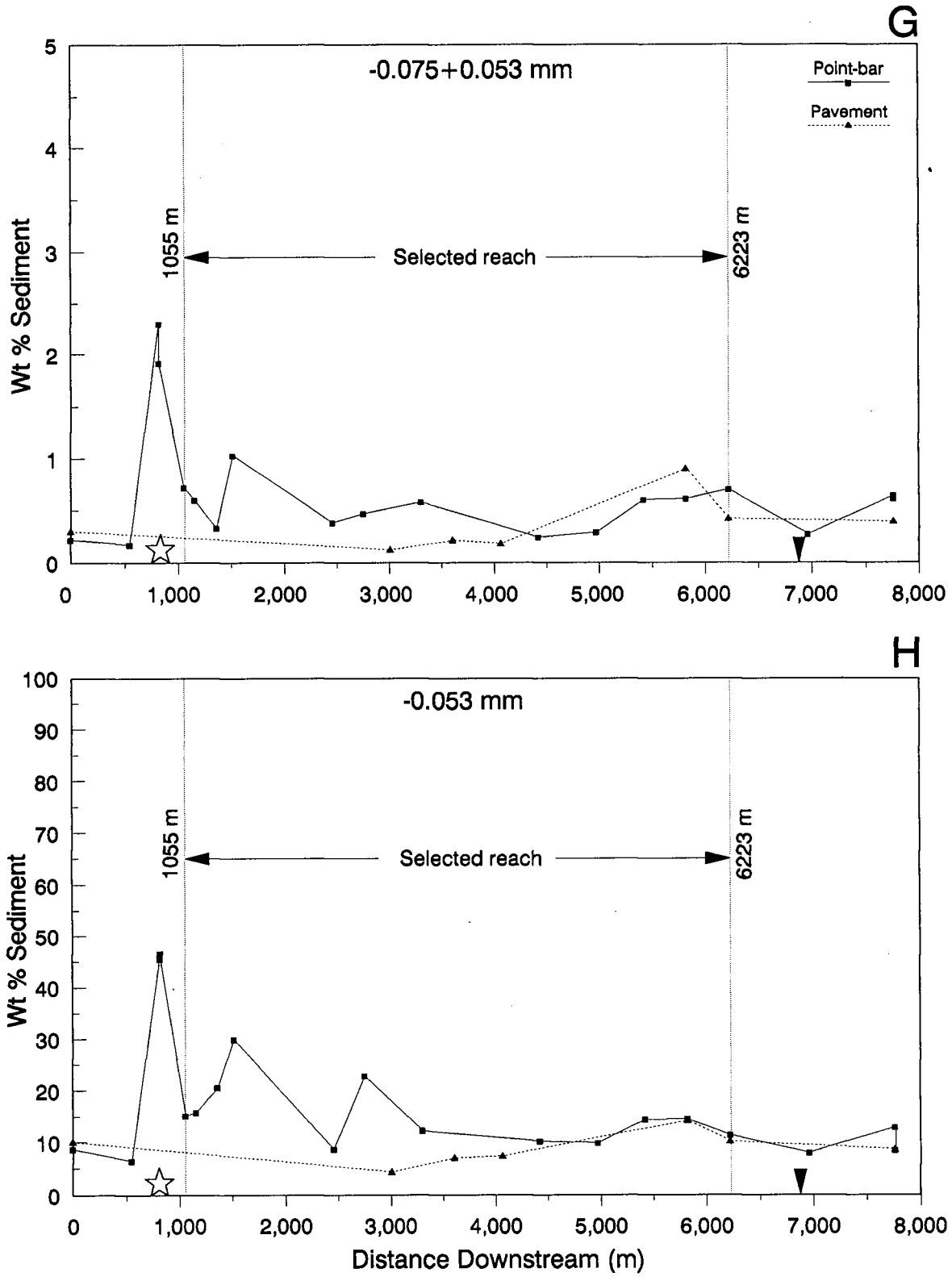

Fig. 4-7. (continued) g) -0.075+0.053 mm fraction and h) -0.053 mm fraction. Star indicates the supposed source of gold mineralization. Arrow indicates the confluence with the Huai Kho Lo.

3,000 and 6,000 m whereas content of sediment finer than 2.0 mm increases. The Wald-wolfowitz total-number-of-runs test and Spearman rank correlation coefficients suggest only the changes in texture of pavement with distance along the selected reach are significant (Table 4-6).

4.3.4 Correlations between stream characteristics and sediment properties

Relations between stream width, channel depth, flow velocity, mean grain size (M_0 and M_C), sediment sorting (S_0 and S_C) and bed roughness, based on Spearman rank correlation coefficients, are summarized in Table 4-7. In the reach between 1,055 and 6,223 m, stream width is positively correlated with depth, but negatively correlated with flow velocity and sediment sorting (S_0) at point-bar sites. Stream depth is also negatively correlated with sediment sorting (S_0). These relations indicate that as stream width and depth increase, flow velocity decreases (as it must to maintain continuity) and sediment sorting (S_0) improves. Additionally, mean grain size (both M_0 and M_C) are positively correlated with sorting (S_C) suggesting that with increasing grain size the coarse component of the point-bar sediment becomes moor poorly sorted. Bed roughness is positively correlated with distance downstream indicating that it increases downstream.

Table 4-6. Results of the Wald-wolfowitz total-number-of-runs test (μ) and Spearman rank correlation coefficient (r) for downstream trends of weight percent sediment in 8 size fractions from point-bar and pavement sites along the whole reach and between the supposed source of gold and the confluence with the Huai Kho Lo (1,055 and 6,223 m).

Fraction/ Source of Variation	Cut point (median)	N n_1 (+)	N n_2 (-)	μ	P(μ)	Spearman's r values
Whole reach						
Point-bar (n = 19)						
-12.0+2.0 mm	51.93	9	10	9	0.2426	0.061
-2.0+0.425 mm	28.09	9	10	12	0.2349	0.090
-0.425+0.212 mm	3.20	9	10	8	0.1207	0.448*
-0.212+0.150 mm	0.66	10	9	6	0.0171*	0.317
-0.150+0.106 mm	0.61	9	10	4	0.0011*	0.161
-0.106+0.075 mm	0.35	10	9	7	0.0500*	-0.037
-0.075+0.053 mm	0.60	10	9	8	0.1207	0.057
-0.053 mm	12.92	9	10	7	0.0500*	-0.316
Pavement (n = 7)						
-12.0+2.0 mm	62.14	4	3	4	0.3580	-0.429
-2.0+0.425 mm	24.53	4	3	2	0.0196*	0.643
-0.425+0.212 mm	3.13	3	4	4	0.3580	0.250
-0.212+0.150 mm	0.53	3	4	4	0.3580	0.393
-0.150+0.106 mm	0.43	3	4	4	0.3580	0.393
-0.106+0.075 mm	0.27	4	3	3	0.1126	0.607
-0.075+0.053 mm	0.30	4	3	3	0.1126	0.607
-0.053 mm	8.54	4	3	3	0.1126	0.429
Between the supposed source of gold and the confluence with the Huai Kho Lo (1,055 and 6,223 m)						
Point-bar (n = 12)						
-12.0+2.0 mm	53.04	6	6	6	0.2724	0.371
-2.0+0.425 mm	27.73	6	6	6	0.2724	-0.357
-0.425+0.212 mm	2.37	6	6	8	0.2724	0.196
-0.212+0.150 mm	0.65	6	6	7	0.5000	0.231
-0.150+0.106 mm	0.43	6	6	5	0.1129	0.277
-0.106+0.075 mm	0.34	6	6	5	0.1129	-0.270
-0.075+0.053 mm	0.59	6	6	5	0.1129	-0.084
-0.053 mm	14.48	6	6	6	0.2724	-0.490

Table 4-6. (continued).

Fraction/ Source of Variation	Cut point (median)	N n_1 (+)	n_2 (-)	μ	P(μ)	Spearman's r values
Pavement (n = 5)						
-12.0+2.0 mm	63.08	3	2	2	0.0633*	-0.900*
-2.0+0.425 mm	24.90	3	2	2	0.0633*	0.900*
-0.425+0.212 mm	2.91	3	2	2	0.0633*	0.900*
-0.212+0.150 mm	0.38	3	2	4	0.2563	0.800
-0.150+0.106 mm	0.26	3	2	4	0.2563	0.800
-0.106+0.075 mm	0.16	3	2	4	0.2563	0.800
-0.075+0.053 mm	0.21	3	2	4	0.2563	0.800
-0.053 mm	7.92	3	2	2	0.0633*	0.900*

N = total sample number
n_1 = number of samples above median
n_2 = number of samples below median
μ = total number of runs above and below the median
r = Spearman rank correlation coefficient

Note: n = 5; $r_{0.10}$ = 0.90 n = 12; $r_{0.10}$ = 0.50
n = 7; $r_{0.10}$ = 0.71 n = 19; $r_{0.10}$ = 0.39

* = statistically significant at 90% confidence level

Table 4-7. Spearman rank correlation coefficients between stream geometry and sediment characteristics along the whole reach and between the supposed source of gold and the confluence with the Huai Kho Lo (1,055 and 6,223 m).

	Distance	Width	Depth	Velocity	M_0	S_0	M_C	S_C	D_{65}
Whole reach									
Point-bar (n = 19)									
Distance	1.000								
Width	0.362	1.000							
Depth	0.303	0.604*	1.000						
Velocity	0.240	-0.517*	-0.305	1.000					
Mean size (M_0)	0.067	0.143	0.053	0.243	1.000				
Sorting (S_0)	0.100	-0.471*	-0.477*	0.024	-0.370	1.000			
Mean (M_C)	0.149	0.309	0.251	-0.067	0.874*	-0.206	1.000		
Sorting (S_C)	0.447*	0.068	0.111	-0.062	0.248	0.459*	0.425*	1.000	
D_{65}	0.704*	-0.004	0.047	0.347	0.071	0.193	0.207	0.321	1.000
Pavement (n = 7)									
Distance	1.000								
Width	-	-							
Depth	-	-	-						
Velocity	-	-	-	-					
Mean size (M_0)	-0.429	-	-	-	1.000				
Sorting (S_0)	0.643	-	-	-	-0.964*	1.000			
Mean (M_C)	-0.396	-	-	-	0.847*	-0.811*	1.000		
Sorting (S_C)	0.288	-	-	-	-0.847*	0.793*	-0.655	1.000	
D_{65}	0.826*	-	-	-	-0.239	0.441	-0.074	0.120	1.000

Table 4-7. (continued).

	Distance	Width	Depth	Velocity	M_0	S_0	M_C	S_C	D_{65}
Between the supposed source of gold and the confluence with the Huai Kho Lo (1,055 and 6,223 m)									
Point-bar (n = 12)									
Distance	1.000								
Width	0.070	1.000							
Depth	0.322	0.629*	1.000						
Velocity	0.175	-0.809*	-0.455	1.000					
Mean size (M_0)	0.371	0.112	-0.168	0.070	1.000				
Sorting (S_0)	-0.105	-0.657*	-0.601*	0.277	0.000	1.000			
Mean (M_C)	0.425	0.133	-0.154	-0.128	0.891*	0.260	1.000		
Sorting (S_C)	0.343	0.000	-0.133	-0.161	0.867*	0.377	0.867*	1.000	
D_{65}	0.601*	-0.424	-0.138	0.290	0.127	0.258	0.211	0.339	1.000
Pavement (n = 5)									
Distance	1.000								
Width	-	-							
Depth	-	-	-						
Velocity	-	-	-	-					
Mean size (M_0)	-0.900*	-	-	-	1.000				
Sorting (S_0)	0.900*	-	-	-	-1.000*	1.000			
Mean (M_C)	-0.821	-	-	-	0.975*	-0.975*	1.000		
Sorting (S_C)	0.800	-	-	-	-0.900*	0.900*	-0.821	1.000	
D_{65}	0.527	-	-	-	-0.369	0.369	-0.189	0.369	1.000

Note: n = 5; $r_{0.10}$ = 0.90 n = 12; $r_{0.10}$ = 0.50
n = 7; $r_{0.10}$ = 0.71 n = 19; $r_{0.10}$ = 0.39
* = statistically significant at 90% confidence level
M = mean grain size; S_0 = sediment sorting; D_{65} = bed roughness

At pavement sites, mean grain size (both M_0 and M_C) is negatively correlated with distance, but positively correlated with sorting (S_0) i.e. pavement grain size becomes finer and sorting poorer downstream. Unlike point-bar sites, sorting improves (negative correlation) with increasing average grain size (both M_0 and M_C).

4.4 Distribution of heavy mineral concentrates

Distribution of heavy minerals is described with respect to stream and sediment properties because i) behaviour and distribution of heavy minerals in streams may be similar to that of gold, and provide a method of correcting gold data for hydraulic effects (Day and Fletcher, 1986, 1989, in press; Fletcher, 1990; Fletcher and Day, 1988b), and ii) heavy minerals are often sampled and analyzed for gold in geochemical exploration programmes.

4.4.1 Heavy mineral morphology and compositions

Qualitative compositions obtained from SEM-EDS show that heavy mineral concentrates contain limonite, hematite, ilmenite, magnetite, zircon, garnet, spinel and barite. Clay minerals can also be observed in the heavy minerals because they coat or adhere to the surface of heavy-mineral grains and are not separated during the concentration process. Heavy mineral grains are subangular to well-rounded with

irregular to spherical shapes (Fig. 4-8). They comprise approximately 15% magnetic and 85% non-magnetic minerals. After magnetic minerals were removed, the non-magnetic fraction was examined with a binocular microscope to estimate the proportion (by volume) of each mineral. Results are presented in Table 4-8.

4.4.2 Size distribution and abundance of heavy minerals

Mean weight percents of heavy mineral concentrates in five size fractions between 0.425 and 0.053 mm of point-bar and pavement sites are plotted in Fig. 4-9. In both types of sediment, the four size fractions between 0.425 and 0.075 mm contain approximately 1% heavy minerals, whereas the very fine sand (-0.075+0.053 mm) fraction contains approximately 0.2%. Along the reach between 2,753 and 6,223 m, abundance of heavies in the two coarser sand (between 0.425 and 0.150 mm) fractions at pavement sites is slightly greater than at point bars. However, statistical results (two-sample t test) show that the difference is not significant.

4.4.3 Downstream trends of heavy mineral concentrates in point-bar and pavement deposits

Downstream trends of heavy mineral concentrates are shown in Fig. 4-10. The distribution is somewhat erratic. Nevertheless, in the reach between 1,055 and 6,223 m, heavy

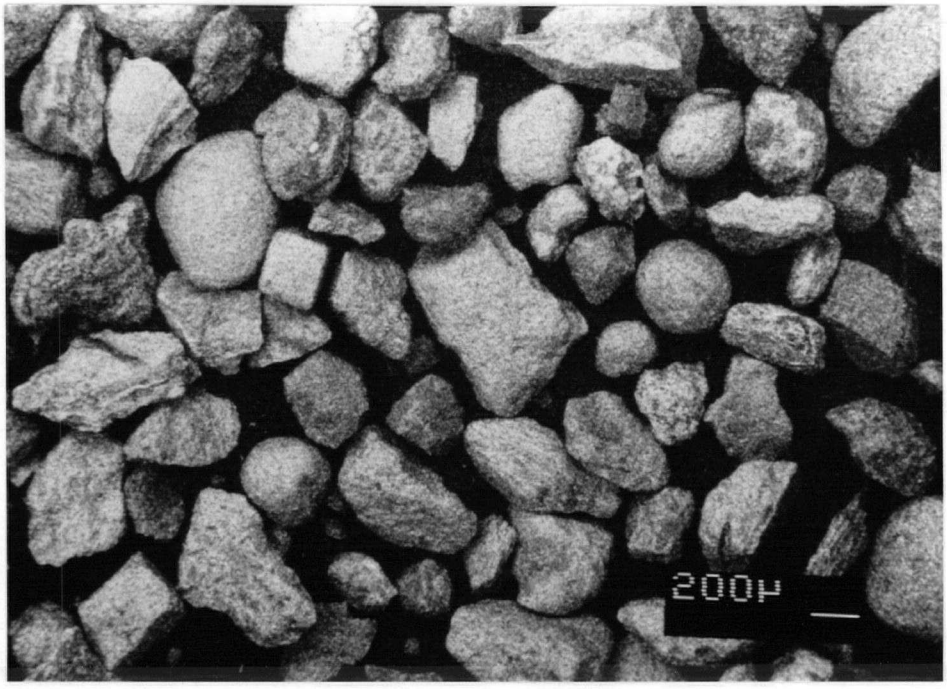

Fig. 4-8. Grain morphology of heavy mineral concentrates.

Table 4-8. Proportion (% by volume) of non-magnetic heavy mineral compositions in stream sediment.

Mineral	Proportion (% by volume)
Limonite	40
Hematite	25
Ilmenite	25
Zircon	5
Garnet	3
Barite	1
Spinel	1

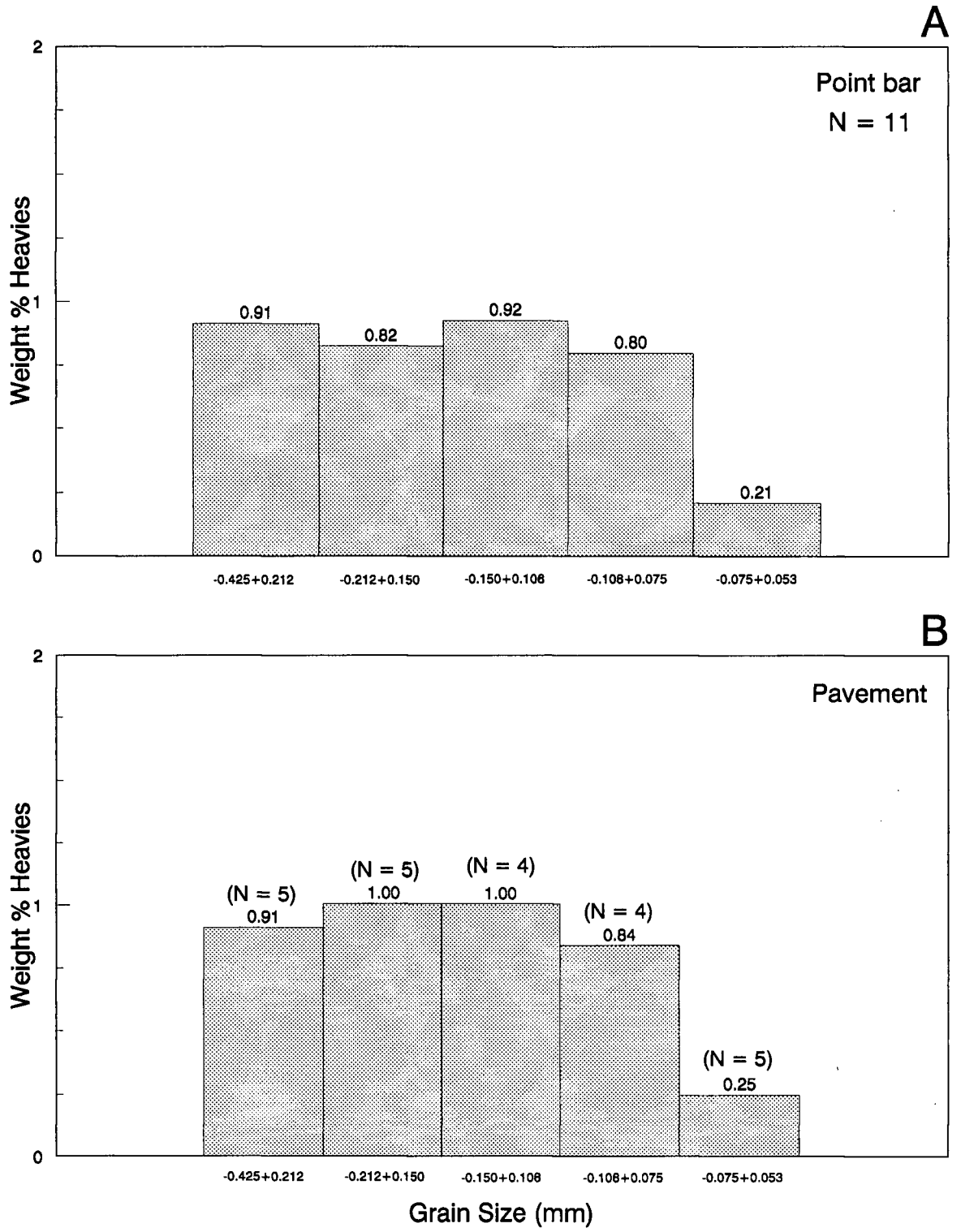

Fig. 4-9. Mean weight percent of heavy mineral distributions in a) point-bar (n = 11) and b) pavement (n = 5) sediments.

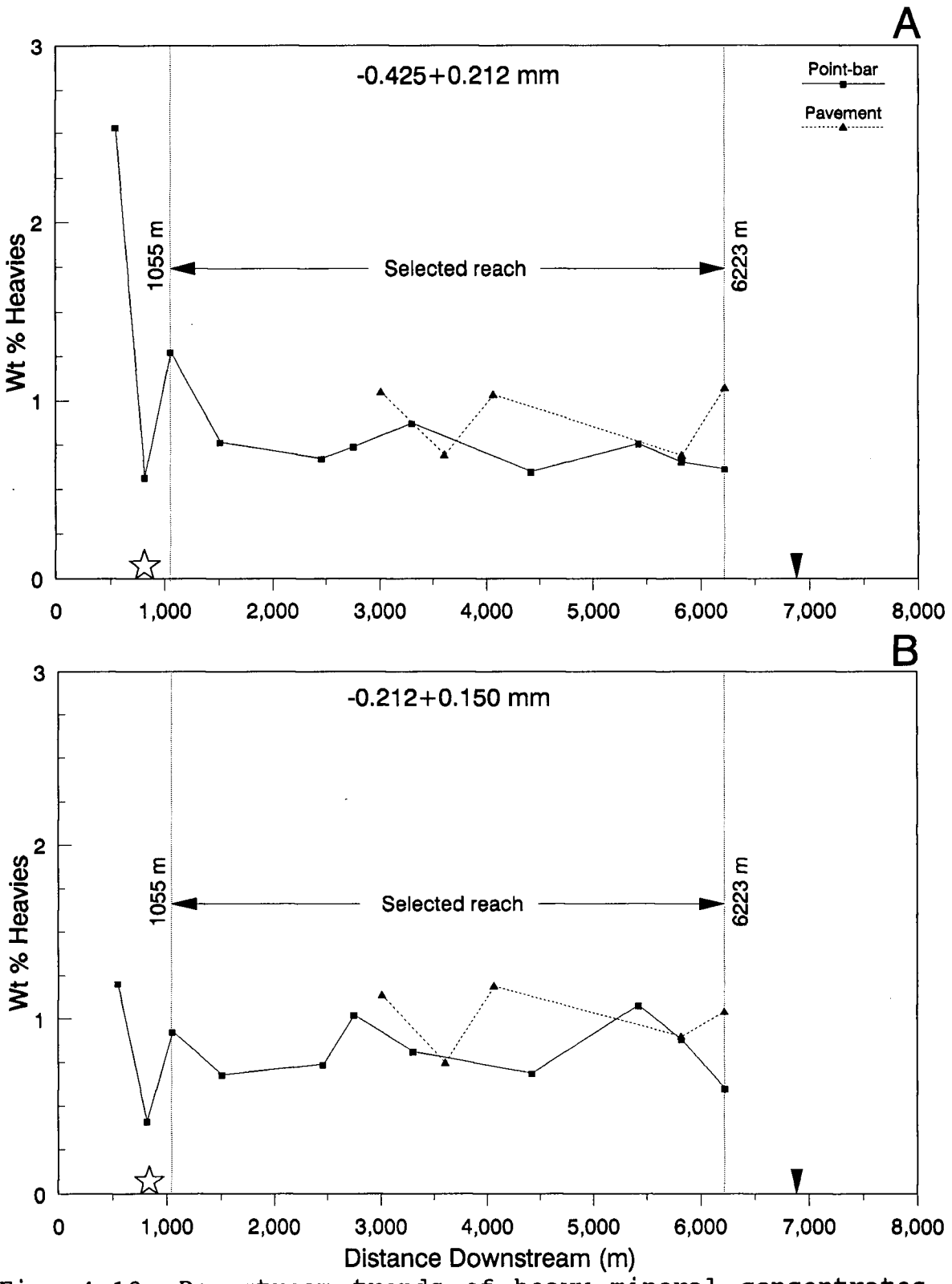

Fig. 4-10. Downstream trends of heavy mineral concentrates at point-bar (solid square) and pavement (solid triangle) sites for a) -0.425+0.212 mm fraction, b) -0.212+0.150 mm fraction,

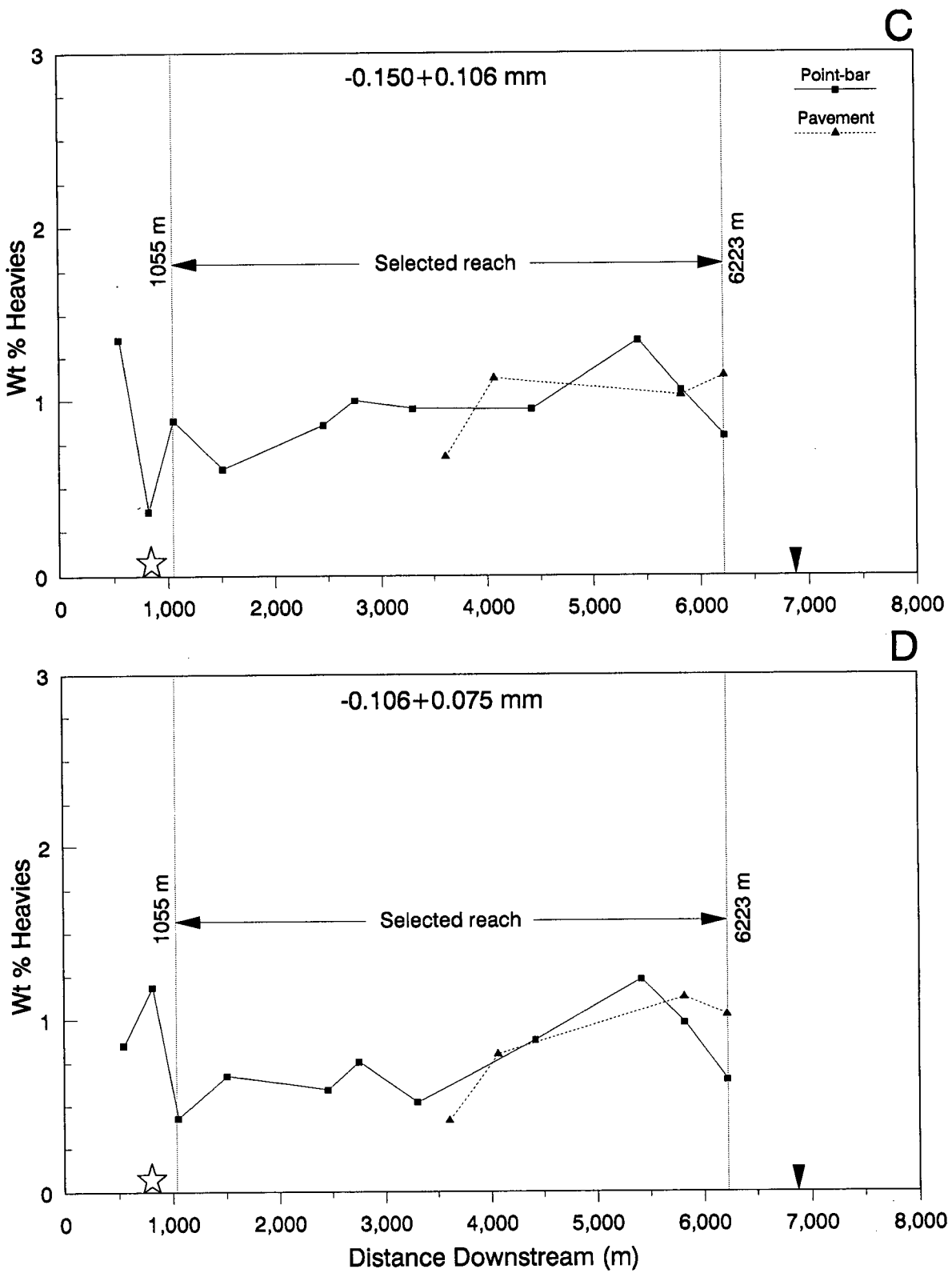

Fig. 4-10. (continued) c) -0.150+0.106 mm fraction, d) -0.106+0.075 mm fraction and

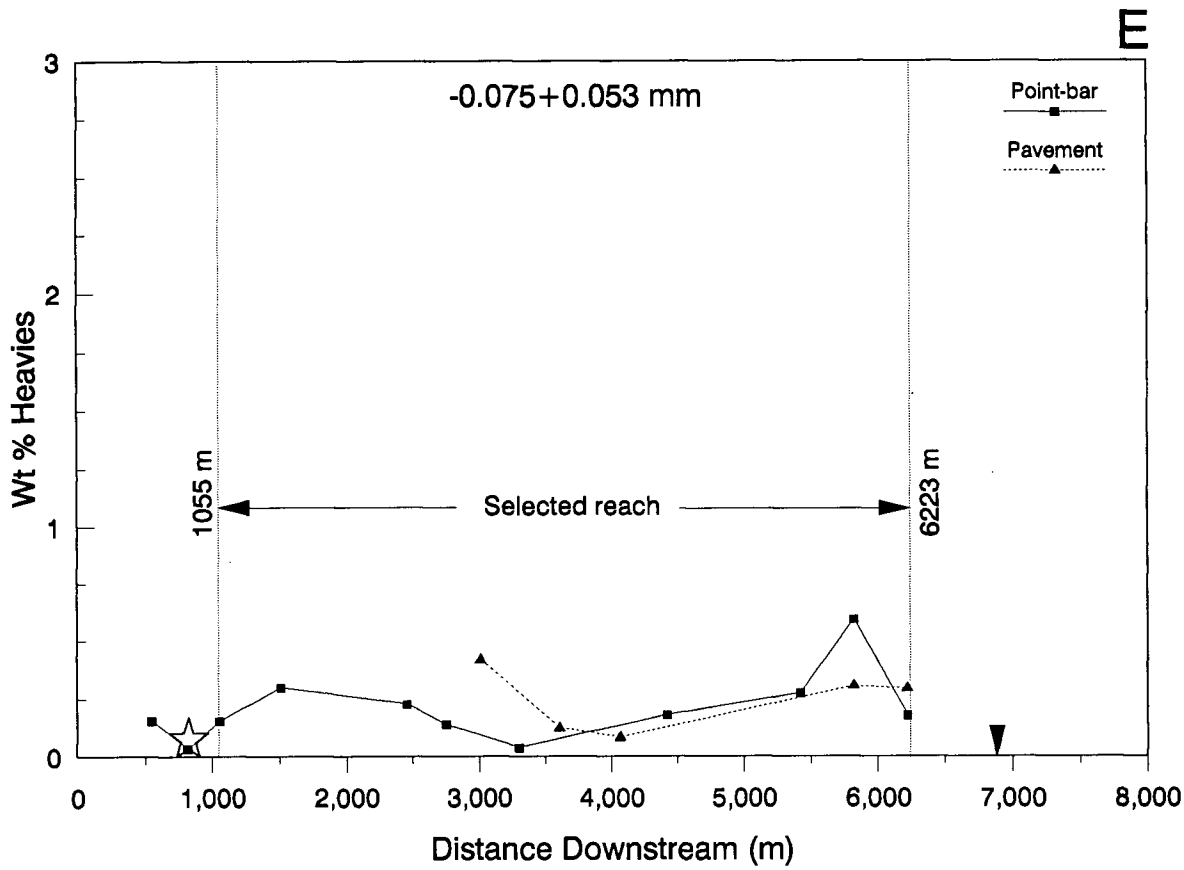

Fig. 4-10. (continued) e) -0.075+0.053 mm fraction. Star indicates the supposed source of gold mineralization. Arrow indicates the confluence with the Huai Kho Lo.

mineral content of coarse sand (-0.425+0.212 mm) fraction from point bars appears to decrease slightly downstream. Conversely, for the two fractions between 0.150 and 0.075 mm concentrations seem to increase erratically downstream. Abundance of heavies in the finest fraction decreases from 1,500 to 3,300 m and then increases again. There are no obvious systematic trends in the abundance of heavy minerals at pavement sites. Statistical evaluations based on the Wald-wolfowitz total-number-of-runs test and Spearman rank correlation coefficients (Table 4-9) suggest that trends for decrease in abundance of coarse grained heavies downstream versus increased abundance of the -0.150+0.106 mm heavies may be real.

4.4.4 Relations between heavy mineral abundance and stream characteristics and sediment properties

Spearman rank correlation coefficients (Table 4-10) are evaluated to examine the relations between the abundance of heavy minerals and stream characteristics and sediment properties in the selected reach. Results indicate that at point-bar sites only stream width and sorting (S_0) are significantly correlated with abundance of heavies, and then only in two finest size fractions. However, it is notable that heavy mineral contents in all size fractions are negatively correlated with stream width and depth, and positively correlated with flow velocity and bed roughness.

Table 4-9. Results of the Wald-wolfowitz total-number-of-runs test (μ) and Spearman rank correlation coefficient (r) for downstream trends of heavy mineral concentrates from point-bar and pavement sediments along the whole reach and between the supposed source of gold and the confluence with the Huai Kho Lo (1,055 and 6,223 m).

Fraction/ Source of Variation	Cut point (median)	N n_1 (+)	N n_2 (-)	N μ	$P(\mu)$	Spearman's r values
Whole reach						
Point-bar (n = 11)						
-0.425+0.212 mm	0.74	6	5	8	0.1607	-0.409
-0.212+0.150 mm	0.88	5	6	8	0.1607	-0.109
-0.150+0.106 mm	0.95	6	5	4	0.0577*	0.164
-0.106+0.075 mm	0.85	5	6	4	0.0577*	0.145
-0.075+0.053 mm	0.18	5	6	5	0.1754	0.436
Pavement (n = 5)						
-0.425+0.212 mm	1.04	2	3	3	0.3313	0.100
-0.212+0.150 mm	1.04	3	2	5	0.0404*	-0.100
-0.150+0.106 mm	1.08	2	2	4	0.1103	0.800
-0.106+0.075 mm	0.91	2	2	2	0.1103	0.800
-0.075+0.053 mm	0.29	3	2	3	0.3313	-0.200
Bewteen the supposed source of gold and the confluence with the Huai Kho Lo (1,055 and 6,223 m)						
Point-bar (n = 9)						
-0.425+0.212 mm	0.74	5	4	6	0.3440	-0.667*
-0.212+0.150 mm	0.81	5	4	6	0.3440	-0.117
-0.150+0.106 mm	0.95	5	4	3	0.0386*	0.393
-0.106+0.075 mm	0.68	5	4	7	0.1304	0.567
-0.075+0.053 mm	0.20	4	5	5	0.3740	-0.150
Pavement (n = 5) as above						

N = total sample number
n_1 = number of samples above median
n_2 = number of samples below median
μ = total number of runs above and below the median
r = Spearman's correlation coefficient

Note n = 5; $r_{(0.10)} = 0.90$
n = 9; $r_{(0.10)} = 0.60$
n = 11; $r_{(0.10)} = 0.54$

* = statistically significant at 90% confidence level

Table 4-10. Spearman rank correlation coefficients between weight percent heavy mineral concentrates and stream characteristics and sediment properties in the whole reach and between the supposed source of gold and the confluence with the Huai Kho Lo (1,055 and 6,223 m).

	Width	Depth	Velocity	M_O	S_O	D_{65}	M_C	S_C
Whole reach								
Point-bar (n = 11)								
-0.425+0.212 mm	-0.164	-0.333	0.319	0.064	-0.145	0.257	-0.100	-0.500
-0.212+0.150 mm	-0.209	-0.319	0.446	0.218	-0.418	0.202	0.073	-0.282
-0.150+0.106 mm	-0.269	-0.288	0.609*	0.397	-0.434	0.447	0.293	-0.064
-0.106+0.075 mm	-0.664*	-0.196	0.405	-0.109	0.245	0.202	-0.087	0.445
-0.075+0.053 mm	-0.023	-0.108	0.378	0.407	0.362	0.379	0.544*	0.371
Pavement (n = 5)								
-0.425+0.212 mm	-	-	-	0.229	-0.229	0.567	0.310	-0.381
-0.212+0.150 mm	-	-	-	0.229	-0.229	0.000	0.000	-0.686
-0.150+0.106 mm (n=4)	-	-	-	-0.424	0.424	0.674	-0.467	-0.076
-0.106+0.075 mm (n=4)	-	-	-	-0.990	0.990	0.674	-0.934	0.680
-0.075+0.053 mm	-	-	-	0.000	0.000	0.567	0.232	0.000
Between the supposed source of gold and the confluence with the Huai Kho Lo (1,055 and 6,223 m)								
Point-bar (n = 9)								
-0.425+0.212 mm	-0.217	-0.250	-0.100	-0.500	0.367	0.067	-0.418	-0.233
-0.212+0.150 mm	-0.300	-0.217	0.167	-0.267	0.000	0.136	-0.167	0.067
-0.150+0.106 mm	-0.427	-0.192	0.477	0.075	-0.084	0.460	0.130	0.360
-0.106+0.075 mm	-0.600*	-0.083	0.583	0.033	0.183	0.526	0.109	0.433
-0.075+0.053 mm	-0.527	-0.318	0.544	0.268	0.661*	0.187	0.412	0.586
Pavement (n = 5) as above								

Table 4-10. (continued).

Note: n = 4; $r_{0.10}$ = 1.00 n = 9; $r_{0.10}$ = 0.60
n = 5; $r_{0.10}$ = 0.90 n = 11; $r_{0.10}$ = 0.54

* = statistically significant at 90% confidence level
M_0 = mean grain size of the entire sediment
S_0 = sediment sorting of the entire sediment
D_{65} = bed roughness
M_C = mean grain size of coarse grained sediment component
S_C = sorting of coarse grained sediment component

These relations suggest that abundances of heavy minerals at point-bar sites increase where reduction in channel width and depth causes flow velocity and bed roughness to increase.

4.5 Summary

1) In the Huai Hin Laep sediments from point-bar and pavement sites have strongly bimodal distributions. They consist mainly of gravel and silt-clay with only minor amounts of sand.

2) Pavement sediments contain significantly more gravel but less silt-clay than point bar sediments.

3) Trends in sediment texture and mean grain size at point-bar sites along the reach between 1,055 and 6,223 m are very erratic, whereas bed roughness increases and sorting improves downstream. However, at pavement sites mean grain size increases and sediment sorting decreases downstream. At point-bar sites sediment sorting is negatively correlated with stream width and depth.

4) Abundance of heavy minerals at point-bar and pavement sites is similar, approximately 1%. At point-bar sites their abundance generally increases in zones of convergent flow (narrow channel width) characterized by higher flow velocities, increased bed roughness and poorer sorting.

CHAPTER FIVE

GEOCHEMISTRY OF GOLD IN THE HUAI HIN LAEP

5.1 Distribution of gold between size and density fractions

Gold concentrations in heavy mineral concentrates, and -0.150 mm and -0.053 mm sediment fractions are listed in Table 5-1. Concentrations in heavy mineral concentrates range from <15 ppb to a maximum of 198,000 ppb, but are typically in the several thousands of ppb range. Of the corresponding light mineral fractions all but six contain less than 5 ppb gold (Appendix). In all cases, Au concentrations in the -0.053 mm sediment fraction are less than 5 ppb (Table 5-1). Similarly, except for 85 ppb in a single point-bar sample and two values of 80 and 95 ppb at pavement sites, Au concentrations in the -0.150 mm sediment fraction are at or less than 5 ppb. These low values in the lights, the -0.150 mm and the -0.053 mm sediment fractions contrast strongly with the high values in the heavy mineral fractions. Summary statistics are shown in Table 5-2.

The data for Au concentrations in heavy mineral concentrates (Table 5-1) were converted to Au concentrations in the whole corresponding sediment fraction using the equation:

$$Au_{TOTAL} = (Au_H x Wt_H)/Wt_{TOTAL} \qquad (5\text{-}1)$$

where Au_{TOTAL} is the Au concentration (ppb) in the sediment fraction, Au_H is the Au concentration (ppb) in heavy mineral concentrates, Wt_H is the weight (g) of the heavy mineral fraction, and Wt_{TOTAL} is the combined weight (g) of heavy mineral and sediment fraction, and assuming that Au

Table 5-1. Gold concentrations (ppb) in heavy mineral concentrates, -0.150 and -0.053 mm sediment fractions.

	Heavy mineral fraction (mm)*			Sediment (mm)	
Sample	-.425+.212	-.212+.106	-.106+.053	-.150	-.053
Point-bar					
PP-16	<15	14700	<200	<5	<5
PP-96	185000	86300	7540	<5	<5
PP-09	380	<25	930	<5	<5
PP-94	3080	<30	4000	<5	<5
PP-10	<20	2290	11000	<5	<5
PP-89	3260	1465	3500	<5	<5
PP-81	14800	46000	18700	<5	<5
PP-75	<30	<75	21300	5	<5
PP-70	28900	28400	11800	85	<5
PP-67	29200	58500	36100	<5	<5
PP-64	25	1790	14200	<5	<5
Pavement					
PP-87	90	55400	38200	95	<5
PP-100	58800	46000	11300	<5	<5
PP-79	800	23000	15200	<5	<5
PP-68	26700	37800	18800	<5	<5
PP-65	72000	198000	67200	80	<5

* = In all but six samples the corresponding light fractions contain < 5 ppb gold. Reported Au detection limits depend on weight of heavy mineral concentrates.

Table 5-2. Summaries statistics of gold content (ppb) in heavy mineral fractions.

	Size fraction (mm)		
	-0.425+0.212	-0.212+0.106	-0.106+0.053
Bar (n = 11)			
Mean	24060	21775	11745
Median	3080	2290	11000
Range	(<15-185000)	(<25-86300)	(<200-36100)
Pavement (n = 5)			
Mean	31678	72040	30140
Median	26700	46000	18800
Range	(90-72000)	(23000-198000)	(11300-67200)

concentration in the light mineral fractions is less than 5 ppb. Results (Table 5-3) show that calculated Au concentrations in all three corresponding sediment fractions are greater than those in the -0.150 and -0.053 mm sediment fractions.

5.2 Gold distribution in the Huai Hin Laep

5.2.1 Comparison between Au concentrations at point bar and pavement sites

In all three size fractions mean and median gold concentrations at pavement sites exceed these for point-bar sites (Tables 5-2 and 5-3). However, values are extremely erratic, with a very wide range of gold concentrations, and a statistical comparison of concentrations shows none of the differences are significant at 90% confidence level (Table 5-4).

5.2.2 Downstream trends of Au concentrations in point-bar and pavement sediments

Gold values in heavies from point-bar and pavement sites are plotted against the distance downstream for four size fractions in Fig. 5-1. Corresponding gold values recalculated for sediments are shown in Fig. 5-2. Because sediment texture remains reasonably constant throughout the

Table 5-3. Calculated gold concentrations* (ppb), mean, median and range of gold concentrations in sediment fractions.

	Size fraction (mm)		
Sample	-0.425+0.212	-0.212+0.106	-0.106+0.053
Point-bar			
PP-16	<1	180	<1
PP-96	1050	340	40
PP-09	5	<1	5
PP-94	25	<1	15
PP-10	<1	20	40
PP-89	25	15	15
PP-81	130	395	30
PP-75	<1	<1	95
PP-70	220	435	85
PP-67	190	555	275
PP-64	<1	10	45
Mean	150	180	60
Median	25	20	40
Range	<1-1050	<1-555	<1-275
Pavement			
PP-87	<1	625	190
PP-100	410	330	25
PP-79	10	270	55
PP-68	185	360	120
PP-65	770	2160	410
Mean	275	750	160
Median	185	360	120
Range	<1-770	270-2160	25-410

* = calculated from data in Table 5-1, values less than the detection limit were taken at mid-point.

Table 5-4. Statistical two-sample test means of Au concentrations* (ppb) in heavy-mineral concentrates and in sediments from point bars and pavements in the reach between 2,753 and 6,223 m.

Null hypothesis: μ Au in point-bar = μ Au in pavement

Fraction/ Source of Variation	N	Mean	S	S_e	Degrees of Freedom
Au in heavies					
-0.425+0.212 mm					
Point-bar	6	12700.00	13782.44		
Pavement	5	31678.00	32929.85		
				14676.77	5
T_{Calc} = -1.20 $T_{(5, 0.10)}$ = 2.015 Null hypothesis accepted					
-0.212+0.106 mm					
Point-bar	6	22698.75	25529.44		
Pavement	5	72040.00	71411.12		
				31045.16	5
T_{Calc} = -1.45 $T_{(5, 0.10)}$ = 2.015 Null hypothesis accepted					
-0.106+0.053 mm					
Point-bar	6	17600.00	10965.04		
Pavement	5	30140.00	23157.89		
				10577.66	5
T_{Calc} = -1.11 $T_{(5, 0.10)}$ = 2.015 Null hypothesis accepted					
-0.212+0.053 mm					
Point-bar	6	21623.22	20904.51		
Pavement	5	62147.76	58446.43		
				25410.57	5
T_{Calc} = -1.47 $T_{(5, 0.10)}$ = 2.015 Null hypothesis accepted					
Au in sediments					
-0.425+0.212 mm					
Point-bar	6	93.90	98.75		
Pavement	5	274.61	323.69		
				138.06	5
T_{Calc} = -1.20 $T_{(5, 0.10)}$ = 2.015 Null hypothesis accepted					

Table 5-4. (continued).

Fraction/ Source of Variation	N	Mean	S	S_e	Degrees of Freedom
<u>-0.212+0.106 mm</u>					
Point-bar	6	235.94	253.85		
Pavement	5	748.31	800.22		
				342.75	5
T_{Calc} = -1.38 $T_{(5, 0.10)}$ = 2.015 Null hypothesis accepted					
<u>-0.106+0.053 mm</u>					
Point-bar	6	90.36	94.75		
Pavement	5	160.76	152.85		
				75.08	6
T_{Calc} = -0.90 $T_{(6, 0.10)}$ = 1.943 Null hypothesis accepted					
<u>-0.212+0.053 mm</u>					
Point-bar	6	174.57	182.15		
Pavement	5	521.41	554.82		
				238.59	5
T_{Calc} = -1.34 $T_{(5, 0.10)}$ = 2.015 Null hypothesis accepted					

* = values lower than detection limits were taken at mid-point.
N = number of samples
Mean = population mean
S = standard deviation
S_e = standard error of difference

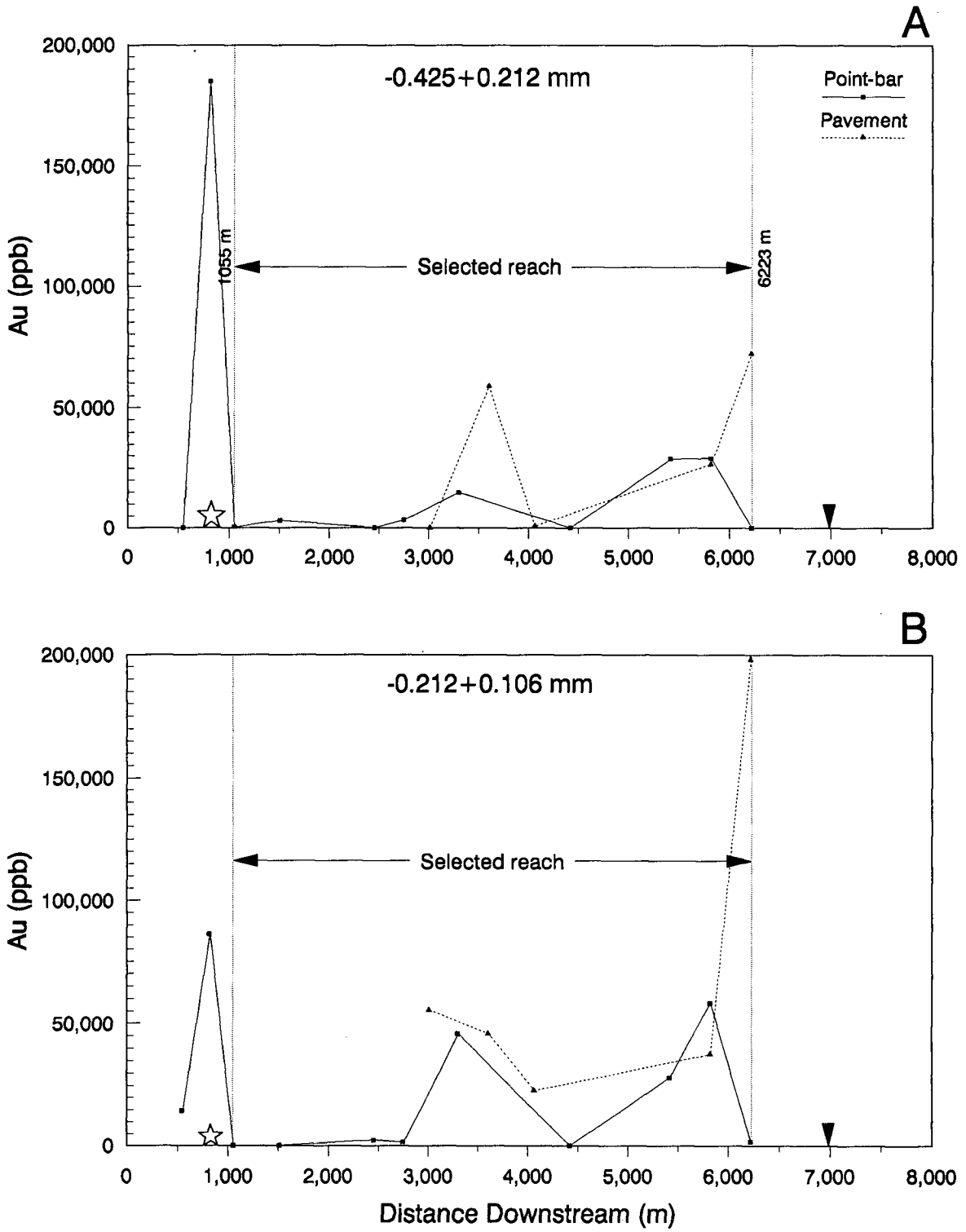

Fig. 5-1. Downstream trends for Au concentrations in heavy mineral concentrates at point bars (solid squares) and pavements (solid triangles) for a) -0.425+0.212 mm fraction, b) -0.212+0.106 mm fraction,

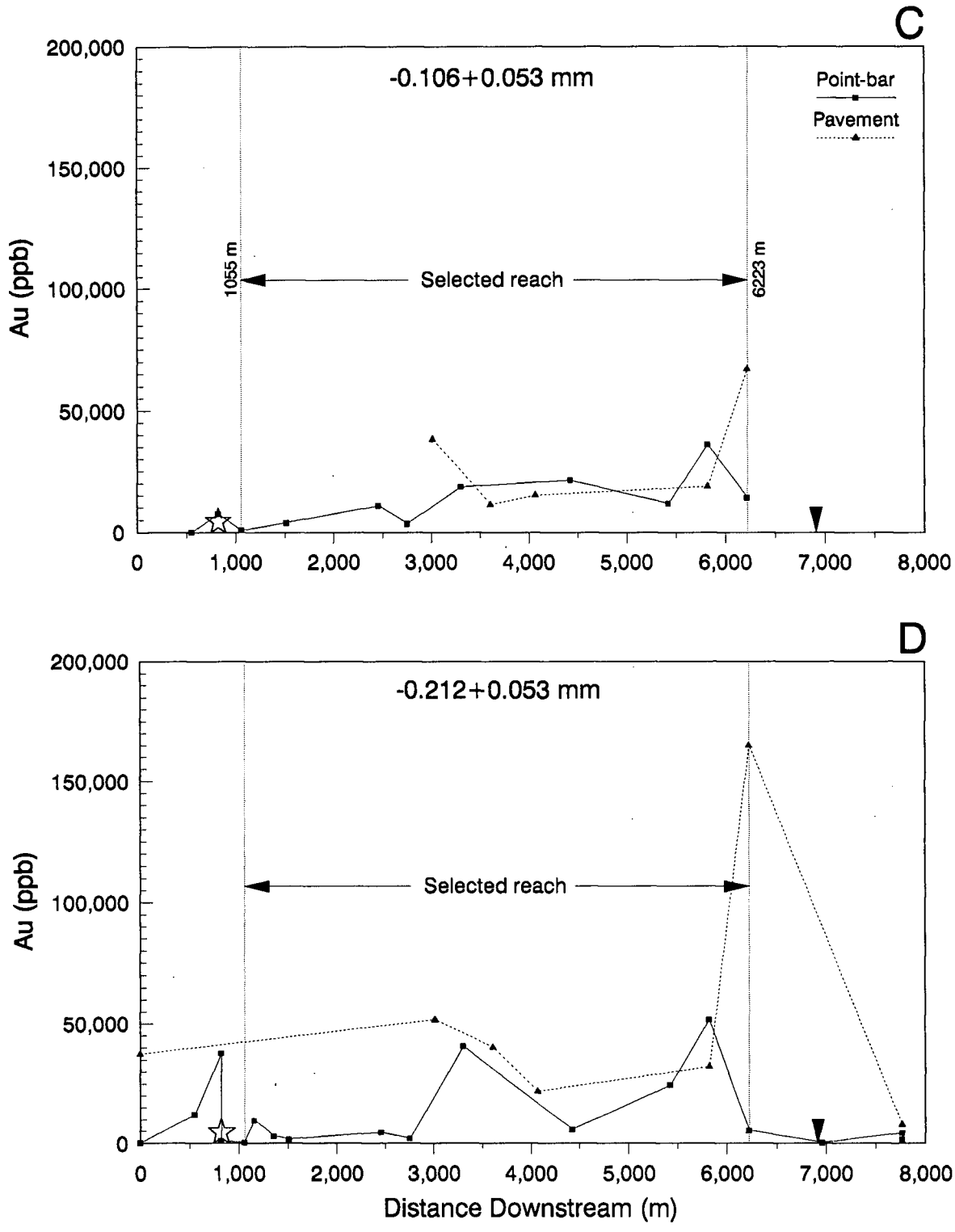

Fig. 5-1. (continued) c) -0.106+0.053 mm fraction and d) ideally combined -0.212+0.053 mm fraction. Star indicates the supposed source of gold mineralization. Arrow indicates the confluence with the Huai Kho Lo.

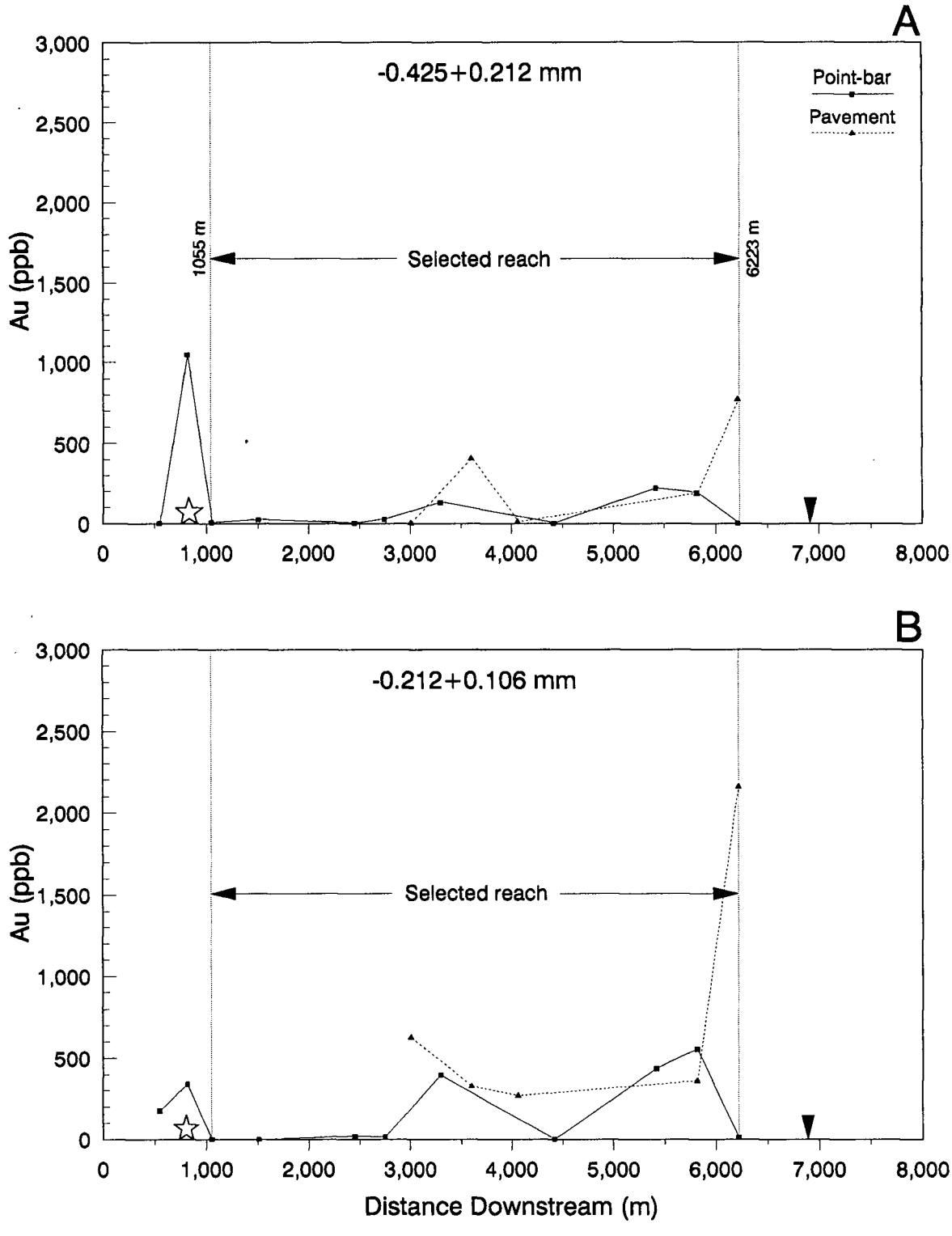

Fig. 5-2. Downstream trends for Au concentrations in sediment fractions at point bars (solid squares) and pavements (solid triangles) for a) -0.425+0.212 mm fraction, b) -0.212+0.106 mm fraction,

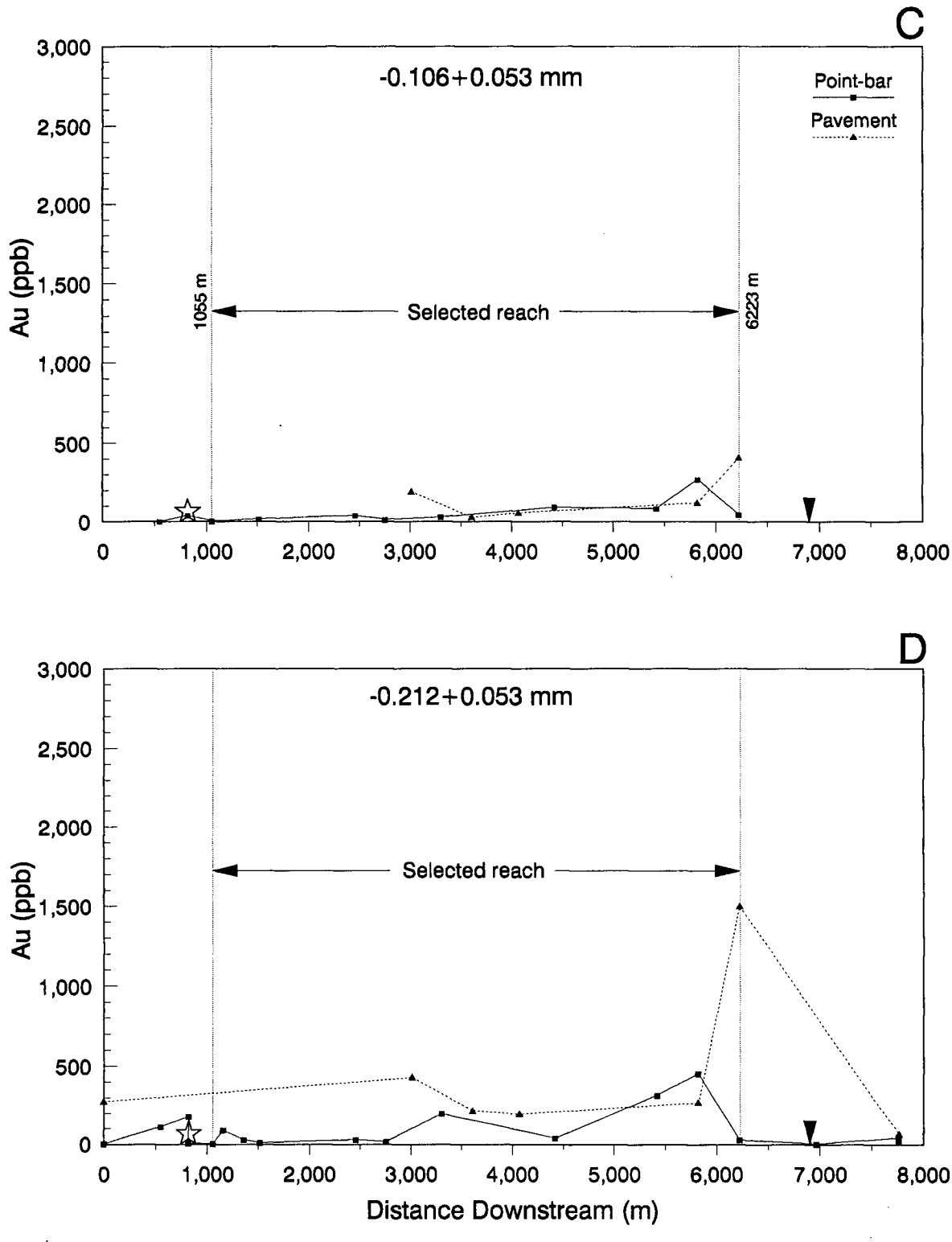

Fig. 5-2. (continued) c) -0.106+0.053 mm fraction and d) ideally combined -0.212+0.053 mm fraction. Star indicates the supposed source of gold mineralization. Arrow indicates the confluence with the Huai Kho Lo.

reach, downstream distribution patterns of Au concentrations in heavy mineral concentrates and in sediments are similar, except that Au concentrations in heavies are approximately 100 times higher than those in sediments.

It is notable that there is a single high gold value in all size fractions of the point-bar sample at 820 m near the supposed bedrock source of the mineralization, where the sediment (PP-96, Appendix) contains mainly of silt and clay (> 46%) and minor gravel (~ 18%). Gold concentrations at this site decrease with decreasing grain size. In the reach downstream from this site, trends in gold concentrations in all three fractions are erratic but show similarities with high gold values at 3,250 and 5,750 m. Especially in the very fine sand (-0.106+0.053 mm) and combined -0.212+0.053 mm fractions, gold concentrations appear to increase downstream as far as the confluence with the Huai Kho Lo. The Wald-wolfowitz total-number-of-runs test and Spearman rank correlation coefficients (Table 5-5) suggest that the trend of Au concentrations in these two fractions is significant.

There are too few results for pavement sediments to identify downstream trends. Nevertheless, it should be noted that the highest concentration of Au is found at 6,223 m (i.e. approximately 5 kilometers downstream of the supposed bedrock source of gold).

Table 5-5. Results of the Wald-wolfowitz total-number-of-runs test (μ) and Spearman rank correlation coefficient (r) for downstream trends of Au concentrations (ppb) in point-bar and pavement sediments in the Huai Hin Laep.

Fraction/ Source of Variation	Cut point (median) (ppb)	N n_1 (+)	n_2 (-)	μ	P(μ)	Spearman's r values
Whole reach						
Point-bar (n = 11)						
-0.425+0.212 mm	23.53	6	5	9	0.0512*	0.009
-0.212+0.106 mm	17.98	5	6	6	0.3853	0.255
-0.106+0.053 mm	39.27	6	5	6	0.3853	0.782*
-0.212+0.053 mm(n=18)	28.20	9	9	9	0.3135	0.201
Pavement (n = 5)						
-0.425+0.212 mm	184.24	2	3	4	0.2563	0.700
-0.212+0.106 mm	360.71	3	2	3	0.3313	0.300
-0.106+0.053 mm	120.35	3	2	3	0.3313	0.400
-0.212+0.053 mm(n=7)	268.35	4	3	4	0.3580	-0.321
Between supposed source of mineralization and confluence with Huai Kho Lo (1,055 and 6,223 m)						
Point-bar (n = 9)						
-0.425+0.212 mm	23.53	5	4	7	0.1304	0.283
-0.212+0.106 mm	14.94	4	5	7	0.1304	0.567
-0.106+0.053 mm	40.24	4	5	2	0.0064*	0.800*
-0.212+0.053 mm(n=11)	36.70	5	6	5	0.1754	0.536*

n_1 = number of samples above median
n_2 = number of samples below median
μ = total number of runs above and below the median

* = statistically significant at 90% confidence level

Note: $n = 5$, $r_{(0.10)} = 0.90$ $n = 11$, $r_{(0.10)} = 0.54$
$n = 7$, $r_{(0.10)} = 0.71$ $n = 14$, $r_{(0.10)} = 0.46$
$n = 9$, $r_{(0.10)} = 0.60$ $n = 18$, $r_{(0.10)} = 0.40$

5.2.3 Relations between Au concentrations, sediment textures and stream geometry

Relations between Au concentrations in sediments and sediment textures (i.e. mean grain size, sediment sorting, bed roughness and weight percent of selected sediment fractions) and stream geometry (i.e. stream width, depth and flow velocity) were examined using Spearman rank correlation coefficients. Results (Table 5-6) show that at point-bar sites along the selected reach, Au concentrations are positively correlated with mean grain size (M_0), bed roughness (D_{65}), mean grain size (M_C) and poorer sorting (S_C) of the coarse grained component of the bed, and also with gravel content, but negatively correlated with coarse sand content. The relations with gravel content, M_C, S_C, bed roughness (D_{65}) and coarse sand content are most prominent. At pavement sites the only significant correlation is between Au concentrations in the two fine fractions and bed roughness. These relations all indicate that gold is preferentially accumulated with relatively coarse grained sediments.

Because stream geometry data at pavement sites are not available, relations between Au concentrations and stream geometry are shown only for point-bar sites in Table 5-7. In the reach between 1,055 and 6,223 m, Au concentrations in all size fractions are negatively correlated with stream width, and positively correlated with flow velocity.

Table 5-6. Spearman rank correlation coefficient (r) between gold concentrations (ppb) in sediments at point-bar and pavement sites and sediment textures of the Huai Hin Laep.

Fraction (mm)	M_0	S_0	D_{65}	M_C	S_C	Weight % sediment			
						-12.0 +2.0	-2.0 +0.425	-0.425 +0.212	-0.053
Whole reach									
Point bar (n = 11)									
-0.425+0.212	-0.509	0.545*	0.248	-0.273	0.518	-0.382	-0.500	0.773*	0.682*
-0.212+0.106	0.300	0.073	0.248	0.415	0.682*	0.400	-0.664*	0.336	-0.100
-0.106+0.053	0.363	0.245	0.422	0.629*	0.745*	0.355	-0.645*	0.164	-0.127
-0.212+0.053 (n=18)	0.495	0.140	0.247	0.358	0.507	0.348	-0.474*	-0.121	0.057
Pavement (n = 5)									
-0.425+0.212	-0.100	0.500	0.316	-0.359	0.700	-0.500	0.600	0.500	0.500
-0.212+0.106	0.500	0.100	0.949*	0.103	0.200	-0.100	0.100	0.100	0.100
-0.106+0.053	0.200	0.200	0.949*	-0.051	0.100	-0.200	0.300	0.200	0.200
-0.212+0.053 (n=7)	-0.179	0.036	0.092	-0.018	0.252	-0.179	0.000	-0.107	0.179
Between supposed source of mineralization and the confluence with Huai Kho Lo (1,055 and 6,223 m)									
Point bar (n = 9)									
-0.425+0.212	-0.283	0.467	0.695*	0.000	0.417	-0.083	-0.417	0.717*	0.517
-0.212+0.106	0.483	0.000	0.373	0.661*	0.817*	0.600*	-0.750*	0.367	-0.267
-0.106+0.053	0.683*	0.100	0.458	0.695*	0.700*	0.683*	-0.567	-0.133	-0.517
-0.212+0.053 (n=11)	0.518	0.164	0.520*	0.548*	0.574*	0.600*	-0.545*	0.045	-0.309

Table 5.6. (continued).

n = 5; $r_{0.10}$ = 0.90	n = 9; $r_{0.10}$ = 0.60
n = 7; $r_{0.10}$ = 0.71	n = 11; $r_{0.10}$ = 0.52
	n = 18; $r_{0.10}$ = 0.40

* = statistically significant at 90% confidence level
M_0 = mean grain size of the entire sediment
S_0 = sorting of the entire sediment
M_C = mean grain size of coarse grained sediment component
S_C = sorting of coarse grained sediment component
D_{65} = bed roughness

Table 5-7. Spearman rank correlation coefficient (r) between gold concentrations (ppb) in sediments at point-bar sites and stream geometry of the Huai Hin Laep.

Fraction (mm)	Width	Depth	Velocity
Whole reach (n = 11)			
-0.425+0.212	-0.518	-0.068	0.091
-0.212+0.106	-0.345	-0.005	0.292
-0.106+0.053	0.100	0.191	0.132
-0.212+0.053 (n=18)	-0.202	0.053	-0.014
Between supposed source of gold and the confluence with the Huai Kho Lo (n = 9)			
-0.425+0.212	-0.633*	-0.167	0.417
-0.212+0.106	-0.167	0.133	0.283
-0.106+0.053	-0.317	-0.100	0.600*
-0.212+0.053 (n=11)	-0.345	-0.045	0.369

n = 9; $r_{0.10}$ = 0.60
n = 11; $r_{0.10}$ = 0.52
n = 18; $r_{0.10}$ = 0.40

* = statistically significant at 90% confidence level

However, only the correlations between Au concentrations in the medium sand (-0.425+0.212 mm) fraction and stream width, and Au concentrations of the very fine sand (-0.106+0.053 mm) fraction and flow velocity are statistically significant.

5.3 Estimated numbers of gold particles

The numbers of gold particles in heavy mineral concentrates were calculated based on the assumption that 1) gold occurs as free spherical particles, 2) the sieve diameter of particles is the geometric midpoint of the bounding sieve openings, and 3) the density of the particles is 15 g/cm^3. Depending on the actual shape of the gold particles and their size distribution within each sieve fraction, these estimates could be too high or too low by a factor of about five. The total number of gold particles in all three size fractions (-0.425+0.053 mm) was obtained by summing the numbers of gold particles in each size fraction, and also in the two size fractions (-0.212+0.053 mm). Results of the estimates (Table 5-8) suggest that in most samples the number of gold particles in the -0.425+0.212 mm fraction from point-bar sites is fewer than one (median = 0.12). However, the number of gold particles increases with decreasing grain size. For example, at point-bar sites median numbers of gold particles increase from 0.12, to 0.21 to 2.83. Corresponding values for pavement sites are 1.26,

Table 5-8. Estimated* numbers of gold particles in heavy mineral concentrates.

Sample	Fractions (mm)			Total	
	-0.425 +0.212	-0.212 +0.106	-0.106 +0.053	-0.425 +0.053	-0.212 +0.053
Point-bar (n = 11)					
PP-16	0.00	1.15	0.00	1.15	1.15
PP-96	6.90	10.46	11.94	29.30	22.40
PP-09	0.02	0.00	0.33	0.35	0.33
PP-94	0.12	0.00	2.83	2.95	2.83
PP-10	0.00	0.20	2.59	2.79	2.79
PP-89	0.20	0.21	1.07	1.48	1.28
PP-81	0.40	3.08	2.47	5.95	5.55
PP-75	0.00	0.00	3.21	3.21	3.21
PP-70	1.94	9.09	9.45	20.48	18.54
PP-67	0.95	12.78	28.23	41.96	41.01
PP-64	0.00	0.20	5.00	5.20	5.20
Mean	0.96	3.38	6.10	10.44	9.48
Median	0.12	0.21	2.83	3.21	3.21
Range	0.00-6.90	0.00-12.78	0.00-28.23	0.35-41.96	0.33-41.01
Score	3	5	9	10	10
Pavement (n = 5)					
PP-87	0.00	1.19	1.92	3.11	3.11
PP-100	1.26	2.46	0.99	4.71	3.45
PP-79	0.04	1.85	1.62	3.51	3.47
PP-68	1.48	10.01	17.01	28.50	27.02
PP-65	3.65	30.78	28.92	63.35	59.70
Mean	1.29	9.26	10.09	20.64	19.35
Median	1.26	2.46	1.92	4.71	3.47
Range	0.00-3.65	1.19-30.78	0.99-28.92	3.11-63.35	3.11-59.70
Score	3	5	5	5	5

* = estimated from data in Table 5-1.

Score = number of samples containing one or more gold particles

2.46 and 1.92 particles.

Based on the above results, the estimated numbers of gold particles were standardized to 40 kg (-12.0 mm) field samples and 30 g analytical subsamples. The probability (from the Poisson distribution, equation 1-2) of recovering one or more particles of gold (P>0) in a random sample was then estimated (Table 5-9). Of the 40 kg field samples, only three out of eleven samples contain more than one gold particle in the -0.425+0.212 mm fraction of point-bar sediment, whereas in the finest (-0.106+0.053 mm) fraction there are nine out of eleven samples that contain more than one gold particle. The median of the standardized number of gold particles increases from 0.15 to 3.54, with a corresponding increase in the probabilities of obtaining one or more gold grains from 21% to 97%.

At pavement sites three out of five samples of the -0.425+0.212 mm and all of the finer fractions contain one or more gold particles. The median number of gold particles increases from 1.61 to 3.13 and 2.88 and the corresponding probability of obtaining one or more gold grains increases from 80 to 96 and 94%, respectively.

In the case of 30 g analytical subsamples, only the median of the standardized number of gold particles in the finest (-0.106+0.053 mm) fraction from pavement sites is greater than one particle with a corresponding probability of finding one or more gold particles of 68%.

Table 5-9. Estimated numbers of gold particles (n) in the standardized 40 kg (-12.0 mm) field samples and 30 g analytical subsamples and probability of containing one or more gold grains (P>0).

Sample	Fractions (mm) -0.425+0.212 n	P>0	-0.212+0.106 n	P>0	-0.106+0.053 n	P>0
40 kg field samples						
Point bar						
PP-16	0.00	0.00	1.48	0.77	0.00	0.00
PP-96	11.38	1.00	17.63	1.00	19.70	1.00
PP-09	0.02	0.02	0.00	0.00	0.43	0.35
PP-94	0.15	0.14	0.00	0.00	3.54	0.97
PP-10	0.00	0.00	0.24	0.21	3.08	0.95
PP-89	0.23	0.21	0.23	0.21	1.21	0.70
PP-81	0.51	0.40	3.98	0.98	3.19	0.96
PP-75	0.00	0.00	0.00	0.00	4.53	0.99
PP-70	2.47	0.92	14.99	1.00	12.04	1.00
PP-67	1.22	0.71	16.36	1.00	36.45	1.00
PP-64	0.00	0.00	0.25	0.22	6.22	1.00
Mean	1.45	0.31	5.01	0.49	8.22	0.81
Median	0.15	0.21	0.25	0.22	3.54	0.97
Range	0.00-11.38	0.00-1.00	0.00-17.63	0.00-1.00	0.00-36.45	0.00-1.00
Score	3	3	5	5	9	9

Table 5-9. (continued).

Sample	Fractions (mm) -0.425+0.212 n	P>0	-0.212+0.106 n	P>0	-0.106+0.053 n	P>0
Pavement						
PP-87	0.00	0.00	1.37	0.75	2.88	0.94
PP-100	1.61	0.80	3.13	0.96	1.27	0.72
PP-79	0.05	0.05	2.33	0.90	2.04	0.87
PP-68	2.01	0.87	13.61	1.00	23.16	1.00
PP-65	4.87	0.99	41.40	1.00	38.70	1.00
Mean	1.71	0.54	12.37	0.92	13.61	0.91
Median	1.61	0.80	3.13	0.96	2.88	0.94
Range	0.00-4.87	0.00-1.00	1.37-41.40	0.75-1.00	1.27-38.70	0.72-1.00
Score	3	3	5	5	5	5
30 g analytical subsamples						
Point bar						
PP-16	0.00	0.00	0.20	0.19	0.00	0.00
PP-96	0.15	0.14	0.39	0.33	0.37	0.31
PP-09	0.00	0.00	0.00	0.00	0.02	0.02
PP-94	0.00	0.00	0.00	0.00	0.16	0.15
PP-10	0.00	0.00	0.02	0.02	0.38	0.32
PP-89	0.00	0.00	0.02	0.02	0.12	0.11
PP-81	0.02	0.02	0.46	0.37	0.30	0.26
PP-75	0.00	0.00	0.00	0.00	0.87	0.58
PP-70	0.03	0.03	0.50	0.40	0.80	0.55
PP-67	0.03	0.03	0.64	0.47	2.58	0.92
PP-64	0.00	0.00	0.01	0.01	0.44	0.36

Table 5-9. (continued).

Sample	Fractions (mm) -0.425+0.212 n	-0.425+0.212 P>0	-0.212+0.106 n	-0.212+0.106 P>0	-0.106+0.053 n	-0.106+0.053 P>0
Mean	0.02	0.02	0.20	0.16	0.55	0.33
Median	0.00	0.00	0.02	0.02	0.37	0.31
Range	0.00-0.15	0.00-0.14	0.00-0.64	0.00-0.47	0.00-2.58	0.00-0.92
Score	0	0	0	0	1	1
Pavement						
PP-87	0.00	0.00	0.72	0.51	1.81	0.84
PP-100	0.06	0.06	0.38	0.31	0.25	0.22
PP-79	0.00	0.00	0.31	0.27	0.52	0.40
PP-68	0.03	0.03	0.42	0.34	1.13	0.68
PP-65	0.11	0.11	2.49	0.92	3.86	0.98
Mean	0.04	0.04	0.86	0.47	1.51	0.62
Median	0.03	0.03	0.42	0.34	1.13	0.68
Range	0.00-0.11	0.00-0.11	0.31-2.49	0.27-0.92	0.25-3.86	0.22-0.98
Score	0	0	2	2	3	3

Score = number of samples containing one or more gold particles

Downstream trends of the estimated numbers of gold particles in heavy mineral fractions are shown in Fig. 5-3. As expected downstream trends of the number of Au particles in all fractions of both environments behave similarly to Au concentrations (Figs. 5-1 and 5-2). Based on the Wald-wolfowitz total-number-of-runs test (Table 5-10) the numbers of gold particles in the combined -0.212+0.053 mm fraction are clustered, with sites containing greater than the median number of particles all in the lower part of the reach. Statistically, this is highly significant. Similarly, spearman rank correlation coefficients show that trends for the estimated numbers of gold particles in the -0.106+0.053 mm and the combined -0.212+0.053 mm fractions increase significantly downstream. This also occurs at pavement sites.

5.4 Gold grain morphology and compositions

The numbers of visible gold grains counted in the field pan-concentrates are listed in Table 5-11 and plotted against distance (Fig. 5-4). The distribution of visible gold grains from point-bar sites along the entire reach is roughly similar to the distribution of Au concentrations (Figs. 5-1 and 5-2) and the estimated numbers of gold particles (Fig. 5-3). Five selected pan concentrates samples were recounted for visible gold grains in the laboratory prior to further study. It is notable that, except in one

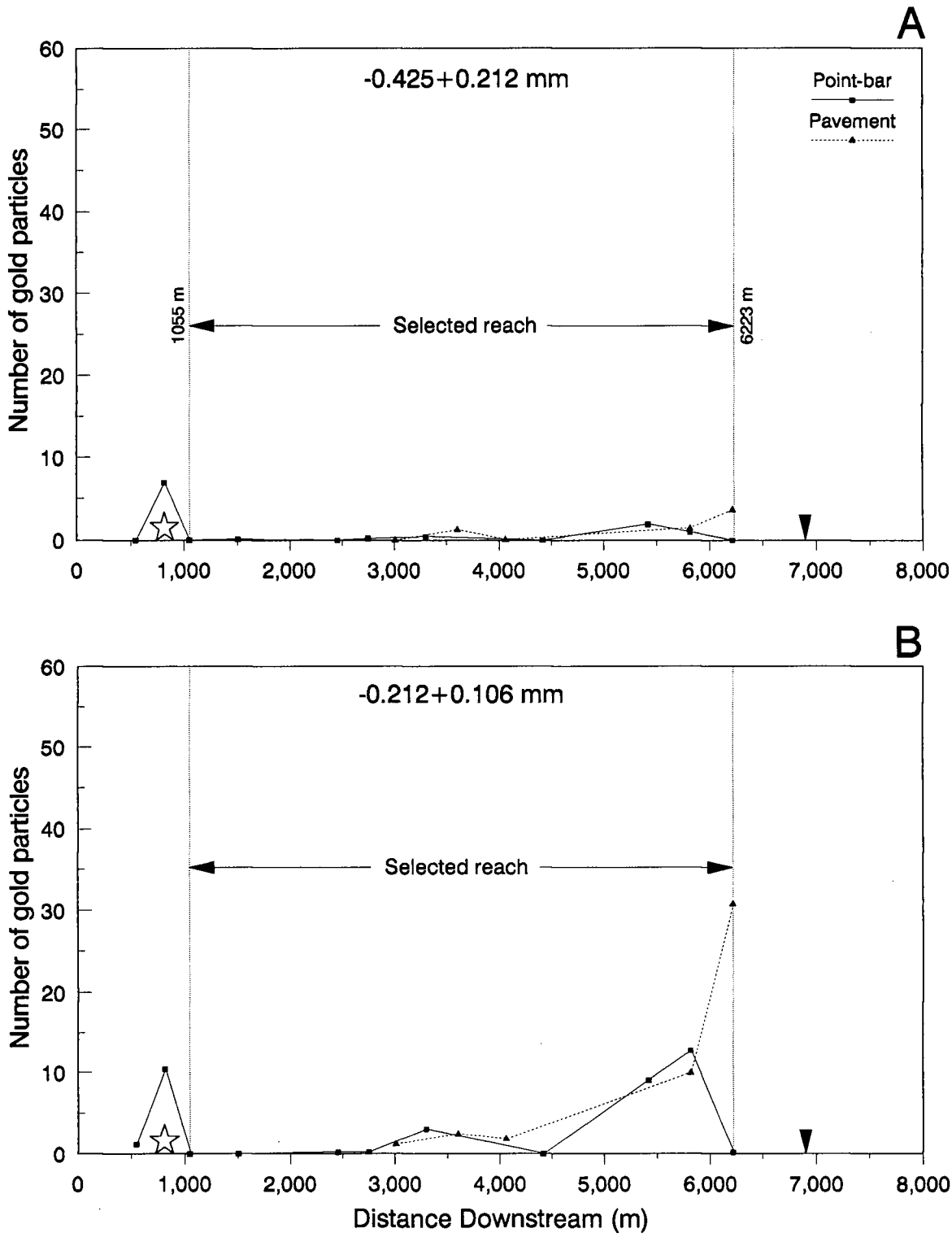

Fig. 5-3. Downstream trends of the estimated numbers of gold particles in heavy mineral concentrates at point bars (solid squares) and pavements (solid triangles) for a) -0.425+0.212 mm fraction, b) -0.212+0.106 mm fraction,

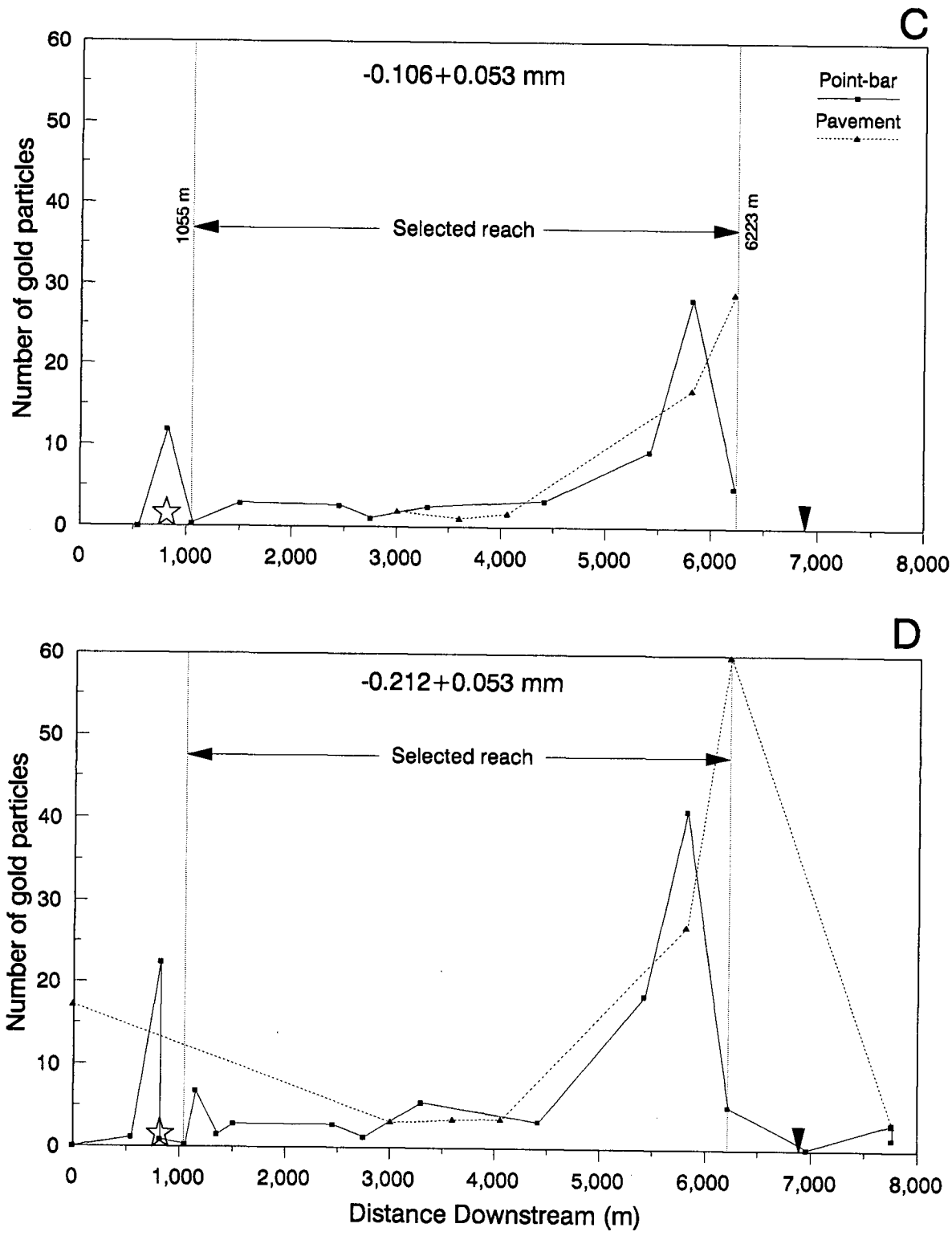

Fig. 5-3. (continued) c) -0.106+0.053 mm fraction and d) ideally combined -0.212+0.053 mm fraction. Star indicates the supposed source of gold mineralization. Arrow indicates the confluence with the Huai Kho Lo.

Table 5-10. Results of the Wald-wolfowitz total-number-of-runs test (μ) and Spearman rank correlation coefficient (r) for downstream trends of number of gold particles in heavy mineral fractions from point-bar and pavement samples of the Huai Hin Laep.

Fraction/ Source of Variation	Cut point (median)	N n_1 (+)	N n_2 (-)	μ	P(μ)	Spearman's r values
Whole reach						
Point bar (n = 11)						
-0.425+0.212 mm	0.12	6	5	9	0.0512*	0.051
-0.212+0.106 mm	0.21	6	5	6	0.3853	0.147
-0.106+0.053 mm	2.83	6	5	6	0.3853	0.555*
-0.212+0.053 mm	3.21	6	5	4	0.0577*	0.536*
Pavement (n = 5)						
-0.425+0.212 mm	1.26	3	2	4	0.2563	0.900*
-0.212+0.106 mm	2.46	3	2	4	0.2563	0.900*
-0.106+0.053 mm	1.92	3	2	3	0.3313	0.700
-0.212+0.053 mm	4.10	3	2	3	0.3313	1.000*
Between supposed source of mineralization and confluence with Huai Kho Lo (1,055 and 6,223 m)						
Point bar (n = 9)						
-0.425+0.212 mm	0.12	5	4	7	0.1304	0.186
-0.212+0.106 mm	0.20	6	3	4	0.2071	0.579
-0.106+0.053 mm	2.83	5	4	4	0.1482	0.800*
-0.212+0.053 mm	3.21	5	4	2	0.0064*	0.800*

N = total sample number
n_1 = number of samples above median
n_2 = number of samples below median
μ = total number of runs above and below the median

* = statistically significant at 90% confidence level

n = 5; $r_{0.10}$ = 0.90 n = 9; $r_{0.10}$ = 0.60
n = 6; $r_{0.10}$ = 0.83 n = 11; $r_{0.10}$ = 0.52

Table 5-11. Numbers of gold particles counted from pan concentrates in the field and in laboratory.

Sample Number	Distance (m)	Number of gold particles	
		Field	Laboratory
Point bar			
PP-17	550	3	-
PP-97	820	25	27
PP-03	1055	20	-
PP-95	1513	0	-
PP-12	2458	17	25
PP-90	2753	0	-
PP-82	3303	5	-
PP-76	4423	2	-
PP-71	5423	11	-
PP-69	5823	14	12
PP-66	6223	10	15
Pavement			
PP-88	3013	5	-
PP-101	3608	3	6
PP-80	4068	0	-

- = sample not processed in laboratory.

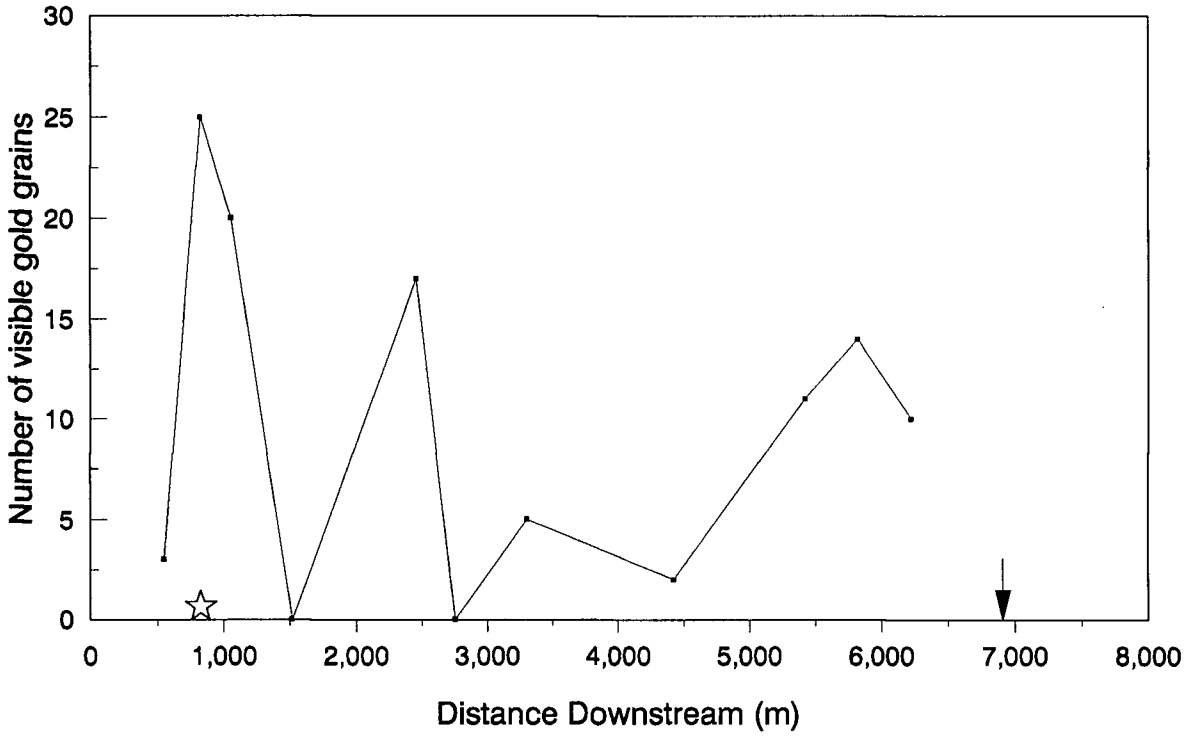

Fig. 5-4. Downstream trend for numbers of visible gold particles recovered in the field pan-concentrates from point bars. Star indicates the supposed source of gold mineralization. Arrow indicates the confluence with the Huai Kho Lo.

case, the number of gold particles counted in the laboratory (Table 5-11) is greater than that counted in the pan.

5.4.1 Grain morphology

Shape of gold particles was obtained using the modified Corey shape factor equation (Corey, 1949):

$$SF = (D_S * D_L)^{1/2} / D_I$$

where D_S, D_I and D_L are the smallest, intermediate and longest diameters, respectively (Day, 1988). An SF value of 1 represents a spherical grain, greater than 1 a long cylindrical grain, and less than 1 a tabular particle (flake).

Estimation of population distribution of 85 gold grains using a probability plot (Fig. 5-5) indicates that at least two populations of grain shapes are present. Population 1 has a mean SF of 0.748 (standard deviation = 0.106) and comprises 65% of the grains. This corresponds to a tabular grain or "flake" with diameter to thickness ratio of 1.79. Population 2 accounts for 35% of the grains and has a mean SF = 1.052 (standard deviation = 0.105), close to a spherical shape with diameter to thickness ratio of 0.90. Between the 52nd and 70th percentiles, there is an overlap between the two populations in the range of SF values between 0.842 and 0.960. This indicates a transition of grain shape from a slightly flatted to nearly spherical shape. Summary of shape factor data of individual sample is

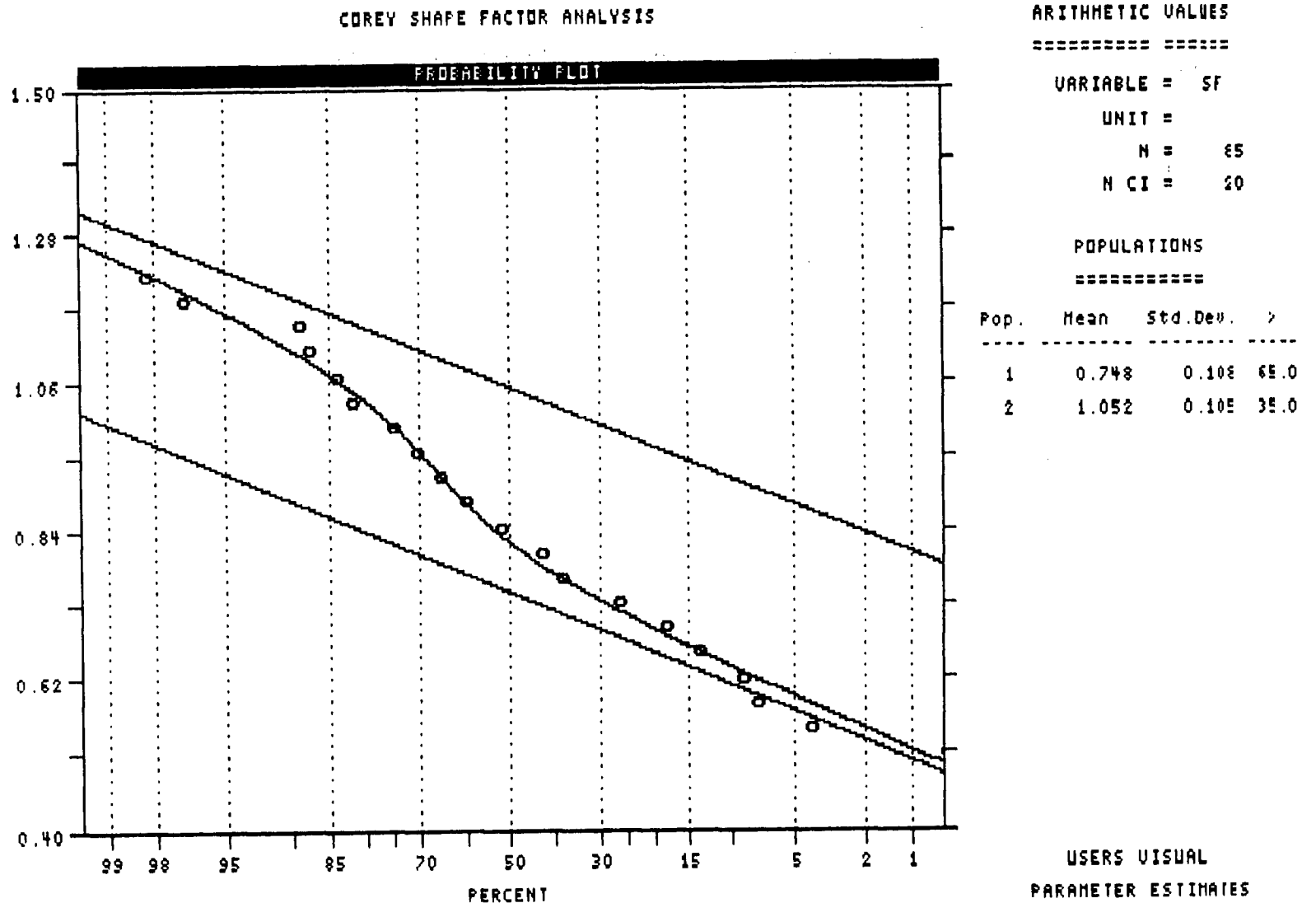

Fig. 5-5. Probability plot of shape factors (SF) of visible gold particles (n = 85) in the selected field pan-concentrates showing inferred component normal populations.

given in Table 5-12. It is apparent that the proximal sample (PP-97) consists 86% of nearly spherical and cylindrical gold grains (Fig. 5-6a) whereas the distal samples (PP-12 to PP-66) contain greater than 65% of the tabular (flake) gold grains (Fig. 5-6b).

5.4.2 Grain composition

Electron microprobe analysis of 39 polished gold grains (Table 5-13) shows that most of the gold grains have patchy rims (Fig. 5-7) of high fineness gold. The rims are very thin (~ 2 to 5 microns). Gold composition varies widely, ranging between 42.02 and 83.44% at cores and 72.62 and 100.17% at rims. Mean fineness (ratio of Au/(Au+Ag) * 1000) for the 39 grain cores is 622.56 (standard deviation = 112.49), whereas mean fineness for 10 rims is 967.98 (standard deviation = 29.94). Concentrations of Cu and Hg are generally at or less than the detection limits and therefore cannot be considered reliable.

The difference of Au compositions in core between proximal and distal samples is statistically examined in Table 5-14. Result shows no significant difference between Au compositions of cores of distal grains (mean = 65.87) and proximal grains (mean = 59.62).

Table 5-12. Summary statistics of shape factor (SF) data.

Sample Number	Distance Downstream	Number Au Grains	SF Populations (%) 1	2
PP-97	820	27	14	86
PP-12	2458	25	67	33
PP-101	3608	6	80	20
PP-69	5823	12	75	25
PP-66	6223	15	65	35
Total		85	65	35

Population 1 = flat grain
Population 2 = nearly spherical and cylindrical grain

A

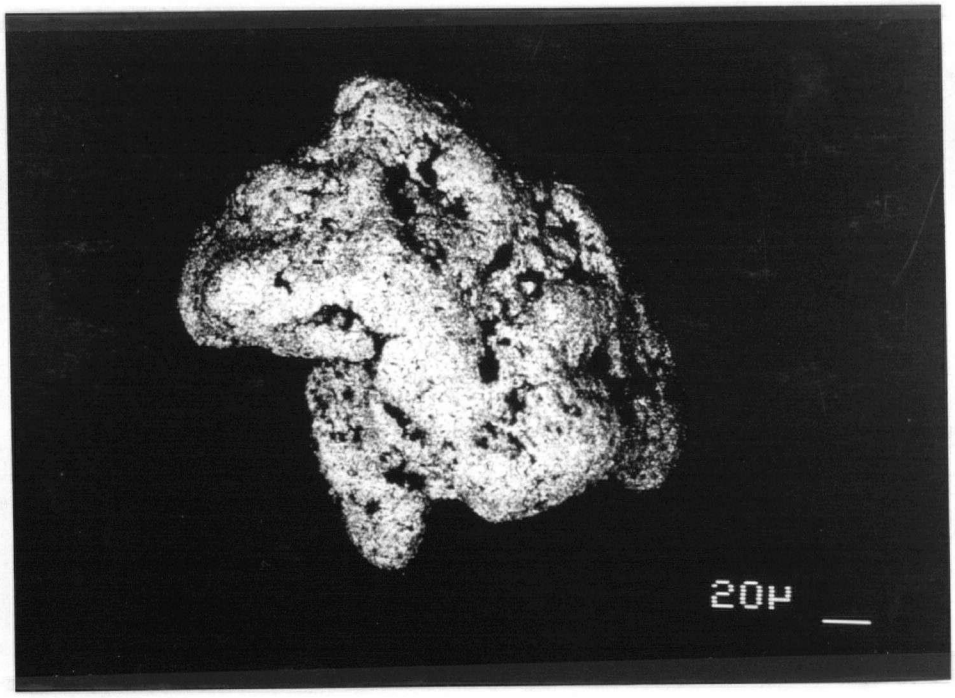

B

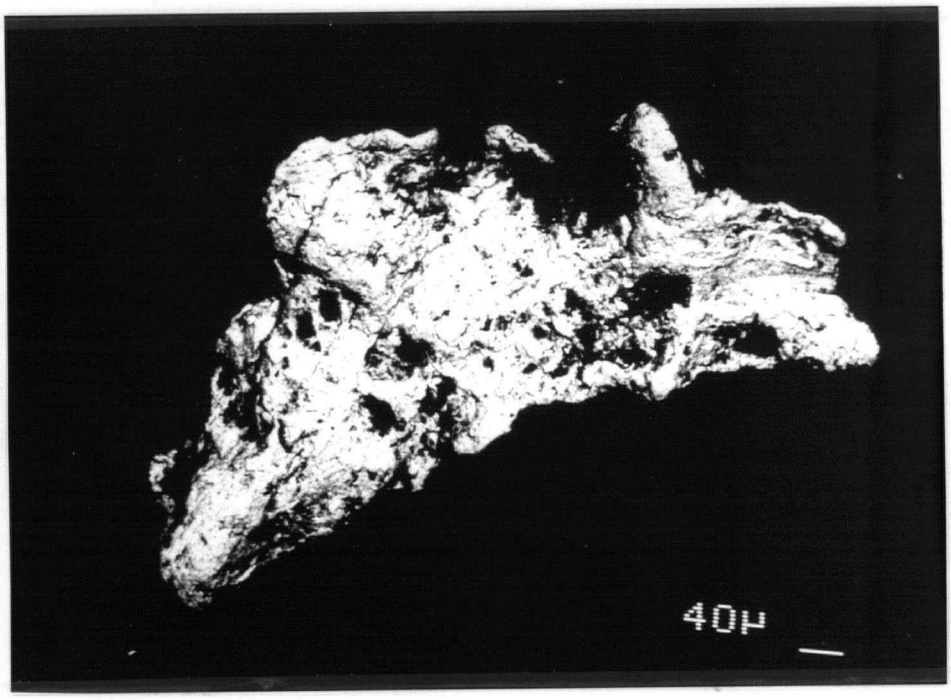

Fig.5-6. Morphology of a) proximal and b) distal gold grain relative to the supposed bedrock source of gold.

Table 5-13. Results of electron microprobe analyses for chemical compositions of the cores and rims of 39 gold grains.

Grain Number	Core Au	Core Ag	Rim-1 Au	Rim-2 Au	Rim-1 Ag	Rim-2 Ag
PP-97-01	57.18	42.41	96.67	97.48	3.04	2.42
PP-97-02	49.17	49.66	-	-	-	-
PP-97-03	82.83	17.13	-	-	-	-
PP-97-04	68.34	31.69	-	-	-	-
PP-97-05	65.71	33.48	91.79	-	5.84	-
PP-97-06	60.78	38.83	-	-	-	-
PP-97-07	72.27	25.66	-	-	-	-
PP-97-08	65.17	34.16	-	-	-	-
PP-97-09	53.87	45.07	-	-	-	-
PP-97-10	53.61	45.53	-	-	-	-
PP-97-11	48.21	50.76	-	-	-	-
PP-97-12	62.56	36.21	-	-	-	-
PP-97-13	52.31	46.51	-	-	-	-
PP-97-14	61.67	37.60	-	-	-	-
PP-97-15	55.41	43.43	-	-	-	-
PP-97-16	55.03	43.96	-	-	-	-
PP-97-17	63.97	34.60	97.98	97.79	1.29	1.65
PP-97-18	65.30	33.73	-	-	-	-
PP-97-19	76.82	22.77	-	-	-	-
PP-97-20	57.33	41.45	-	-	-	-
PP-97-21	43.15	55.86	-	-	-	-
PP-97-22	54.93	44.08	-	-	-	-
PP-97-23	73.32	26.15	-	-	-	-
PP-97-24	50.38	49.19	-	-	-	-
PP-97-25	47.55	52.16	-	-	-	-
PP-97-26	65.82	33.55	-	-	-	-
PP-97-27	46.93	52.30	-	-	-	-

Table 5-13. (continued)

Grain Number	Core Au	Core Ag	Rim-1 Au	Rim-2 Au	Rim-1 Ag	Rim-2 Ag
PP-97 (continued)						
Mean	59.61	39.55	95.48	97.63	3.39	2.03
Median	57.33	41.45	96.67	97.63	3.04	2.03
Range	43.15-82.83	17.13-55.86	72.62-97.98	97.48-97.79	1.29-17.46	1.65-2.42
PP-69-01	74.60	24.13	-	-	-	-
PP-69-02	55.69	43.05	89.57	95.23	10.63	4.66
PP-69-03	61.76	37.18	98.77	-	1.41	-
PP-69-04	78.76	20.48	-	-	-	-
PP-69-05	72.12	27.17	-	-	-	-
PP-69-06	45.29	53.24	-	-	-	-
PP-69-07	83.44	16.03	-	-	-	-
PP-69-08	77.58	21.98	98.63	100.17	0.67	0.27
PP-69-09	71.18	27.77	-	-	-	-
PP-69-10	69.25	21.06	-	-	-	-
PP-69-11	42.02	56.01	-	-	-	-
PP-69-12	58.73	40.11	-	-	-	-
Mean	65.87	32.35	95.66	97.70	4.24	2.46
Median	74.38	27.47	98.63	97.70	1.41	2.46
Range	42.02-83.44	16.03-56.01	89.57-98.77	95.23-100.17	0.67-10.63	0.27-4.66

A

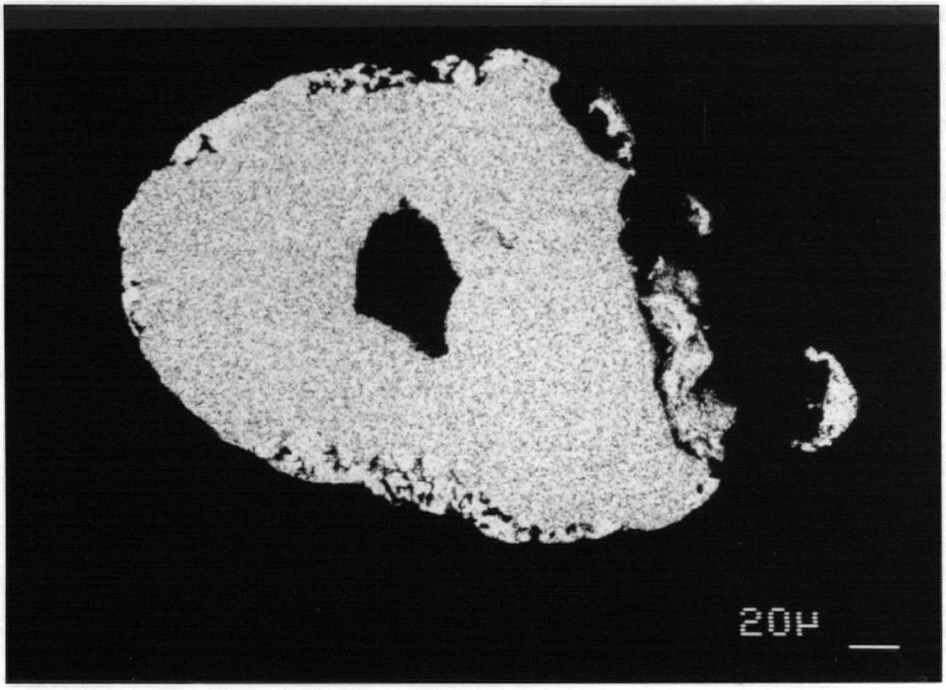

B

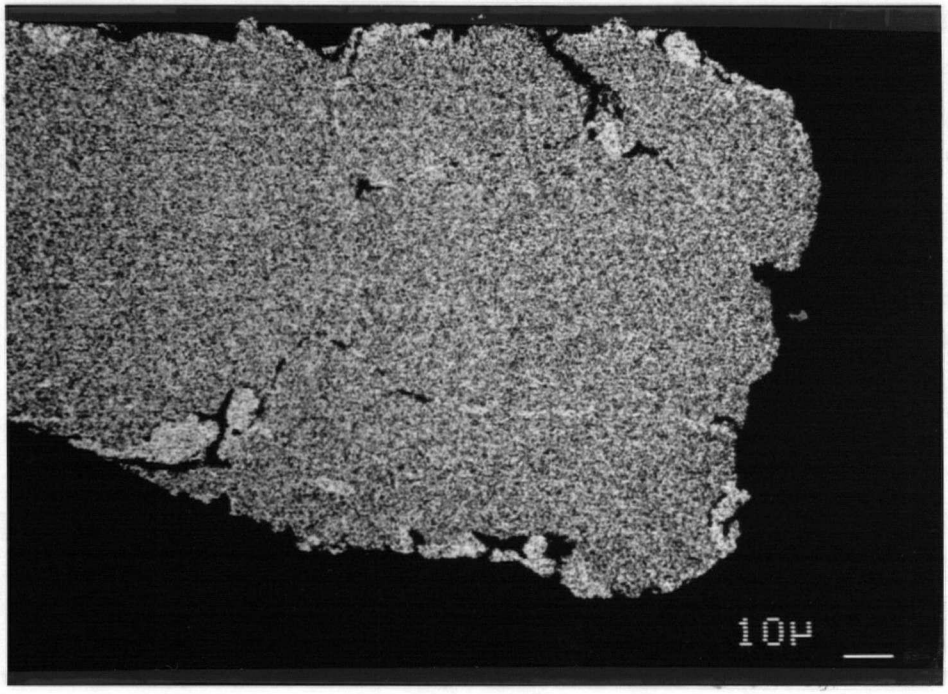

Fig. 5-7. Polished gold grain showing patchy rim of high fineness gold compositions along the edges for a) proximal and b) distal relative to the supposed bedrock source of gold.

Table 5-14. Statistical two-sample t test for the difference between means of Au compositions at cores of proximal (PP-97) and distal (PP-69) gold grains.

Null hypothesis:
μ Au compositions in proximal $=$ μ Au compositions in distal

Fraction/ Source of Variation	N	Mean	S	S_e	Degrees of Freedom
Cores					
Proximal	27	59.615	9.858		
Distal	12	65.868	13.247		
				3.808	17

$T_{Calc} = -1.47$ $T_{(17,\ 0.10)} = 1.740$ Null hypothesis accepted

N = number of samples
Mean = population mean
S = standard deviation
S_e = standard error of difference

5.5 Summary

1) Gold concentrations in heavy mineral concentrates are typically in the several thousand ppb range, versus < 5 ppb in most of the corresponding light and sediment fractions.

2) In the reach between 2,753 and 6,223 m, gold concentrations in all size fractions are slightly greater at pavement than at point-bar sites. However, differences are not statistically significant.

3) Strongly anomalous concentrations of gold are found in all three size fractions of a single sample close to the supposed source of gold. Downstream from this point concentrations of gold are erratic but appear to increase downstream, particularly in the finest sand (-0.106+0.053 mm) and the combined -0.212+0.053 mm fractions of point bars.

4) Gold concentrations in several size fractions from point-bar sites are positively correlated with gravel content, mean grain size (M_0), mean grain size (M_C) and decreased sorting (S_C) of coarse grained component of sediment, and bed roughness; and negatively correlated with coarse sand content.

5) The estimated numbers of gold particles in heavy mineral concentrates increase with decreasing grain size. In a 40 kg field sample, numbers of gold particles in the finest fraction from point-bar and all three size fractions

from pavement provide a reasonable chance of containing free gold, whereas a 30 g analytical subsample is unreliably to contain even a single gold grain.

6) The number of gold particles in point-bar and pavement deposits, particularly the two fine fractions, increases downstream.

7) Gold particles are nearly spherical near their source but are more flattened downstream. They have thin, patchy rims of high fineness gold.

CHAPTER SIX

DISCUSSION

6.1 Introduction

Based on results presented in Chapter 5, gold content is greatest in heavy mineral fractions, whereas, with a few exceptions, concentrations in the corresponding light mineral, -0.150 mm and -0.053 mm sediment fractions are at or below the detection limit. The average concentration of Au in heavy mineral and in sediment fractions from pavement is slightly greater than from point-bar sites, but Au concentrations in sediment from point-bar sites increase with increasing flow velocity and bed roughness where channel width and depth decrease. These controls result in Au concentrations increasing downstream, away from the source, towards the confluence with the Huai Kho Lo.

6.2 Distribution of gold between size and density fractions

High concentrations of gold (Table 5-1) are typically present in heavy mineral fractions (between 0.425 and 0.053 mm). This contrasts with the absence of gold (< 5 ppb) in the corresponding light mineral fractions, only six of which (Appendix) contain gold values greater than the detection limit. These six samples, which with one exception contain less than 50 ppb gold, probably represent cases of incomplete separation during preparation of the heavy mineral concentrate. Low Au values in the light mineral fractions indicate that either 1) gold does not occur as

inclusions in low density minerals, or 2) gold may occur as inclusions in low density minerals but its concentrations are diluted by large amounts of barren light minerals.

Concentrations of gold in the corresponding -0.150 mm and silt-clay (-0.053 mm) fractions (Table 5-1), with exception of 85 ppb from one point bar and 80 and 95 ppb from two pavement sites, are also at or below the detection limit. The -0.150+0.053 mm heavy minerals (Table 5-1) and the corresponding sediment fractions (Table 5-3) contain considerable amounts of gold. Failure to detect gold in the -0.150 mm fraction of sediments must therefore result from its dilution by large amounts of barren sediment. This dilution greatly reduces the probability of even a single grain of gold being encountered in a 30 g assay sample (Table 5-9). It seems unlikely that there is an abrupt cut off in gold particle size at 0.053 mm fraction. Absence of gold from the -0.053 mm sediment fraction therefore probably also results from dilution by large amounts of barren silt and clay. Nuchanong and Nichol (1990) also reported high Au concentrations in field pan concentrates from the Huai Hin Laep versus low values in the silt-clay (-0.063 mm) sediment fraction. Low gold content of the Huai Hin Laep sediments (as opposed to the heavy mineral concentrates) thus seems to result from dilution of free gold by large quantities of fine sediment derived from erosion of the lateritic soils that consist mainly of silt and clay (Fig. 2-6).

The bimodal distribution of sediments in the Huai Hin Laep, with large amounts of silt and clay (~ 10%), contrasts with only 0.8% of these size fractions found in a Malaysian stream also draining lateritic soils, containing more than 60% silt and clay, in a mature rubber plantation (Sirinawin et al, 1987). In this case winnowing of fine sediments from the stream bed enhanced the Sn (cassiterite) concentrations in the sediments relative to concentrations in soils. In the Huai Hin Laep the substantial amounts of silt and clay appear to result from land clearing and in particular the practice of ploughing to plant corn just before the onset of the rainy season. A similar circumstance was also found in corn fields in Kalasin province (Lekhakul, 1990). However, the effects of soil erosion and land use on stream sediment geochemistry require further study.

6.3 Distribution of gold between bed forms

The size distribution of both point-bar and pavement sediments in the Huai Hin Laep is strongly bimodal (Figs. 4-2 and 4-4). However, pavement contains significantly more gravel and less silt-clay than do point bars. This is consistent with pavement sites being higher energy environments where fine sediments are either not deposited or they are winnowed more effectively than from point-bar sites. The removal of fine sediment might account for the somewhat higher heavy mineral and Au concentrations at

pavement than at point-bar sites. However, the coarser grain size and lower abundance of silt-clay might also promote accumulation of gold and heavy minerals by its preferential deposition and trapping in voids. Once preferentially trapped in the pavement, winnowing of fine light minerals could further increase concentrations of heavy minerals and gold. This is consistent with observations elsewhere of preferential accumulation of heavy minerals at high energy sites (Sleath and Fletcher, 1982; Fletcher et al, 1987; Saxby and Fletcher, 1987; Fletcher and Day, 1988b; Day and Fletcher, 1989). The preferential accumulation of heavy minerals and gold at such sites is also consistent with predictions of their behaviour based on bedload transport models proposed by Slingerland (1984), Slingerland and Smith (1986) and Day and Fletcher (in press).

6.4 Distribution of gold along the stream's longitudinal profile

When considering the distribution of gold along the stream's longitudinal profile, the effects of sediment supply and changes in stream characteristics must be taken into account. Although the supposed bedrock source(s) of gold is probably located in the stream headwaters (Fig. 2-5), it is not possible to demonstrate that this is the source of the gold in the Huai Hin Laep without a comprehensive programme of bank soil analysis: this was

beyond the scope of this thesis. However, anomalous Au concentrations are found in the Huai Hin Laep near, but not upstream from, the supposed bedrock source of the gold (Figs. 5-1 and 5-2). It is therefore assumed that this site is at or close to the entry point of gold into the stream.

The abnormally high Au concentration at the point-bar site near the supposed source of gold (Figs. 5-1 and 5-2) probably result from the sediment at this site being directly derived from anomalous soils. This is consistent with the unusual texture of the sediment (PP-96, Appendix) which contains greater than 46% silt and clay but only 18% gravel. At the next site downstream, Au concentrations are much lower, probably as a result of large amounts of barren light minerals derived from upstream sediments that dilute the concentration of gold.

Increased Au concentrations at point-bar sites further downstream contrast with the downstream dilution model presented by Polikarpochkin (1971) and Hawkes (1976). However, it is consistent with observations elsewhere that concentrations of cassiterite (Fletcher et al, 1986, 1987) scheelite (Saxby and Fletcher, 1986) and gold (Fletcher and Day, 1988b; Fletcher, 1990 and Day and Fletcher, in press) can increase downstream from their source in response to changing hydraulic conditions.

In this study, concentrations of gold at point-bar sites are most frequently positively correlated (Table 6-1) with sediment properties such as mean grain size (M_C) and

Table 6-1. Summary significant correlations between Au concentrations in sediments at point-bar sites and stream characteristics and sediment properties in the reach between the supposed source of gold mineralization and the confluence with the Huai Kho Lo.

Fraction (mm)	w	d	v	M_C	S_C	M_0	S_0	D_{65}	wt % sediment			
									-12.0 +2.0	-2.0 +0.425	-0.425 +0.212	-0.053
Point-bar (n = 9)												
-0.425+0.212	-							+			+	
-0.212+0.106				+	+				+	-		
-0.106+0.053			+	+	+	+			+			
-0.212+0.053 (n=11)				+	+			+	+	-		
Score	-1	0	1	3	3	1	0	2	3	-2	1	0

w = stream width; d = channel depth; v = flow velocity
M_C = mean grain size of coarse grained sediment component
S_C = sorting of coarse grained sediment component
M_0 = mean grain size of sediment
S_0 = sorting of sediment
D_{65} = bed roughness
Score = total numbers of significant correlations between gold concentrations in sediment fractions stream characteristics and sediment properties
- = negatively significant correlation
+ = positively significant correlation

poor sorting (S_C, i.e. increasing) of the coarse grained sediment component, and gravel content. They are also positively correlated with other parameters such as bed roughness, mean grain size (M_0), abundance of medium sand (-0.425+0.212 mm) and flow velocity, but negatively correlated with abundance of coarse sand (-2.0+0.425 mm) and channel width. Thus, abundance of Au is positively correlated with those sediment properties that indicate high energy environments and removal of fine sediment. As would be expected these parameters are positively correlated with flow velocity and negatively correlated with channel width. Accumulation of gold at point-bar sites is thus associated with flow convergent zones where decreased channel width results in increased flow velocity, increased bed roughness and decreased (poor) sorting.

It would be useful to establish a model for concentrations of gold in sediment fractions in terms of easily measured field parameters, such as stream width, depth and flow velocity, and estimates of sediment textures such as mean grain size, sediment sorting and amount of gravel. These can be done by linear regressions of the form:

$$Au_{(-0.425+0.212\ mm)} = 0.29 - 40w + 368d + 594v$$

$$(r^2 = .675,\ Se = 64.138)$$

$$Au_{(-0.212+0.106\ mm)} = -130 - 78w + 920d + 2053v$$

$$(r^2 = .671,\ Se = 167.931)$$

$Au_{(-0.106+0.053\ mm)} = -158 + 24w + 60d + 1353v$

$(r^2 = .939, Se = 26.033)$

where w = stream width (m), d = channel depth (m), v = flow velocity (m/sec) and Se = standard error of estimation.

and:

$Au_{(-0.425+0.212\ mm)} = 925 - 1440M_0 + 2D_{65} - 15S_0 + 93G$

$(r^2 = .890, Se = 41.746)$

$Au_{(-0.212+0.106\ mm)} = 2396 - 3974M_0 + 3D_{65} - 40S_0 + 263G$

$(r^2 = .804, Se = 144.775)$

$Au_{(-0.106+0.053\ mm)} = 968 - 1673M_0 - D_{65} - 13S_0 + 112G$

$(r^2 = .764, Se = 57.257)$

where M_0 = mean grain size (mm), D_{65} = bed roughness (mm), S_0 = sediment sorting and G = weight percent gravel.

Gold concentrations (Figs. 5-1 and 5-2) tend to increase downstream as the slope of the Huai Hin Laep (Fig. 2-3) decreases from 0.013 in the headwaters to 0.003 at the confluence with the Huai Kho Lo. Although statistical correlations between slope and heavy mineral and gold concentrations were not carried out, this is consistent with observations elsewhere (Day, 1988; Fletcher, 1990; Day and Fletcher, in press) that as slope decreases abundance of gold increases.

6.5 Gold grain shape and composition

The proportion of nearly spherical to flat gold grains in field pan concentrates decreases from 86:14 close to the source, to 35:65 downstream (Table 5-12). Thus, gold grains either tend to become more flattened during their transport downstream or flattened grains are selectively transported. This is consistent with observations by Giusti (1986) and Poling (1987) that the more flattened, the more easily the gold grains are transported by stream current. Use of changes of gold grain shape in estimating the proximal or distal (relative to source) occurrence of gold might be applicable in the Huai Hin Laep.

Composition of placer gold particles has been extensively studied. The presence of high fineness gold has been interpreted to indicate either leaching of silver (Desborough, 1970; Mann, 1984; Freyssinet et al, 1989; Grimm and Friedrich, 1990) or precipitation of pure gold (Mann, 1984; Webster and Mann, 1984; Wilson, 1984; Freyssinet et al, 1990; Groen et al, 1990). In the Huai Hin Laep, high fineness rims are present on only a few gold grains and are very patchy and incomplete (Fig. 5-7). This suggests that, despite the lateritic weathering environment, which has been associated with hydromorphic mobility of gold in Australia (Mann, 1984; Webster and Mann, 1984), dispersion of gold is principally mechanical rather than chemical. Nuchanong and Nichol (1990) reached a similar conclusion.

6.6 Recommendations for mineral exploration

Several gold occurrences were visited during preliminary site selection. The Huai Hin Laep was chosen to represent a typical small stream in an area of deforested agricultural land use in northeastern Thailand. The following recommendations should be applicable to similar streams containing relatively coarse, sand size, gold particles.

6.6.1 Regional survey

The purpose of a regional reconnaissance survey is to reliably detect presence or absence of gold in large survey areas using the minimum number of samples, i.e. a low sample density. This usually restricts sampling to relatively large drainage catchments. In such cases, the probability that a single sample, in an area of known gold mineralization, will fail to detect the presence of gold must be considered. Recommendations for this surveying stage should consider: i) representative field sample size, ii) sample location along the stream reach, and iii) preferred sampling sites or types of sample.

6.6.1.1 Sample fraction

The presence of gold in the Huai Hin Laep is readily detected in heavy mineral fractions that contain Au concentrations up to 100 times greater than those in individual sediment fractions. The high gold content of the heavy mineral fractions indicates that these will be much more effective than conventional sediment samples in detecting gold in the Huai Hin Laep. Thus, based on estimates of the numbers of free gold particles likely to be present in 40 kg of -12 mm field samples and in 30 g analytical subsamples (Tables 5-9 and 6-2), the median of the total numbers of gold particles in a heavy mineral concentrate from a 40 kg point-bar sample is about 3 grains. The corresponding Poisson probability of detecting one or more gold grains is very high - 95%. Similarly, for pavement samples, the median of the total numbers of gold particles is about 5 grains with a probability of detecting one or more gold grains of 99%. These results indicate that analysis of heavy mineral concentrates from a 40 kg field sample of either point-bar or pavement sediments will have very high chance of detecting the presence of anomalous concentrations of gold. This also explains why use of traditional field pan concentrates is a very effective method in the Huai Hin Laep. Use of the -2.0 mm sediment fraction would reduce the field sample size, like that of the Harris Creek, south central British Columbia (Day,

Table 6-2. Summary statistics of median, range and probability of containing one or more gold grains (P>0) for the estimated numbers of gold particles in the standardized 40 kg (-12.0 mm) field samples and 30 g analytical subsamples.

	Fractions (mm)			
				Total
	-0.425 +0.212	-0.212 +0.106	-0.106 +0.053	-0.425 +0.053
40 kg field samples				
Point bar (n = 11)				
Median	0.15	0.25	3.54	3.21
Range	0.00-11.38	0.00-17.63	0.00-36.45	0.35-41.96
P>0	0.14	0.22	0.97	0.96
Pavement (n = 5)				
Median	1.61	3.13	2.88	4.71
Range	0.00-4.87	1.37-41.40	1.27-38.70	3.11-59.70
P>0	0.80	0.96	0.94	0.99
30 g analytical subsamples				
Point bar				
Median	0.00	0.02	0.37	0.45
Range	0.00-0.15	0.00-0.64	0.00-2.58	0.02-3.25
P>0	0.003	0.02	0.31	0.36
Pavement				
Median	0.03	0.42	1.13	1.58
Range	0.00-0.11	0.31-2.49	0.25-3.86	0.69-6.46
P>0	0.03	0.34	0.68	0.79

Statistical data are based on data in Tables 5-8 and 5-9.

1988). However, because of the large amounts of silt and clay in the Huai Hin Laep sediment, the difficulty may arise when these sediment fractions block the screen opening preventing sand sized particles to pass through it, and then the field sieving process becomes very time consuming.

These findings are consistent with those of Nuchanong and Nichol (1990) who also found that relatively high Au concentrations were present in field pan concentrates from high energy environments in the Huai Hin Laep. However, there are some potential disadvantages to use of field pan concentrate samples in mineral exploration, for example, differences in gold recovery by different individuals and substantial losses of fine grained gold (Wang and Poling, 1983; Giusti, 1986 and Poling, 1987). To improve recovery of fine gold particles, methylene iodide heavy liquid can be employed to prepare the concentrates. However, the disadvantages of this are 1) the high cost of sample transportation and laboratory preparation and 2) inability to separate gold or heavy minerals finer than about 0.053 mm fraction.

Compared to numbers of gold particles in heavy mineral concentrates prepared from 40 kg field samples, the median number of gold particles in all size fractions of a 30 g subsample is only about 0.15 grains for point-bar samples and 0.53 grains for pavement samples. The corresponding probabilities of detecting one or more gold grains are 14 and 41%, respectively. In addition, the inability of

conventional sediment samples to reliably detect anomalous concentrations is confirmed by Au concentrations in the -0.150 mm and -0.053 mm sediment fractions below the detection limit (Table 5-1). Absence of Au from the -0.053 mm fractions implies that analysis of 30 g sediment samples will have even lower probabilities of detecting the presence of gold than indicated by probabilities based on estimates of numbers of gold particles. Thus, conventional stream sediment samples will fail to reliably detect the presence of a gold anomaly in the Huai Hin Laep.

6.6.1.2 Sample location at catchment scale

In a large scale stream sediment survey, it is necessary to consider the dispersion pattern of anomalous sediment along the drainage. With the anomaly dilution model of Polikarpochkin (1971) and Hawkes (1976), the anomaly decreases exponentially from the source, in proportion to catchment basin area, as a consequence of dilution by barren sediment. To detect such an anomaly it may be necessary to do detailed sediment sampling along the entire stream reach. However, with Au concentrations increasing downstream in response to changing stream and sediment properties, dispersion of gold in the Huai Hin Laep does not follow this conventional model. It follows that collection of sediment samples along the lower reaches of third order streams may be capable of detecting the presence of a source of coarse

gold much further upstream. Thus, providing that heavy mineral concentrates are prepared from bulk sediment samples of sufficient size (~ 40 kg), relatively low density regional surveys should be effective in exploration for gold deposits containing coarse gold.

6.6.1.3 Preferred sampling sites at local scale

Gold concentrations in sediments are slightly greater at pavement than at point bar sites. The entire 40 kg of -12 mm sediment or field pan concentrate should therefore be taken from pavement sites where possible. Where this is not possible point-bars characterized by narrowing of the stream channel and increased bed roughness and flow velocity should be chosen. Because gold concentrations are closely related to sediment properties that can easily be evaluated during sample collection, it is important to record this information as a guide to subsequent interpretation. Parameters to be recorded include 1) channel width and depth at the water level where very easily measured in the field, 2) flow velocity by timing a float over a known distance, and 3) sediment texture, particularly the amount of gravel and bed roughness estimated in the field. These parameters must be recorded prior to sample collection: a scaled photograph of the bed provides a useful record of bed texture.

6.6.2 Follow-up survey

The purpose of the follow-up survey is to locate the source of gold in the drainage basin. Since the auriferous catchment has been identified, the follow-up survey should consist of more detailed sampling of either the 40 kg of -12 mm sediment or field pan concentrates along the stream channel. A pan sample should be sufficiently large (i.e. panned from 8 shovels-full or at least 20 kg of sediment) to detect the presence of very rare gold particles. Together with stream sediment sampling, soil samples should be collected from both sides of the stream banks to identify the point of entry of gold into the stream.

Because of the possibility of gold concentrations increasing downstream away from the source as a function of stream characteristics and sediment textures, gold anomalies along the lower reaches of stream should not be interpreted as being in the immediate vicinity of gold mineralization. Anomalous concentrations of gold must therefore be carefully evaluated in relation to stream characteristics and sediment textures, for example, possibly using regression equations similar to those in section 6.4. High gold concentrations at locations where the channel narrows and flow velocity and bed roughness increase may indicate a local accumulation of gold in response to these conditions. Conversely, high concentrations of gold at sites not favourable to its accumulation are more likely to indicate proximity to a

source.

It must be emphasized that these recommendations apply only to exploration for coarse sand sized gold in streams like the Huai Hin Laep. They are probably not applicable to exploration for deposits of fine grained gold of the type described by Nuchanong and Nichol (1990) in the Loei region.

CHAPTER SEVEN

CONCLUSIONS

7.1 Conclusions

1) Sediments of the Huai Hin Laep have a strongly bimodal distribution with large amounts of gravel and silt-clay but little sand. Pavement sediments contain greater amounts of gravel but less silt and clay than point-bar sediments. Abnormally high silt and clay probably results from increased soil erosion that results from the practice of ploughing the lateritic soils to plant corn just before the onset of the rainy season.

2) Downstream trends in sediment texture at point-bar sites are very erratic but sediment sorting and flow velocity are negatively correlated with stream width and depth. That is, sediment sorting at point-bar sites becomes poorer in the convergent zones characterized by high flow velocity, narrow channel and shallow depth.

3) Heavy mineral content of sediments from point-bar and pavement sites is approximately 1%. At point-bar sites, heavy mineral content increases in high energy convergent zones.

4) Gold concentrations in the heavy mineral fractions (SG > 3.3) are typically several thousand ppb ranging up to 198,000 ppb. In comparison, concentrations in light mineral fractions and whole sediments are generally less than 5 ppb.

5) Gold concentrations in all three size fractions at pavement sites are slightly higher than at point-bar sites. At point-bar sites gold is preferentially accumulated where narrow stream channel, shallow depth, high flow velocity leads to high bed roughness and coarse sediment texture. Changes of these stream characteristics and sedimentological conditions cause concentrations of gold to increase downstream away from the supposed source.

6) The estimated numbers of gold particles in heavy mineral concentrates from the 40 kg field samples and the correspondingly high probabilities of detecting the gold anomalies suggest that analysis of heavy mineral concentrates from large bulk sediments has very high chance of detecting the presence of anomalous concentrations of gold.

7) The estimated numbers of gold particles in the 30 g sediment samples give a low probability of detecting the presence of gold with such samples. This results from dilution of Au-rich heavy minerals by large amounts of light and silt-clay fractions.

8) With respect to mineral exploration for coarse grained gold similar to that found in the Huai Hin Laep, because gold concentrations increase downstream, at the regional

survey stage bulk sediment samples (i.e. 40 kg of -12 mm) or field pan concentrates (i.e. at least 20 kg of sediment) can be taken along the lower part of third order streams. Together with sample collection, data regarding stream characteristics and sediment properties should be recorded.

9) At the follow-up survey stage, more detailed samples of either bulk sediments or field pan concentrates should be taken from high energy point-bar sites along the stream channel, together with bank soil samples to identify the point of entry of gold into the stream. Because gold concentrations increase downstream, gold anomalies at the lower reach of the stream may not be the vicinity of gold mineralization. High gold concentrations at sites not favourable to its accumulation may indicate proximity to a source.

REFERENCES

References

Beschta, R.L. and Jackson, W.L. 1979. The intrusion of fine sediments into a stable gravel bed. J. Fish. Res. Board Can. 36: 204-210.

Bradley, J.V. 1968. Distribution-free statistical tests. Prentice-Hall, Inc. Englewood Cliffs, N.J. 388 pages.

Charoenpravat, A., Wongwanich, T., Tantiwanit, W and Theetiparivatra, U. 1976. Regional geological survey, scale 1 : 250,000, Changwat Loei, map sheet NE 47-12. Geological Survey Division, Department of Mineral Resources, Bangkok, Thailand (in Thai).

Chorley, R.J., Schumm, S.A. and Sugden, D.E. 1984. Geomorphology. Methuen & Co. Ltd, London. 605 pages.

Clifton, H.E., Hunter, R.E., Swanson, F.J. and Phillips, R.L. 1969. Sample size and meaningful gold analysis. U.S. Geol. Surv. Prof. Paper 625 C, pp. C1-C17.

Corey, A.T. 1949. Influence of shape on the fall velocity of sand grains. Unpub. M.Sc. thesis, Colorado A & M college, 102 pages.

Day, S.J. 1988. Sampling stream sediments for gold in mineral exploration, southern British Columbia. Unpub. M.Sc. thesis, The University of British Columbia, 232 pages.

Day, S.J. and Fletcher, W.K. 1986. Particle size and abundance of gold in selected stream sediments, southern British Columbia, Canada. J. Geochem. Explor., 26: 203-214.

Day, S.J. and Fletcher, W.K. 1987. Effects of valley and local channel morphology on the distribution of gold in stream sediments. In: Geochemical Exploration 1987: Selected papers of the 12th International geochemical exploration symposium, Orleans, France. Jenness S.E. ed. (Amsterdam, etc.: Elsevier, 1989), 1-6. (Spec. Publ. Ass. Explor. Geochemists no. 15).

Day, S.J. and Fletcher, W.K. 1989. Effects of valley and local channel morphology on the distribution of gold in stream sediments from Harris Creek, British Columbia, Canada, J. Geochem. Explor., 32: 1-16.

Day, S.J. and Fletcher, W.K. Formation of gold placers in a gravel-bed stream. In press: J. Sed. Petrol.

Desborough, G.A. 1970. Silver depletion indicated by microanalysis of gold from placer occurrence, Western United States. Econ. Geol., 65: 304-311.

Einstein, H.A. 1950. The bed-load function for sediment transportation in open channel flows. U.S. Dept. Agric., Tech. Bull. 1026, 71 pages.

Fletcher, W.K. 1981. Analytical methods in geochemical prospecting. Elsevier, 255 pages.

Fletcher, W.K. 1990. Dispersion and behaviour of gold in stream sediments. Open File 1990-28. Mineral Resources Branch, British Columbia Ministry of Energy, Mines and Petroleum Resources, 28 pages.

Fletcher, W.K. and Day, S.J. 1988a. Seasonal variation of gold content of Harris Creek, near Vernon: a progress report. In: Geological fieldwork 1987. BC Ministry of Energy, Mines and Petroleum Resources, Paper 1988-1: 511-513.

Fletcher, W.K. and Day, S.J. 1988b. Behaviour of gold and other heavy minerals in drainage sediments: some implications for exploration geochemical surveys. In: MacDonald, D.R. (Editors), Prospecting in areas of glaciated terrain - 1988. Canadian Institute Mining and Metallurgy, Halifax, 171-183.

Fletcher, W.K. and Wolcott, J. 1989. Seasonal variation in transport of gold in Harris Creek: implications for exploration. Association of Exploration Geochemists, Explore 66: 1, 8 and 9.

Fletcher, W.K. and Wolcott, J. Transportation of magnetite and gold in Harris Creek, British Columbia, and implications for exploration. In press: J. Geochem. Explor.

Fletcher, W.K. and Zhang, W. 1989. Size distribution of gold in drainage sediments: Mount Washington, Vancouver Island (92F/14). British Columbia Ministry of Energy Mines and Petroleum Resources, Geological Fieldwork, 1988, Paper 1989-1, 603-605.

Fletcher, W.K., Dousset, P.E. and Ismail, Y.B. 1987. Elimination of hydraulic effects in stream sediment data behaviour of cassiterite in a Malaysian stream. J. Geochem. Explor., 28: 385-408.

Freyssinet, Ph., Lawrence, L.M. and Butt, C.R.M. 1990. Geochemistry and morphology of gold in lateritic profiles in Savanna and Semi-arid climates (abstract). 2nd International Symposium, Geochemistry of the Earth's surface and of mineral formation. July, Aix en Provence, France. pp. 61-63.

Freyssinet, Ph., Zeegers, H. and Tardy, Y. 1989. Morphology and geochemistry of gold grains in lateritic profiles of southern Mali. In: S. Jenness et al. (Editors), Geochemical Exploration 1987. J. Geochem. Explor., 32: 17-31.

Frostick, L.E., Lucas, P.M. and Reid, I. 1984. The infiltration of fine matrices into coarse-grained alluvial sediments and its implications for stratigraphical interpretation. J. Geol. Soc. London, Vol. 141, pp. 955-965.

Giusti, L. 1986. The morphology, mineralogy, and behavior of "fine-grained" gold from placer deposits of Alberta: sampling and implications for mineral exploration. Can. J. Earth Sci. 23: 1662-1672.

Grigg, N.S. and Rathbun, R.E. 1969. Hydraulic equivalence of minerals with a consideration of the reentrainment process. U.S. Geol. Surv., Prof. Paper 650-B, pp. B77-B80.

Grimm, B. and Friedrich, G. 1990. Weathering effects on supergene gold in soils of a semiarid environment, Gentio Do Ouro, Brazil (abstract). 2nd International Symposium, Geochemistry of the Earth's surface and of mineral formation. July, Aix en Provence, France. pp. 70-73.

Groen, J.C., Craig, J.R. and Rimstidt, J.D. 1990. Gold-rich rim formation on electrum grains in placers. Canadian Mineralogist, V. 28: 207-228.

Hawkes, H.E. 1976. The downstream dilution of stream sediment anomalies. J. Geochem. Explor., 6:345-358.

Ingamells, C.O. 1981. Evaluation of skewed exploration data - the nugget effect. Geochim. Cosmochim. Acta, 45: 1209-1216.

Knight, J. and McTaggart, K.C. 1986. The composition of placer and lode gold from the Fraser River drainage area, southwestern British Columbia. C.I.M.M. Geol. Journ., v. 1, no. 1, pp. 21-30.

Koch, J.S. and Link, R.F. 1970. Statistical analysis of geological data. John Wiley and Sons. 375 pages.

Komar, P.D. and Wang, C. 1984. Processes of selective grain transport and the formation of placer on beaches. J. Geol., 92: 637-655.

Krumbein, W.C. and Pettijohn, F.J. 1938. Manual of sedimentary petrography. D. Appleton-Century Company, Inc. 549 pages.

Kuhnle, R.A. and Southard, J.B. 1990. Flume experiments on the transport of heavy minerals in gravel-bed streams. J. Sed. Petrol., Vol. 60, pp. 687-696.

Kumanchan, P. 1987. Gold deposits in Changwat Loei and Changwat Nong Khai areas. 4th Symposium, Department of Mineral Resources (in Thai), Bangkok, Thailand. pp. 68-97.

Lekhakul, K. 1990. Soil and plant management for agricultural development in northeastern Thailand. Technical meeting, Agricultural Development Research Center (ADRC), Soil and Water Conservation Research in the Northeast, Land Development Department, Bangkok, Thailand (in Thai). pp. 103-137.

Lynch, J. 1990. Provisional elemental values for eight new geochemical lake sediment and stream sediment reference materials LKSD-1, LKSD-2, LKSD-3, LKSD-4, STSD-1, STSD-2, STSD-3 and STSD-4. Geostandards Newsletter, Vol. 14, No. 1, pp. 153-167.

Mann, A.W. 1984. Mobility of gold and silver in lateritic weathering profiles. Some observations from Western Australia. Econ. Geol., 39: 38-49.

Middleton, G.V. 1970. Experimental studies related to problems of flysch sedimentation. In: Lajoie, J., ed., Flysch Sedimentology in North America: Geological Association of Canada, Spec. Pub. 7, pp. 253-272.

Nuchanong, T. 1988. Geochemical orientation survey over Gold-copper mineralization at Phu Tham Phra and Phu Thong Daeng, Thailand. Progress Report 2, 86 pages.

Nuchanong, T. 1991. Geochemical dispersion of gold associated with copper-gold mineralization in northeastern Thailand. Unpub. Ph.D. thesis, Queen's University, 341 pages.

Nuchanong, T. and Nichol, I. 1990. Distribution of gold in stream sediments associated with two gold prospects in northeastern Thailand. Poster at 14th International Geochemical Exploration Symposium, Prague, Czechoslovakia.

Pholphan, N. and Siriratanamongkol, C. 1967. Copper mineralization at Phu Thong Daeng, Loei province: Base metal project's report, Economic Geology Division, Department of Mineral Resources (in Thai), 211 pages.

Polikarpochkin, V.V. 1971. The quantitative estimation of ore-bearing areas from sample data of the drainage systems (abs). Trans. 3rd Int. Geochem. Explor. Symp. Can. Inst. Min. Metall., Spec. Vol., 11: 585-586.

Poling, G.W. 1987. Recovery of fine gold in placer mining. In: Gold Mining 87, C.O. Brawner, Ed. 1st International Conference on Gold Mining, Vancouver, British Columbia, Canada. pp. 345-360.

Pookcharoen, V. and Ruaisoongnoen, S. 1986. Runoff and sediment yields from sample plot in Acacia auriculaeformis and Leucaena leucocephala, 5 yrs plantation at Chee watershed research station, Chaiyaphum. Research Section, Watershed Management Division, Royal Forest Department (in Thai), 14 pages.

Reid, I. and Frostick, L.E. 1985. Role of settling, entrainment and dispersive equivalence and of interstice trapping in placer formation. J. Geol. Soc. London, Vol. 142, pp. 739-746.

Rittenhouse, G. 1943. Transportation and deposition of heavy minerals: Geol. Soc. America Bull., Vol. 54, pp. 1725-1780.

Rose, W.A., Hawkes, H.E. and Webb, J.S. 1979. Geochemistry in mineral exploration. Academic Press, 657 pages.

Rubey, W.W. 1933. The size-distribution of heavy minerals within a water-laid sandstone. J. Sed. Petrol, Vol. 3, no. 1, pp. 3-29.

Sallenger, A.H. 1979. Inverse grading and hydraulic equivalence in grain-flow deposits. J. Sed. Petrol, Vol. 49, pp. 553-562.

Saxby, D.W. 1985. Sampling problems and hydraulic factors related to the dispersion of scheelite in drainage sediments, Clea Property, Yukon Territory. Unpub. M.Sc. thesis, The University of British Columbia, 152 pages.

Saxby, D.W. and Fletcher, W.K. 1986a. Behaviour of scheelite in a Cordilleran stream. In: GEOEXPO'86: Exploration in the North American Cordillera. I.L. Elliott and B.W. Smee, eds. Association of Exploration Geochemists, pp. 177-183.

Saxby, D. and Fletcher, K. 1986b. The geometric mean concentration ratio (GMCR) as an estimator of hydraulic effects in geochemical data for elements dispersed as heavy minerals. J. Geochem. Explor., 26: 223-230.

Schumm, S.A. 1985. Patterns of alluvial rivers. Ann. Rev. Earth Planet. Sci. 13: 5-27.

Selby, M.J. 1985. Earth's Changing Surface. Clarendon Press, Oxford. 607 pages.

Sinclair, A.J. 1976. Applications of probability graphs in mineral exploration. The Association of Exploration Geochemists, Spec. Vol. 4, 95 pages.

Sirinawin, T. Fletcher, W.K. and Dousset, P.E. 1987. Evaluation of geochemical methods in exploration for primary tin deposits: Batu Gajah-Tanjong Tualang area, Perak, Malaysia. J. Geochem. Explor., 29:165-181.

Sleath, A. and Fletcher, W.K. 1982. Geochemical dispersion in a glacial stream, Purcell Mountains, B.C. In: Prospecting in areas of glaciated terrain. P. Davenport, ed. (Montreal: Canadian Institute of Mining and Metallurgy, 1982), 195-203.

Slingerland, R.L. 1977. The effects of entrainment on the hydraulic equivalence relationships of light and heavy minerals in sands. J. Sed. Petrol., Vol. 47, no. 2, pp. 753-770.

Slingerland, R.L. 1984. Role of hydraulic sorting in the origin of fluvial placers. J. Sed. Petrol., Vol. 54, no. 1, pp. 137-150.

Slingerland, R.L. and Smith, N.D. 1986. Occurrence and formation of water-laid placers. Ann. Rev. Earth Planet. Sci., Vol. 14: 113-147.

Smith, H.H., Bernier, D.W., Bung, F.M., Rintz, F.C., Shinn, R. and Teleki, S. 1968. Area handbook for Thailand. 558 pages.

Smith, N.D. and Minter, W.E.L. 1980. Sedimentological controls of gold and uranium in Witwatersrand paleoplacers. Econ. Geol. 75: 1-14.

Snedecor, G.W. and Cochran, W.G. 1989. Statistical Methods. Iowa State University Press / AMES. 503 pages.

Soil Survey Division, 1975. Detailed reconnaissance soil map of Loei province. Province Series: No. 10., Soil Survey Division, Department of Land Development, Bangkok, Thailand.

Steger, H.F. 1986. Certified reference materials. CM84-14E (revised edition): Energy, Mines and Resources Canada. 42 pages.

Steidtmann, J.R. 1982. Size-density sorting of sand-size spheres during deposition from bedload transport and implications concerning hydraulic equivalence. Sedimentology. 29: 877-883.

Tate, N.M. 1988. Styles and distribution of gold deposits in Thailand (unpublished paper). 15 pages.

Tourtelot, H.A. 1968. Hydraulic equivalence of grains of quartz and heavier minerals, and implications for the study of placers. U.S. Geol. Surv., Prof. Paper 594-F, pp. F1-F13.

Vudhichatvanich, S., Vichit, P. and Suvanves, B. 1980. Gold. Economic Geology Bulletin, no. 25. Economic Geology Division, Department of Mineral Resources (in Thai), 99 pages.

Wang, W. and Poling, G.W. 1983. Methods for recovering fine placer gold. Canadian Institute Mining Metallurgy Bulletin, 76: 47-56.

Webster, J.G. and Mann, A.W. 1984. The influence of climate, geomorphology and primary geology on the supergene migration of gold and silver. J. Geochem. Explor., 22: 21-42.

Wilson, A.F. 1984. Origin of quartz free gold nuggets and supergene gold found in laterites and soils. A review of some new observations. Aust. J. Earth Sci., 31: 303-316.

Yensabai, S. and Jamnongthai, M. 1990. Report on detailed geochemical survey of the Huai Hin Laep area, Ban Nong Khan, Amphoe Na Duang, Changwat Loei. Economic Geology Report, August, 1990. Economic Geology Division, Department of Mineral Resources (in Thai). 34 pages.

Zar, J.H. 1984. Biostatistical analysis. Prentice-Hall Inc. 718 pages.

APPENDIX

Summary of stream characteristics of the Huai Hin Laep.

Sample Number	Width (m)	Depth (m)	Velocity (m/sec)
Point-bar (n = 19)			
PP-22	1.45	.34	0.50
PP-16	0.70	.9	0.45
PP-96	1.00	.20	0.03
PP-98	1.40	.5	0.03
PP-09	2.80	.10	0.05
PP-08	3.30	.38	0.00
PP-06	1.20	.30	0.36
PP-94	1.50	.20	0.11
PP-10	5.40	.55	0.03
PP-89	5.00	.61	0.02
PP-81	2.30	.50	0.08
PP-75	1.90	.18	0.17
PP-73	2.85	.92	0.14
PP-70	1.30	.36	0.12
PP-67	1.70	.15	0.27
PP-64	6.50	.70	0.00
PP-59	2.00	.25	0.30
PP-55	1.60	.25	1.00
PP-56	1.60	.25	1.00
Mean	2.39	.34	0.25
Std	1.60	.29	0.31
Pavement (n = 3)			
PP-23	-	-	-
PP-87	2.40	.15	0.50
PP-100	2.80	.8	0.40
PP-79	2.00	.11	0.33
PP-68	-	-	-
PP-65	-	-	-
PP-58	-	-	-
Mean	2.40	.11	0.41
Std	0.40	.35	0.09

Weight (g) of sediments in each size fraction of point-bar and pavement samples.

Sample	Fractions (mm)							
	-12.0 +2.0	-2.0 +0.425	-0.425 +0.212	-0.212 +0.150	-0.150 +0.106	-0.106 +0.075	-0.075 +0.053	-0.053
Point-bar (n = 19)								
PP-22	2769.50	1382.50	106.60	26.80	17.20	8.70	10.30	409.89
PP-16	19172.00	9530.00	287.60	99.50	69.50	47.00	54.70	2010.58
PP-96	4411.00	5431.00	1354.00	386.45	427.29	411.21	558.23	11293.16
PP-98	520.40	923.20	138.00	37.60	51.80	86.70	64.30	1518.65
PP-09	15364.00	8979.00	811.89	203.03	229.00	187.81	222.01	4659.60
PP-08	2202.90	1187.80	88.30	25.50	19.70	21.80	25.60	670.75
PP-06	2070.80	1558.50	71.10	30.60	9.60	15.40	15.50	978.93
PP-94	11601.00	8770.00	1021.02	300.51	193.60	190.35	329.38	9542.20
PP-10	21174.00	8379.00	693.60	174.76	114.32	76.41	129.18	2901.90
PP-89	12162.00	12695.00	1702.54	227.40	130.09	102.62	164.56	8054.80
PP-81	17910.20	8199.10	635.37	131.76	70.06	67.89	178.56	3794.10
PP-75	16363.00	8373.00	529.97	111.30	56.68	42.10	68.32	2868.10
PP-73	997.70	1390.80	91.80	15.80	10.81	8.08	8.18	274.08
PP-70	17004.00	7013.30	1827.20	442.43	260.12	165.24	190.17	4533.60
PP-67	19992.60	4771.30	1025.72	342.42	250.78	140.34	190.72	4543.60
PP-64	18482.00	8659.60	605.30	217.26	198.52	112.95	226.05	3642.60
PP-59	2367.10	2675.10	632.00	102.30	45.00	23.90	17.30	503.62
PP-55	1751.90	1654.20	458.90	45.90	28.10	19.30	29.30	591.55
PP-56	3026.80	1589.40	416.70	55.50	39.70	19.50	34.50	476.27

Weight (g) of sediments (continued).

Sample	Fractions (mm)							
	-12.0 +2.0	-2.0 +0.425	-0.425 +0.212	-0.212 +0.150	-0.150 +0.106	-0.106 +0.075	-0.075 +0.053	-0.053
Pavement (n = 7)								
PP-23	3438.00	1397.90	216.40	32.80	25.10	15.70	17.30	571.95
PP-87	26664.00	6189.00	325.08	49.66	22.89	18.83	41.24	1491.90
PP-100	21555.00	6776.00	638.39	118.33	80.99	51.74	65.75	2167.64
PP-79	20056.80	8225.00	925.10	115.24	63.36	37.09	57.29	2317.80
PP-68	15082.70	7321.00	1649.60	419.54	300.94	186.30	263.60	4182.40
PP-65	17458.50	7867.80	970.56	230.09	142.46	98.69	126.78	3028.30
PP-58	2825.40	1115.40	142.20	23.90	19.40	14.10	17.80	388.27

Weight percent sediment in each size fraction of point-bar and pavement samples.

Sample	Fractions (mm)							
	-12.0 +2.0	-2.0 +0.425	-0.425 +0.212	-0.212 +0.150	-0.150 +0.106	-0.106 +0.075	-0.075 +0.053	-0.053
Point-bar (n = 19)								
PP-22	58.53	29.22	2.25	0.57	0.36	0.18	0.22	8.66
PP-16	61.31	30.48	0.92	0.32	0.22	0.15	0.17	6.43
PP-96	18.17	22.38	5.58	1.59	1.76	1.69	2.30	46.53
PP-98	15.58	27.64	4.13	1.13	1.55	2.60	1.92	45.46
PP-09	50.12	29.29	2.65	0.66	0.75	0.61	0.72	15.20
PP-08	51.93	28.00	2.08	0.60	0.46	0.51	0.60	15.81
PP-06	43.59	32.81	1.50	0.64	0.20	0.32	0.33	20.61
PP-94	36.31	27.45	3.20	0.94	0.61	0.60	1.03	29.87
PP-10	62.94	24.91	2.06	0.52	0.34	0.23	0.38	8.63
PP-89	34.51	36.03	4.83	0.65	0.37	0.29	0.47	22.86
PP-81	57.80	26.46	2.05	0.43	0.23	0.22	0.58	12.24
PP-75	57.59	29.47	1.87	0.39	0.20	0.15	0.24	10.09
PP-73	35.67	49.72	3.28	0.56	0.39	0.29	0.29	9.80
PP-70	54.09	22.31	5.81	1.41	0.83	0.53	0.60	14.42
PP-67	63.96	15.26	3.28	1.10	0.80	0.45	0.61	14.54
PP-64	57.50	26.94	1.88	0.68	0.62	0.35	0.70	11.33
PP-59	37.18	42.02	9.93	1.61	0.71	0.38	0.27	7.91
PP-55	38.26	36.12	10.02	1.00	0.61	0.42	0.64	12.92
PP-56	53.49	28.09	7.36	0.98	0.70	0.34	0.61	8.42
Mean	46.76	29.72	3.93	0.83	0.62	0.54	0.67	16.93
Std	14.42	7.52	2.70	0.39	0.42	0.60	0.56	11.76
Pavement (n = 7)								
PP-23	60.16	24.46	3.79	0.57	0.44	0.27	0.30	10.01
PP-87	76.61	17.78	0.93	0.14	0.07	0.05	0.12	4.29
PP-100	68.53	21.54	2.03	0.38	0.26	0.16	0.21	6.89
PP-79	63.08	25.87	2.91	0.36	0.20	0.12	0.18	7.29
PP-68	51.29	24.90	5.61	1.43	1.02	0.63	0.90	14.22
PP-65	58.34	26.29	3.24	0.77	0.48	0.33	0.42	10.12
PP-58	62.14	24.53	3.13	0.53	0.43	0.31	0.39	8.54
Mean	62.88	23.62	3.09	0.60	0.41	0.27	0.36	8.77
Std	7.99	2.99	1.45	0.42	0.31	0.19	0.26	3.13

Weight (g) of heavy mineral concentrates in each size fraction from point-bar and pavement samples.

	Fractions (mm)				
Sample	-0.425 +0.212	-0.212 +0.150	-0.150 +0.106	-0.106 +0.075	-0.075 +0.053
Point-bar (n = 11)					
PP-16	7.28	1.10	0.94	0.40	0.09
PP-96	7.68	1.60	1.56	4.86	0.20
PP-09	10.32	1.88	2.02	0.80	0.34
PP-94	7.80	2.05	1.18	1.29	0.98
PP-10	4.67	1.29	0.98	0.45	0.29
PP-89	12.59	2.33	1.30	0.78	0.23
PP-81	5.54	1.07	0.67	0.35	0.07
PP-75	3.18	0.77	0.54	0.37	0.12
PP-70	13.82	4.78	3.51	2.03	0.52
PP-67	6.71	3.02	2.66	1.37	1.13
PP-64	3.72	1.31	1.58	0.73	0.41
Pavement (n = 5)					
PP-87	3.42	0.57	-	-	0.17
PP-100	4.42	0.85	0.55	0.21	0.08
PP-79	9.59	1.37	0.72	0.30	0.05
PP-68	11.38	3.77	3.10	2.09	0.81
PP-65	10.42	2.41	1.63	1.01	0.37

Weight percent heavy mineral concentrates in each size fraction from point-bar and pavement samples.

Sample Number	Size Fractions (mm) -0.425 +0.212	-0.212 +0.150	-0.150 +0.106	-0.106 +0.075	-0.075 +0.053
Point-bar (n = 11)					
PP-16	2.53	1.21	1.35	0.85	0.16
PP-96	0.57	0.41	0.36	1.19	0.04
PP-09	1.27	0.93	0.88	0.43	0.16
PP-94	0.76	0.68	0.61	0.68	0.30
PP-10	0.67	0.74	0.86	0.59	0.23
PP-89	0.74	1.02	1.00	0.75	0.14
PP-81	0.87	0.81	0.95	0.52	0.04
PP-75	0.60	0.69	0.95	0.88	0.18
PP-70	0.76	1.08	1.35	1.23	0.28
PP-67	0.65	0.88	1.06	0.98	0.59
PP-64	0.61	0.60	0.80	0.65	0.18
Mean	0.91	0.82	0.92	0.80	0.21
Std	0.54	0.22	0.27	0.25	0.14
Pavement (n = 5)					
PP-87	1.05	1.14	-	-	0.42
PP-100	0.69	0.75	0.68	0.41	0.13
PP-79	1.04	1.19	1.13	0.80	0.08
PP-68	0.69	0.90	1.03	1.12	0.31
PP-65	1.07	1.04	1.14	1.02	0.29
Mean	0.91	1.00	1.00	0.84	0.25
Std	0.18	0.16	0.19	0.27	0.12

Gold concentrations (ppb) in light mineral fractions.

Sample	Light mineral fractions (mm)				
	-0.425 +0.212	-0.212 +0.150	-0.150 +0.106	-0.106 +0.075	-0.075 +0.053
Point-bar					
PP-16	<5	<5	<5	<5	<5
PP-96	<5	5	10	<5	<5
PP-09	<5	<5	<5	<5	<5
PP-94	<5	<5	<5	<5	<5
PP-10	<5	<5	<5	<5	<5
PP-89	<5	<5	<5	<5	<5
PP-81	<5	<5	<5	<5	<5
PP-75	<5	<5	<5	<5	<5
PP-70	<5	160	<5	<5	<5
PP-67	<5	<5	<5	5	<5
PP-64	<5	<5	<5	<5	<5
Pavement					
PP-87	<5	<5	-	-	45
PP-100	<5	<5	<5	<5	<5
PP-79	<5	<5	<5	<5	<5
PP-68	<5	<5	<5	<5	<5
PP-65	<5	<5	35	<5	<5

Axial measurements (microns) of each visible gold grain and its Corey shape factor (SF).

Sample	L-axis	I-axis	S-axis	SF
PP-97-1-1	180	150	80	0.80
PP-97-1-2	225	189	95	0.77
PP-97-1-3	156	137	80	0.82
PP-97-1-4	544	380	255	0.98
PP-97-1-5	246	138	100	1.14
PP-97-1-6	309	267	95	0.64
PP-97-1-7	686	554	415	0.96
PP-97-1-8	274	260	200	0.90
PP-97-1-9	442	328	210	0.93
PP-97-1-10	266	240	145	0.82
PP-97-1-11	262	238	145	0.82
PP-97-1-12	714	566	320	0.85
PP-97-1-13	321	180	140	1.18
PP-97-1-14	261	183	130	1.01
PP-97-1-15	342	220	160	1.06
PP-97-1-16	153	114	80	0.97
PP-97-1-17	324	228	130	0.90
PP-97-1-18	442	272	175	1.02
PP-97-1-19	270	207	80	0.71
PP-97-1-20	266	218	160	0.95
PP-97-1-21	394	394	190	0.69
PP-97-1-22	528	410	175	0.74
PP-97-1-23	1200	864	290	0.68
PP-97-1-24	442	218	145	1.16
PP-97-1-25	550	350	270	1.10
PP-97-1-26	336	272	175	0.89
PP-97-1-27	237	146	95	1.03
PP-12-1-1	975	758	190	0.57
PP-12-1-2	189	96	65	1.15
PP-12-1-3	180	93	65	1.16
PP-12-1-4	207	207	95	0.68
PP-12-1-5	246	156	65	0.81
PP-12-1-6	346	230	110	0.85
PP-12-1-7	330	218	80	0.75
PP-12-1-8	234	126	95	1.18
PP-12-1-9	895	736	175	0.54
PP-12-1-10	195	135	50	0.73
PP-12-1-11	432	214	120	1.06
PP-12-1-12	650	310	130	0.94
PP-12-1-13	279	255	95	0.64
PP-12-1-14	321	234	145	0.92
PP-12-1-15	153	78	55	1.18
PP-12-1-16	294	165	50	0.73
PP-12-1-17	198	99	50	1.01
PP-12-1-18	432	336	145	0.75
PP-12-1-19	358	278	110	0.71

Axial measurements (continued).

Sample	L-axis	I-axis	S-axis	SF
PP-12-1-20	210	180	110	0.84
PP-12-1-21	330	294	145	0.74
PP-12-1-22	132	99	50	0.82
PP-12-1-23	111	96	30	0.60
PP-12-1-24	114	84	30	0.70
PP-12-1-25	272	246	95	0.65
PP-101-1-1	216	129	80	1.02
PP-101-1-2	576	362	175	0.88
PP-101-1-3	165	126	30	0.56
PP-101-1-4	168	108	50	0.85
PP-101-1-5	325	234	120	0.84
PP-101-1-6	348	219	80	0.76
PP-69-1-1	214	180	140	0.96
PP-69-1-2	297	156	65	0.89
PP-69-1-3	311	153	115	1.24
PP-69-1-4	239	197	95	0.77
PP-69-1-5	347	311	95	0.58
PP-69-1-6	343	251	110	0.77
PP-69-1-7	237	159	80	0.87
PP-69-1-8	357	270	95	0.68
PP-69-1-9	203	90	55	1.17
PP-69-1-10	548	314	130	0.85
PP-69-1-11	256	176	110	0.95
PP-69-1-12	272	180	80	0.82
PP-66-1-1	713	298	175	1.19
PP-66-1-2	604	305	110	0.85
PP-66-1-3	436	156	65	1.08
PP-66-1-4	404	196	110	1.08
PP-66-1-5	218	138	50	0.76
PP-66-1-6	287	200	95	0.83
PP-66-1-7	444	218	110	1.01
PP-66-1-8	633	298	80	0.76
PP-66-1-9	240	185	40	0.53
PP-66-1-10	302	229	50	0.54
PP-66-1-11	189	138	65	0.80
PP-66-1-12	335	207	65	0.71
PP-66-1-13	165	149	65	0.70
PP-66-1-14	149	147	95	0.81
PP-66-1-15	75	75	30	0.63

L = longest, I = intermediate and S = smallest axis.

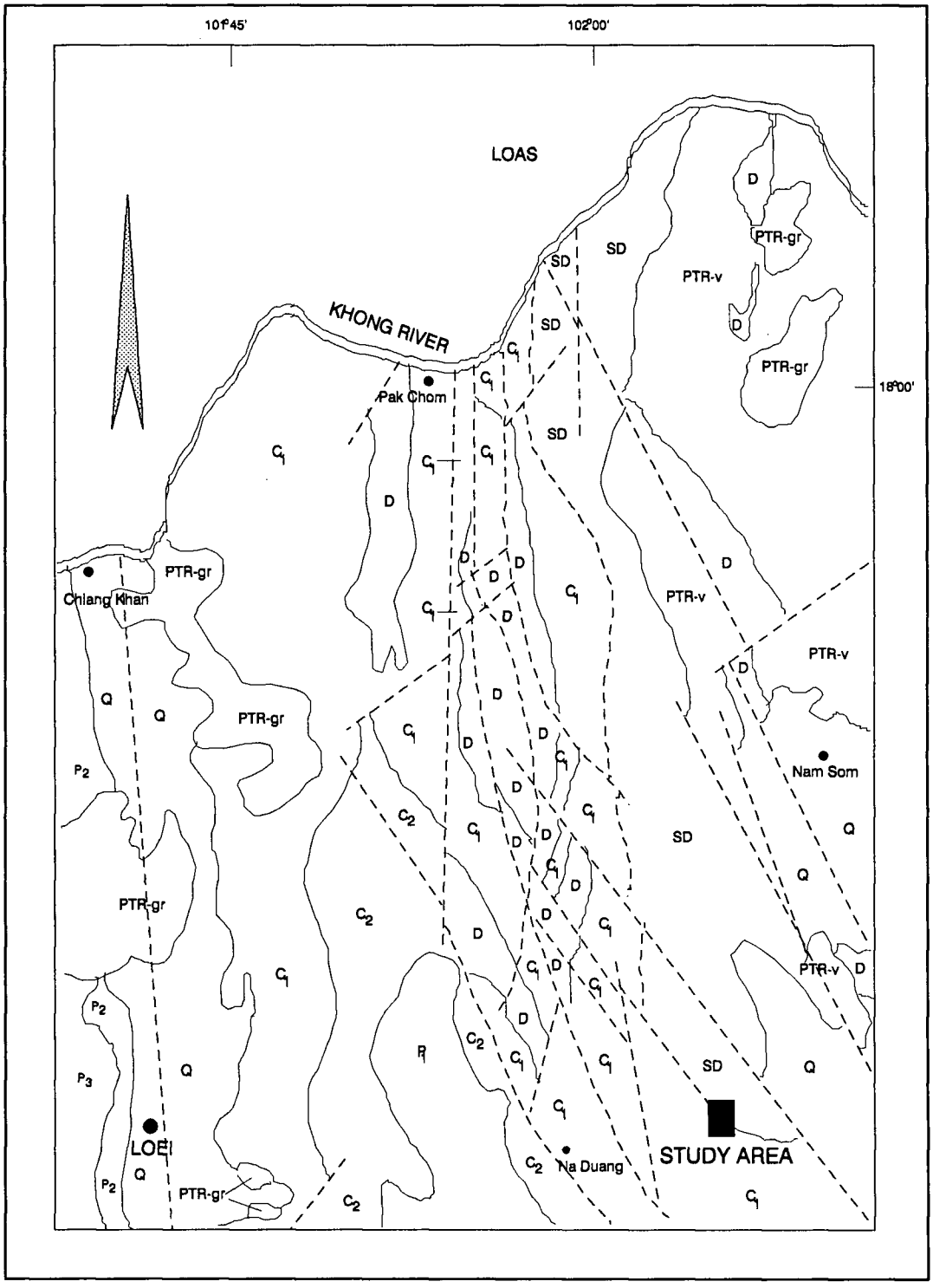

Regional geology of Loei region, northeastern Thailand (after Charoenpravat et al, 1976). SD = Silurian-Devonian; D = Devonian; C_1, C_2 = Carboniferous; P_1 = Permian; PTR-gr = Permo-triassic granite; PTR-v = Permo-triassic volcanic rocks; Q = Quaternary. Shaded arrow indicates north direction.